

Figure 4.25 Slope profiles and contour map of St.1

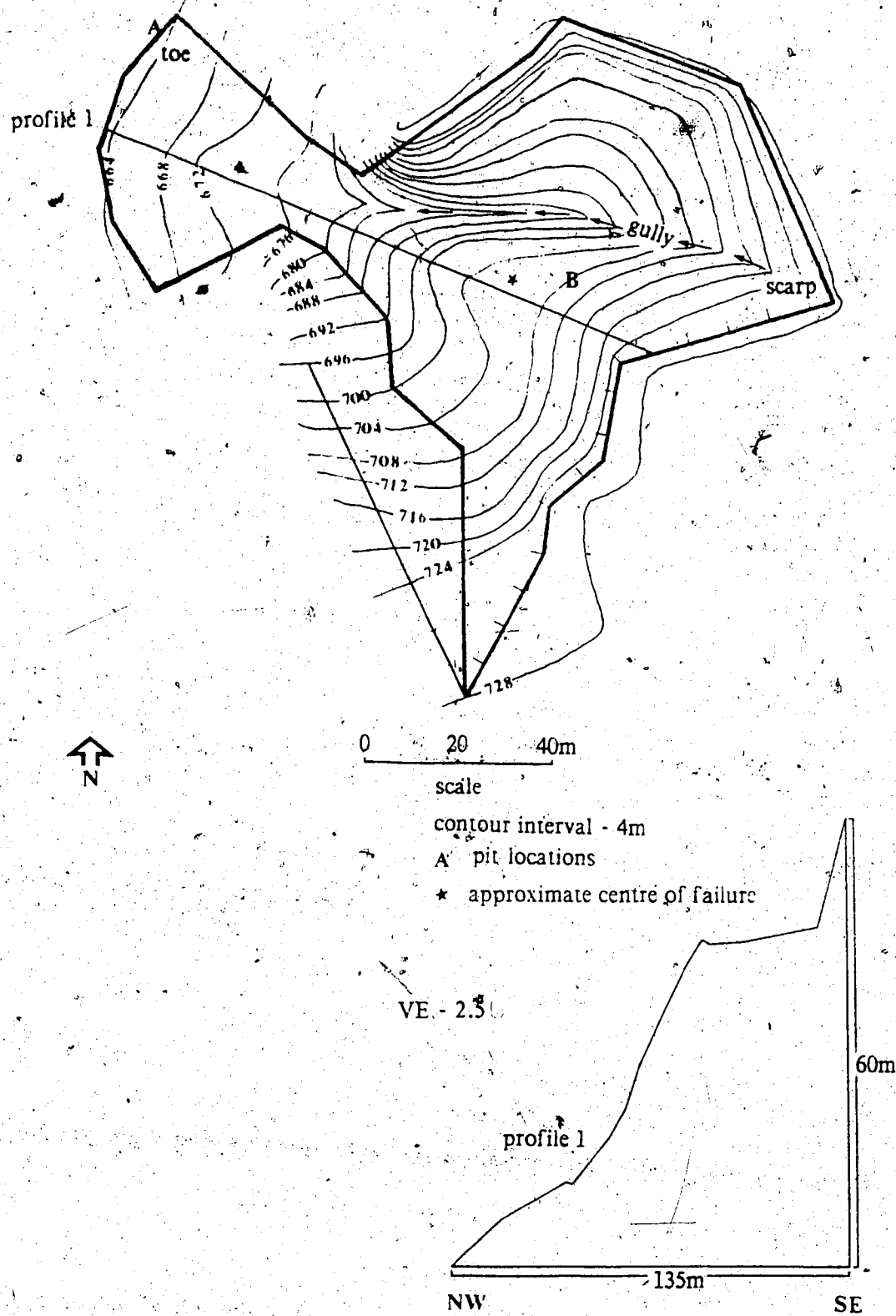


Figure 4.26 Slope profiles and contour map of S/F1

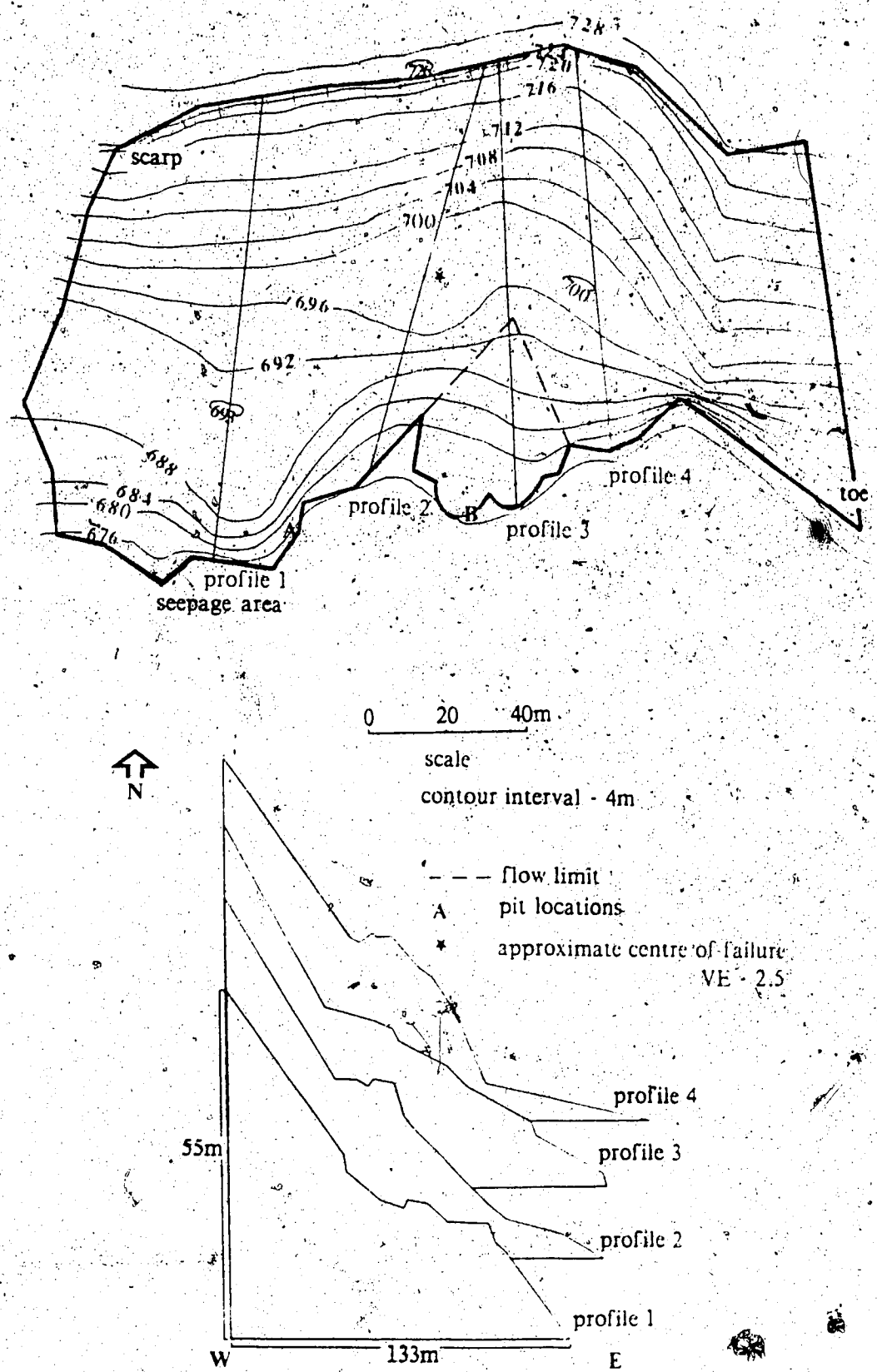


Figure 4.27 Slope profiles and contour map of S/F2

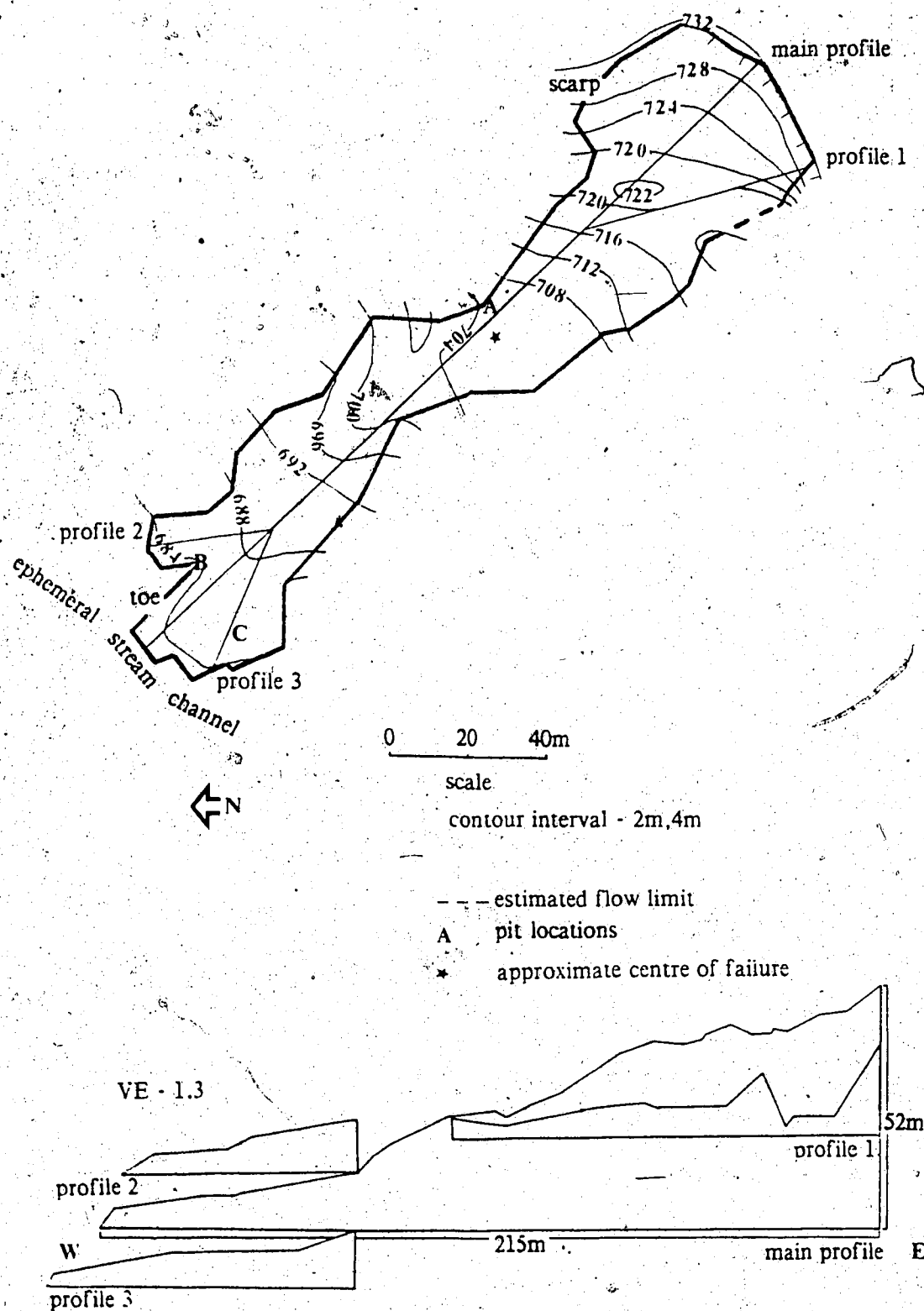


Figure 4.28 Slope profiles and contour map of P/F1

were calculated by multiplying the planimetric area of each failure by the mean depth of failure. Because the original slope forms are approximated (Figures 4.35 and 4.36), so are the depths and calculated volumes. Nevertheless, these estimates are indicative of the amount of badland material moved by mass movements.

With the failures currently visible it is apparent that slides contribute the greatest volume of material removed while complex failures, flows, falls and topples contribute increasingly smaller amounts. The role of each failure type in the current rate of badland extension can also be assessed with respect to the badland perimeter (189,000 m). Assuming an average slope length of 120 m, 4 percent of the current perimeter is affected by mass movements. These observations, however, do not take into account those failures that have occurred but did not persist. Because many of the smaller failures (flows, falls, and topples) may no longer be evident, their contribution to badland denudation may be grossly underestimated. Also, during badland evolution the various failure types may have occurred at significantly different rates than are apparent today. Therefore, analyses of this kind are necessarily restricted by the time factor where only those failures visible at a geologic point in time can be considered.

Table 4.3 - Volumetric analysis of failures occurring in the Dinosaur Badlands Case Failures

Failure	Volume(m ³)	Order of magnitude ¹
Sc1	59,000	4
Sc2	374,000	5
Sc3	7,000	3
Sc4	285,000	5
Sr ²	267,000	4
St1	54,000	3
S/F1	44,000	3
S/F2	158,000	3
P/F1	27,000	3

¹ Order of magnitude was determined by the range in size of each failure type with '1' being the smallest in each failure group.

The reactivated slide (Sr²) was monitored for movement. Cumulative movement, both vertical and horizontal, is revealed by the vector diagram (Figure 4.29). Because the survey

Table 4.4 - Representative volumes of various magnitude events.

Failure type	Magnitude	representative volume(m ³)	Frequency of occurrence	Total volume(m ³)
slides	1	1,800	41	73,800
	2	5,200	25	130,000
	3	30,545	9	274,905
	4	163,090	10	1,630,900
	5	329,675	7	2,307,725
	6	1,655,170	1	<u>1,655,170</u>
				Tot.6,072,500
flows	1	140	125	17,500
	2	350	18	<u>6,300</u>
				Tot.23,800
falls + topples	1	5	15	75
	2	10	8	<u>80</u>
				Tot.155
complex failures	1	6,925	5	34,625
	2	20,550	1	20,550
	3	76,380	3	<u>229,140</u>
				Tot.284,315

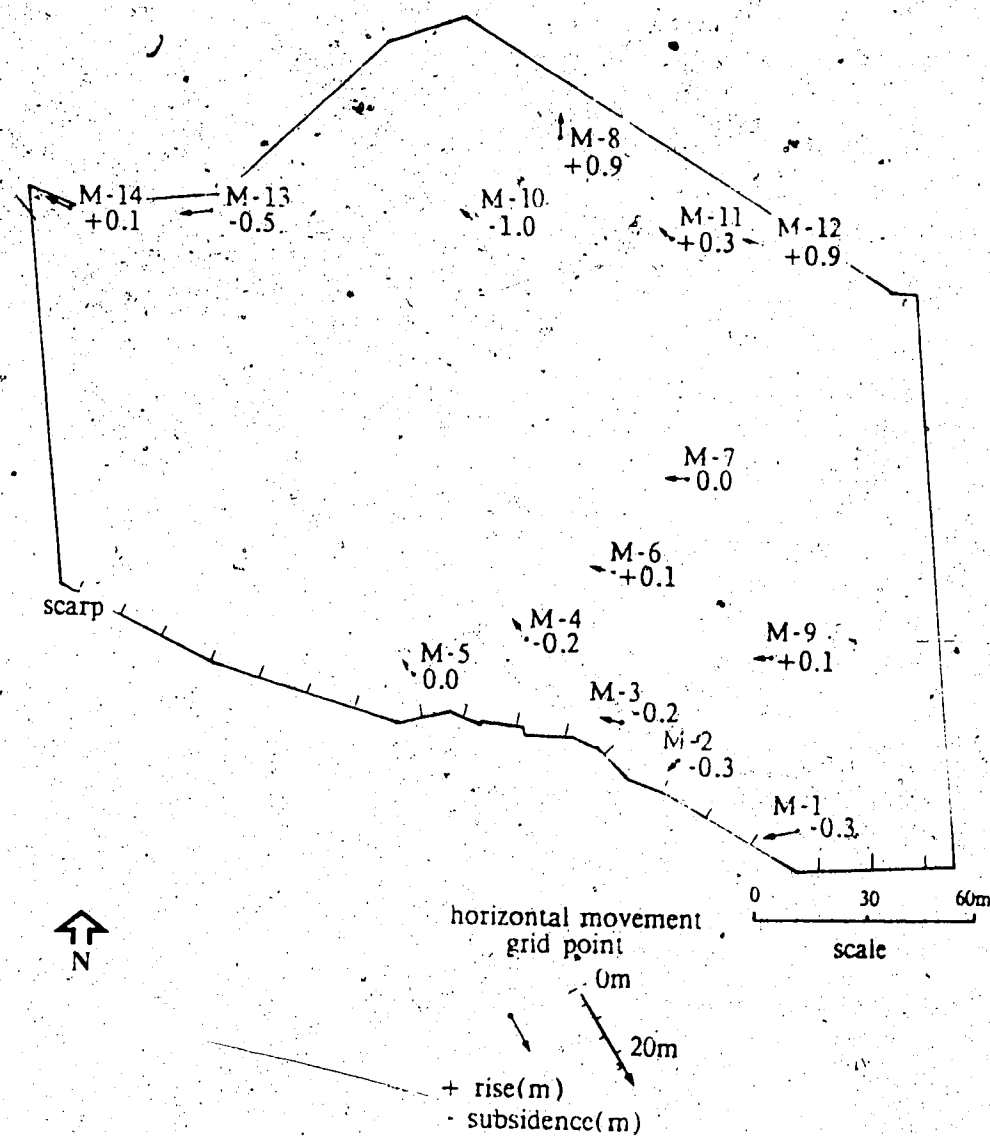


Figure 4.29 Vector diagram showing movement since July 1, 1986, when measurement began.

points were not resected, a true three dimensional pattern has not been represented. Figure 4.29 therefore only illustrates the cumulative distance and elevation changes. The horizontal movement is generally in a westerly direction and not coincident with the actual direction of the slope which is towards the north. The vertical movement is somewhat less defined, but does tend to drop in the head area and rise in the foot area.

When movement was initially suspected (June 11, 1986), the exposed scarp was approximately 0.07 m. By mid July, 1986, the scarp height was 0.63 m (Figure 4.30). This displacement at the head continued and by August 2, 1987 the visible scarp was 0.85 m (Figure 4.31). Movement of the toe area did not keep pace with the displacement along the scarp. Two toe bulges developed, one along the northern perimeter in the center of the slide, and one along the western perimeter. The one in the center appeared on July 1, 1986 (Figure 4.32), and had extended in length by July 6 and then by July 10, 1986. The bulge along the western perimeter developed on August 3, 1986 (Figure 4.33), and had extended in both length and depth by August 2, 1987 (Figures 4.34). Although slight changes were evident after their initial appearance, in contrast to those of the scarp area, these changes were negligible. This is particularly true for the toe bulge in the center of the slide.

The four extensometers along the backscarp of Sr^2 (Figure 4.24) provided information in terms of movement of the mass. The cumulative change in length from July 8, 1986 to June 19, 1987 was as follows:

- ET_1 - +0.27 m
- ET_2 - +0.12 m
- ET_3 - -0.02 m
- ET_4 - -0.22 m

These values are simply measurements of movement and do not separate the vertical and horizontal components. After the initial measurements, the distance between the posts of the first two extensometers increased while the distance of the last two decreased. Thus, the eastern portion of the slide is moving away from the scarp while the western portion is rotating back into it. This suggests that general movement is to the west, confirming the observation made earlier.

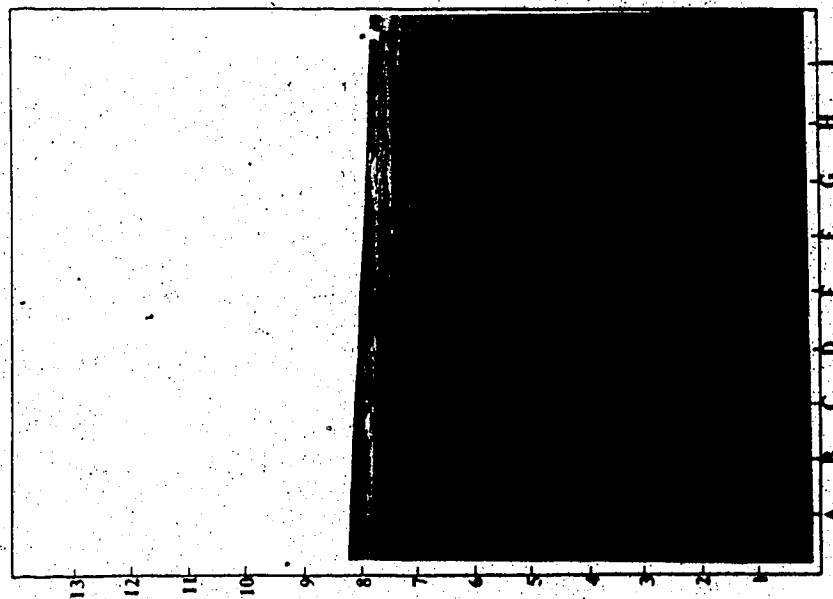


Figure 4.30 Scarp (mid July, 1986) of Sr^2 - looking east.
S. O'Hara for scale.

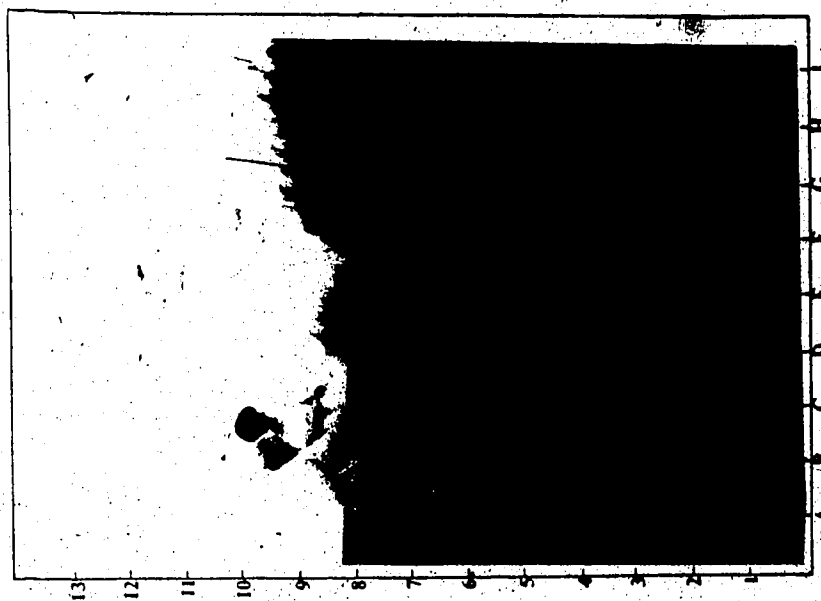


Figure 4.31 Scarp (August 2, 1987) of Sr^2 - looking east.
Kyla (E7) is at the same block evident in Figure 4.30 (H2).

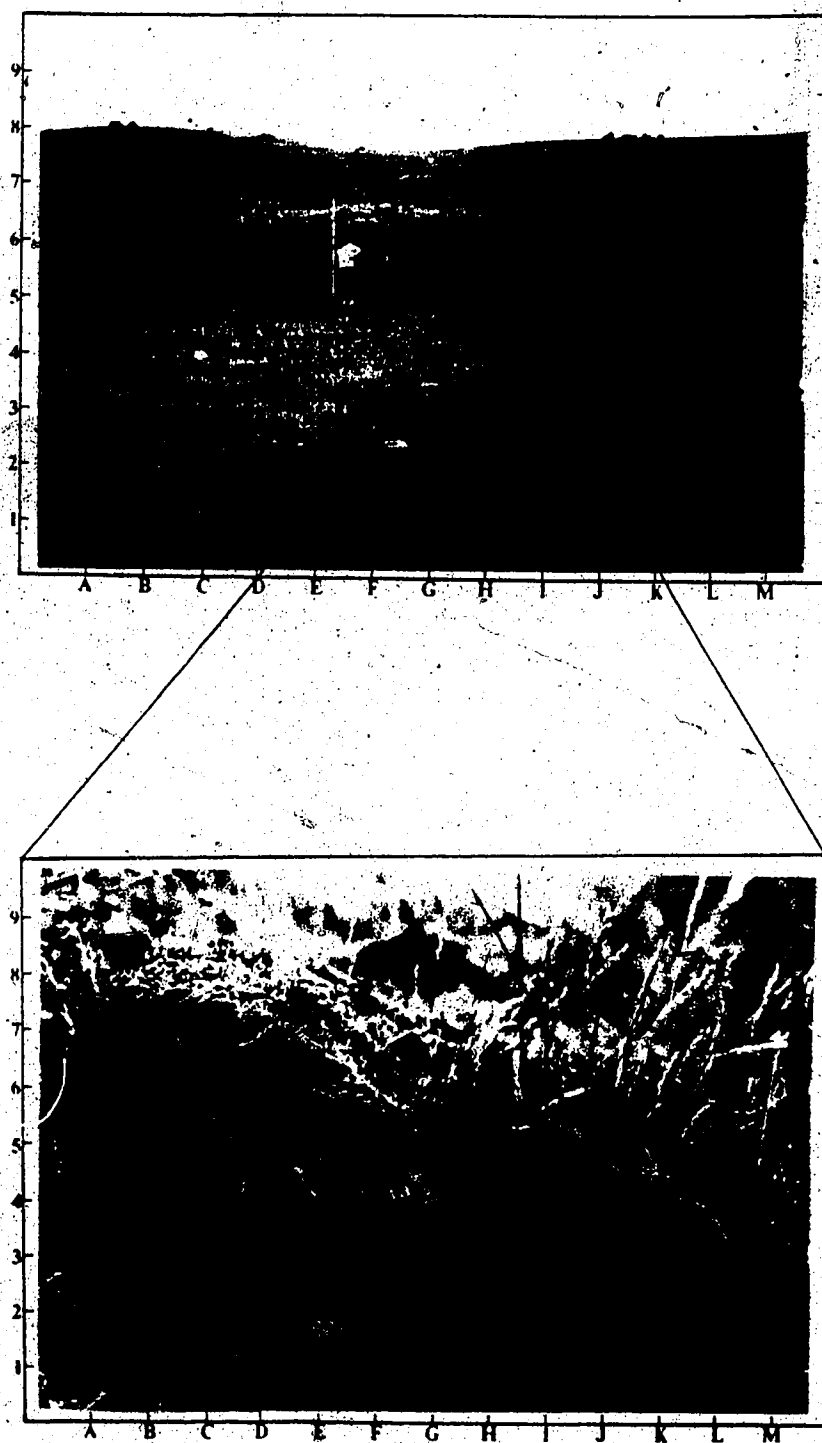


Figure 4.32 Centre toe bulge (July 1, 1986) of Sr^2 - looking south. For actual location see Figure 4.15 (H3).

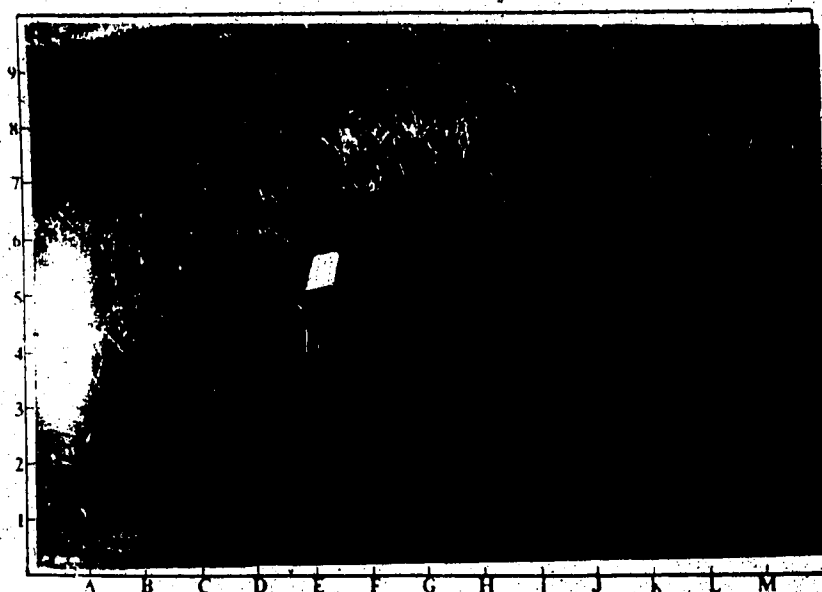


Figure 4.33 Western toe bulge (August 3, 1986) of Sr² - looking northeast. For actual location see Figure 4.15 (K5).

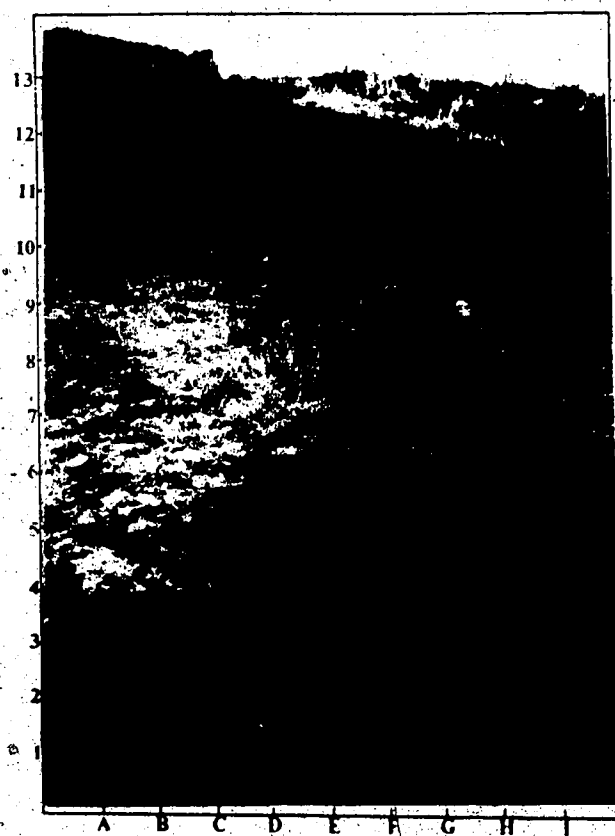


Figure 4.34 Western toe bulge (August 2, 1987) of Sr² - Looking southeast.

The crack depths measured at each of the extensometer locations also varied through time. Initially, these depths increased but as movement slowed, blocks collapsed and infilling occurred, crack depth decreased. The following values are the greatest depths attained before infilling took place:

- ET₁ - 3.50 m (July 8, 1986)
- ET₂ - 6.60 m (July 8, 1986)
- ET₃ - 5.25 m (August 21, 1986)
- ET₄ - 0.44 m (August 4, 1986)

Lateral displacement was initially greater on the eastern portion of the slide. However, by August, 1986, vertical movement was more apparent on the western side. The transfer of movement from the eastern to the western part of the slide also corresponds with the later development of the toe bulge along the western flank.

4.2.3 Geology

Because of the thin regolith and lack of vegetation, bedrock is often exposed. Undisturbed bedrock sequences, depicted in Figures 4.35 and 4.36, were obtained from slopes adjacent to the actual failure. Where possible (if bedding was evident), lithological contacts were also identified on the displaced mass. The debris was designated as either intact or disaggregated, depending on the extent of deformation.

The geological profiles show that although all of the failures involved till and a sequence of shales and sandstones, there is a wide range in the depth and order of each unit and there appeared to be no preferential failure unit. However, virtually all of the mass movements were topped with till (and in places with other glacial sediments) and were then immediately followed by a shale layer. With the exception of two failures (Sc1 and Sc3), sandstone was generally the unit at the base of the slope. Outside these nine studies, however, there were several cases in which the failure interface was between the till unit and the underlying bedrock (Figure 4.37). In these cases, the underlying bedrock unit remained intact while the overlying till slumped over it.

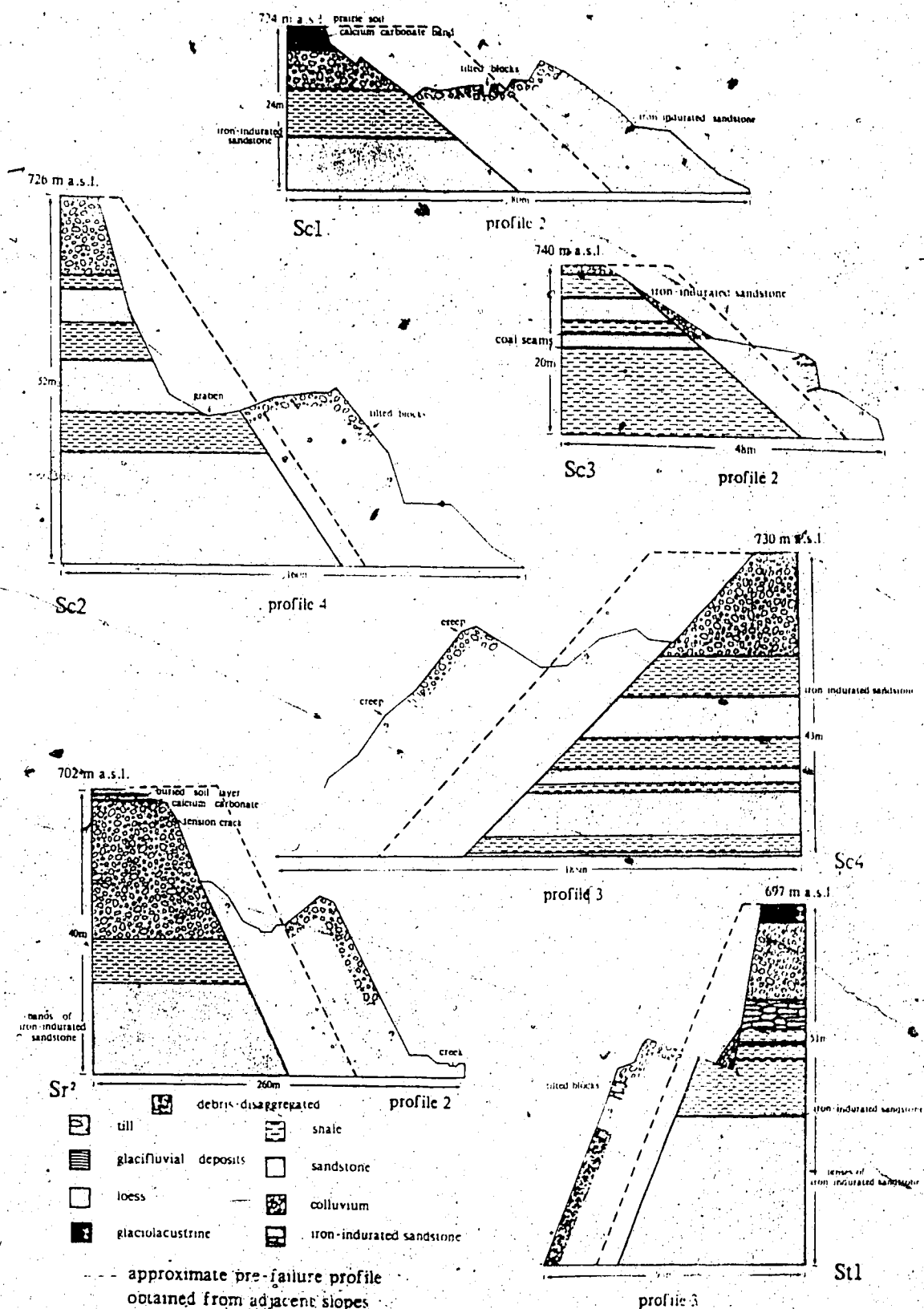


Figure 4.35 Lithological sequence of slide failures

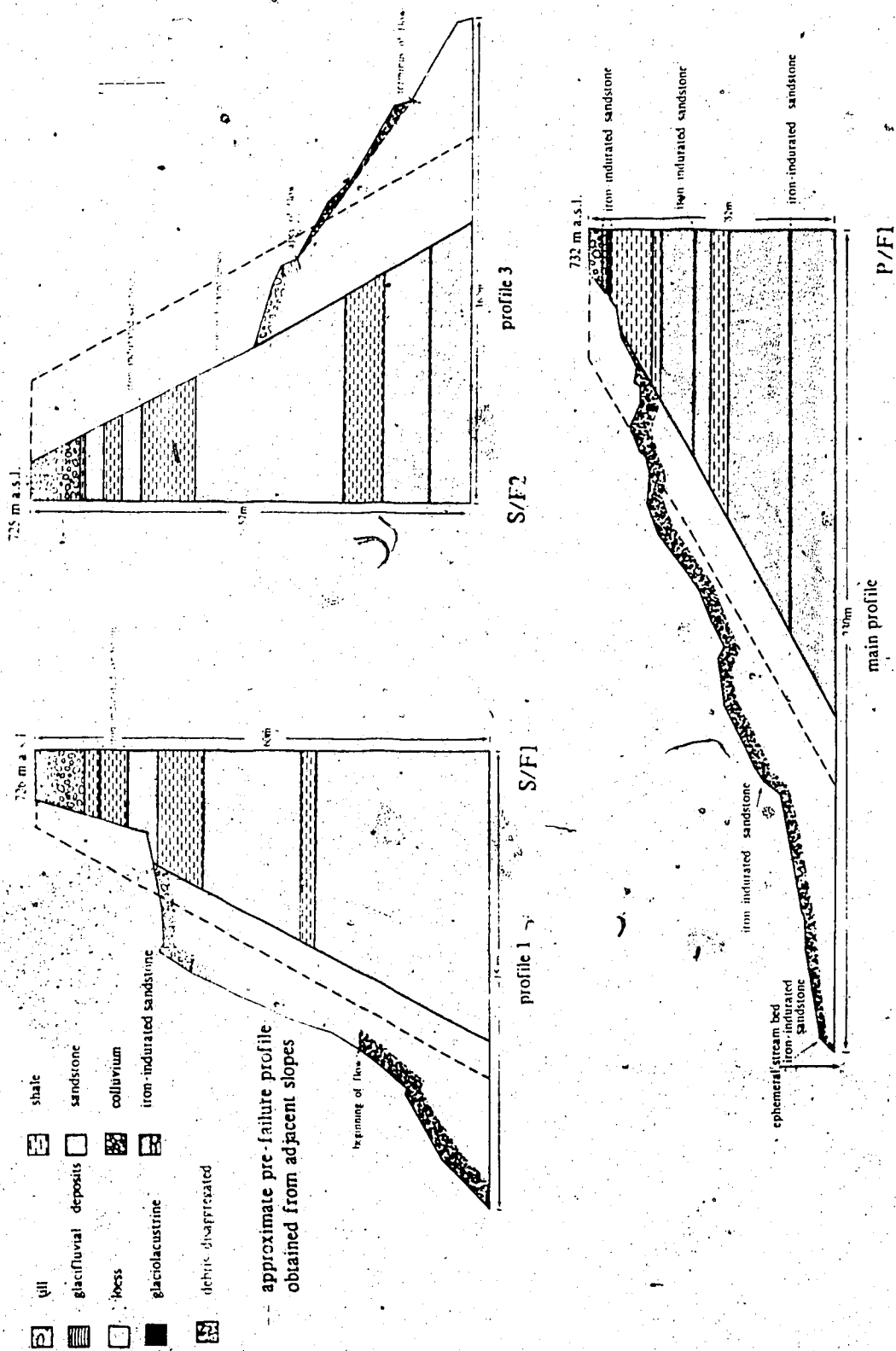


Figure 4.36 Lithological sequence of complex failures

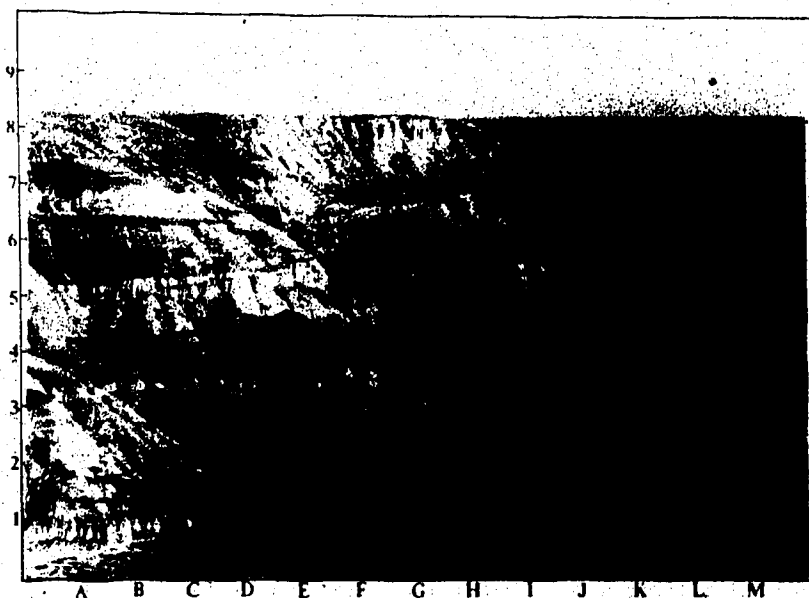


Figure 4.37 Till failure (G7) along Irishman's Coulee - looking southeast. Note the intact bedrock below the failure(I5)

Vegetation type and distribution did not vary significantly between the nine failures. Grasses dominated the vegetation cover, but most have some shrubs and sagebrush, although only two (Sc4 and Sr¹) had trees present. In both of these cases the trees were concentrated in depressions, generally at the head of the failure. These depressions are likely to be wetter and possibly held ponded water.

Specific hydrological details varied from failure to failure. The larger and more noteworthy of these have been included on the contour maps (Figures 4.21 to 4.29). In general, effects of surface flow were evident on all of the failures. On the reactivated slide (Sr¹), after one particularly severe storm in July, transported debris (grass and twigs) was in some places trapped 2-3 cm above the ground surface, providing some indication of the depth of runoff.

Seeps (or springs) were evident in two of the nine failures. The seep of S/F1 was located about 15 m north of the actual failure (Figure 4.38) at the base of the slope, with no evidence of its source. The second seepage area was along the south toe of S/F2 (Figure 4.39); again no source area was identified. Piping channels were noted above the wet area, but did not appear to be connected with the seep.

Wet ground was noted at the toe of Sc1 and St1. A pond at the base of Sc1 (Figure 4.12) had no apparent inflow or outflow. This pond was not in existence before the failure, and was therefore probably created by the damming of irrigation water. As early as 1949 irrigation water was channeled into the valley, immediately to the west of the slide. Standing water was also evident at the base of St1. No channel was evident, so the presence of this water is likely a result of a seep or spring. From the aerial photographs, an interesting configuration of the vegetation above the scarp became apparent (Figure 4.40). In 1949 there appeared to be a seepage area (denser vegetation) immediately above the scarp face. The vegetation ring that was evident then is also currently visible. There is a distinct change in vegetation within the ring itself which is dominated by dense prairie lichen, instead of the prairie grass evident inside and outside the ring. There is a subtle depression within the ring (the ring margin was somewhat elevated). The centre of the depression seemed to be broadly channelized and oriented in the

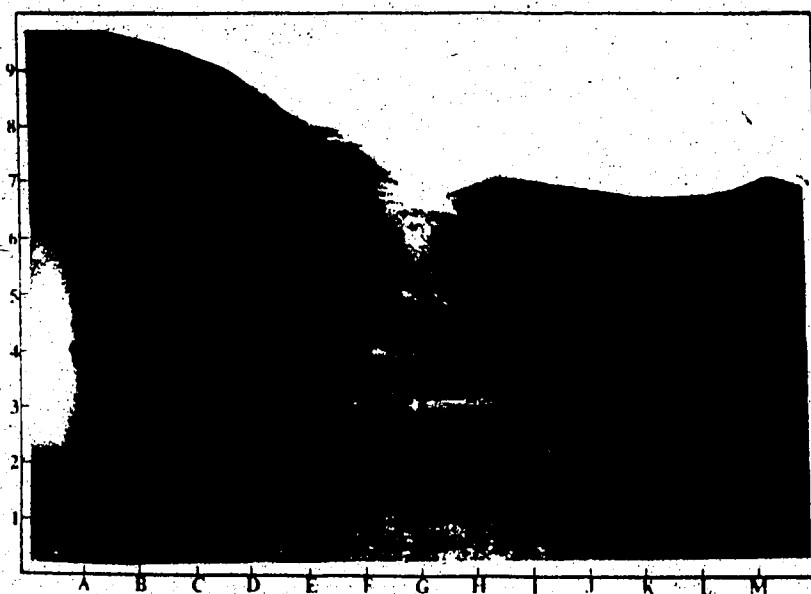


Figure 4.38 Seepage area north of S/F1 (D3), outlined by the denser vegetation.

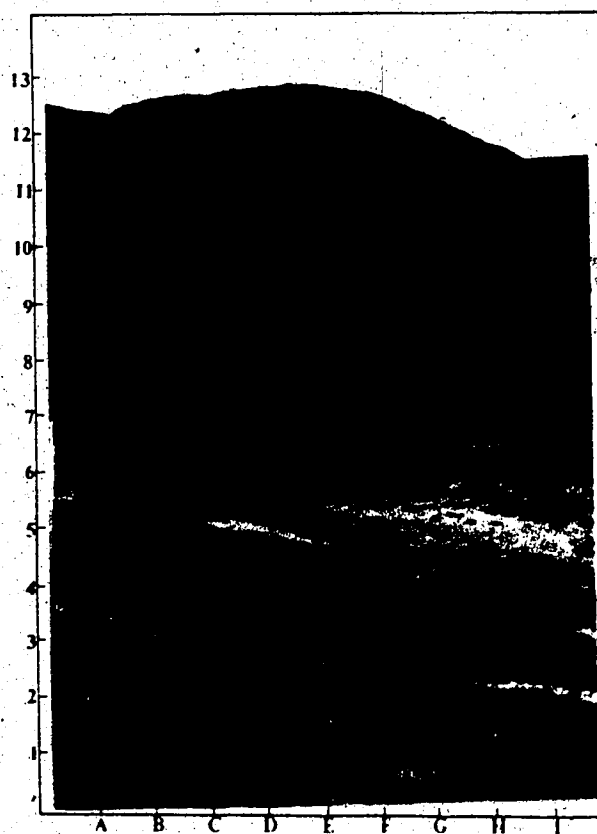


Figure 4.39 Seepage area at south toe of S/F2 (D7). For location, see Figure 4.18 (E4)

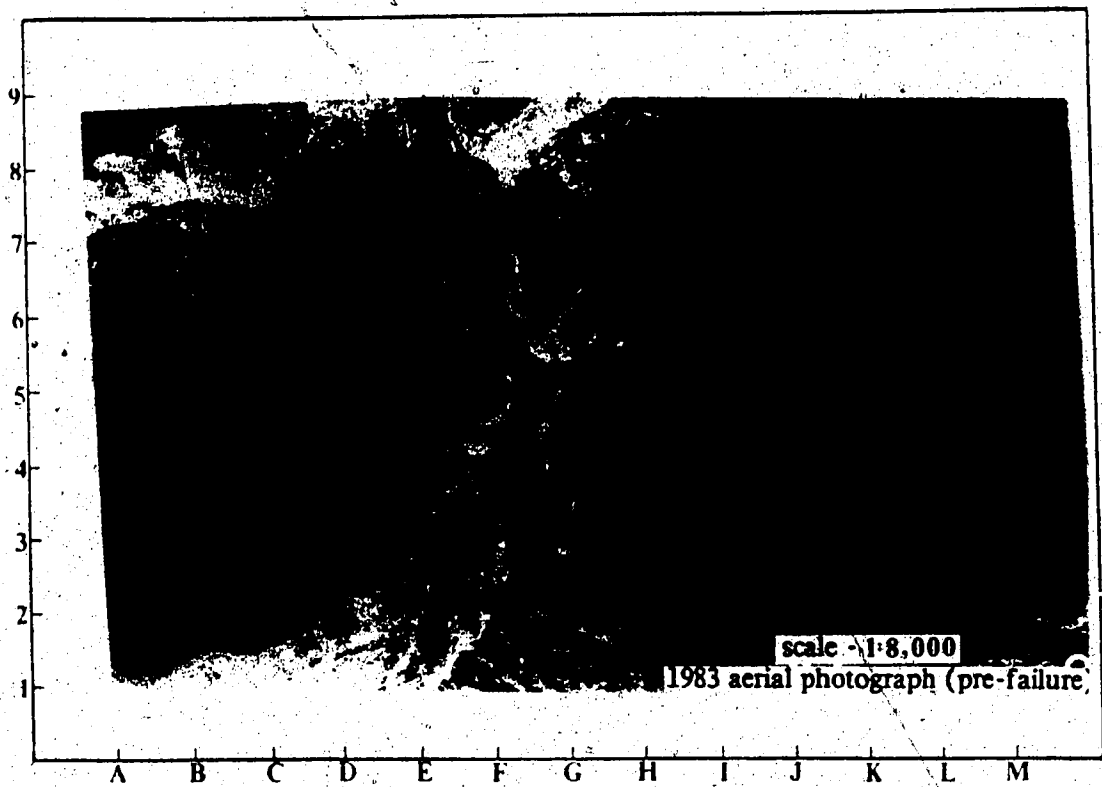


Figure 4.40 Visible ring above St1 (H-J, 4-7). The vegetation inside and outside the ring is typical prairie grass while the ring itself is largely prairie lichen.

direction of the mid-scarp dip (Figure 4.17). It is possible that before 1949 the area was a pond.

In the nine case studies, water appears to have had a major role, and a recent failure (November, 1987) was clearly influenced by water. A portion of a much larger and older failure was reactivated, producing the small debris slide (Figure 4.41). The presence of ice on the sheared surface in November and ponded water (ice) within the debris indicates that water was a key factor in this failure (Figure 4.42). Well above the actual failure a dry depression was evident, possibly representing the source area for the water.

Bedding is generally horizontal. A raised rim is, however, apparent along the prairie perimeter (Figure 4.43) possibly showing valley rebound (Matheson and Thomson, 1973). The raised valley rim did not appear to be associated with the nine mass movements, which generally occurred along coulee walls. The raised rim is most pronounced along the prairie perimeter where extensive badland development has occurred.

The mass structure of the slope failures varied with the type of failure, and was revealed mostly through the test pits. In general, the failed debris is classified as either intact or disaggregated, or in some cases as a combination of the two. If the material failed as a relatively intact unit or units, it is classified as intact debris. This is the case with at least a part of all the failures, with the exception of P/F1, which is completely disaggregated. The two slide/flow combinations have both intact and disaggregated debris, as do St1 and Sc1.

Sc1

Three pits were excavated at Sc1, one along the toe (A), one through the base of a recent dry flow (B), and one along the base of the scarp (C) (Figure 4.20). Pit A was dug to depth of 1.65 m. The fluvial sands and gravels at the base of the pit were overlain by a thin buried soil and vegetation layer (Figure 4.44) indicative of either channel cessation or migration. Overlying the buried soil layer is the failure debris with visible rip-up structures incorporated. These rip-up structures are soil and vegetation from the underlying layer that

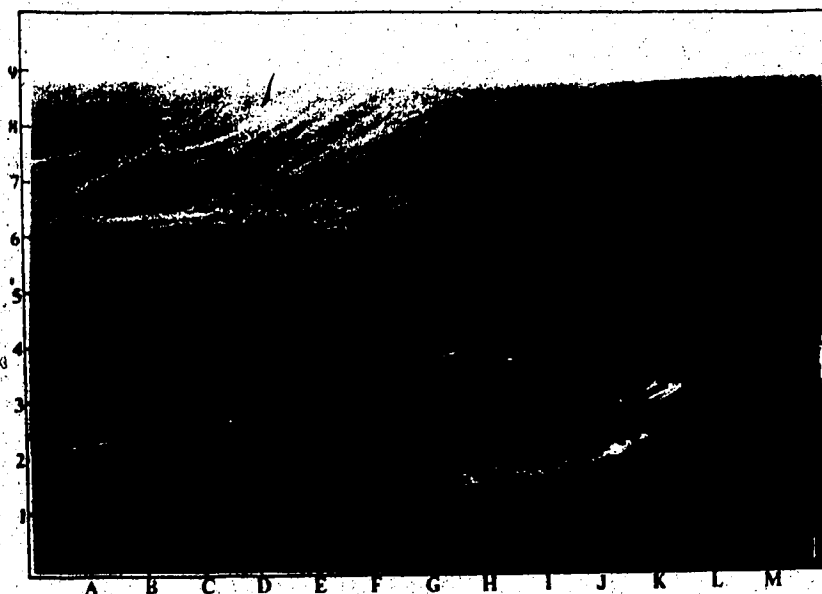


Figure 4.41 Debris slide (I4)(Nov., 1987) along Little Sandhill Coulee. Note the larger and older failure beyond (D5).

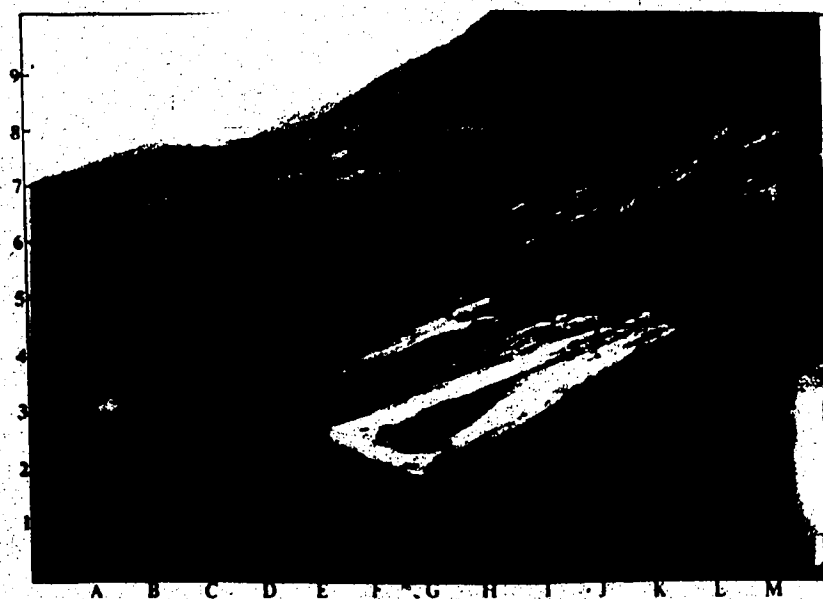


Figure 4.42 Water (on sheared surface and in debris) indicated large amount present during failure. P.Nielsen for scale (L9).

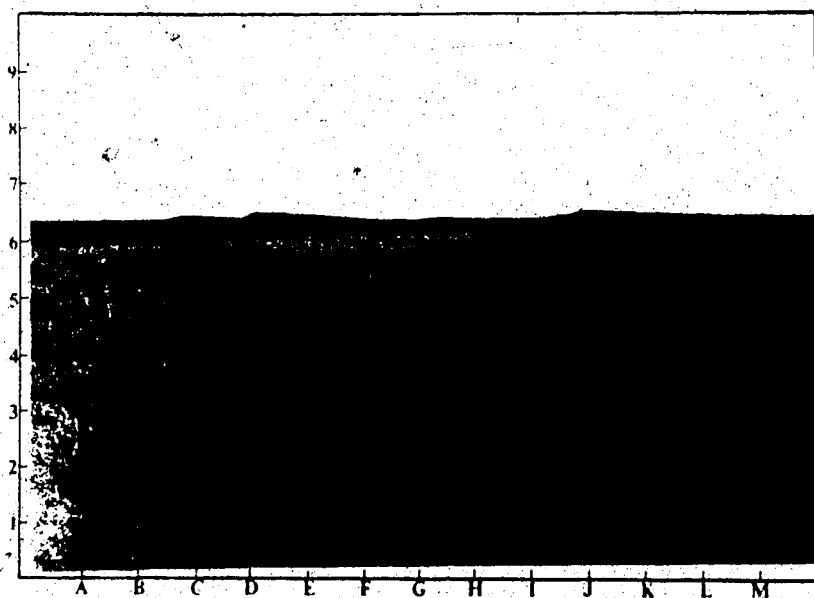


Figure 4.43 Raised prairie perimeter (E6) due to valley rebound (Matheson and Thomson, 1973) is most evident where extensive badland development has occurred

have been dislodged and transported. The debris at this location is somewhat disaggregated with broken sandstone pieces in a matrix of sand and clay-sized particles.

The second pit excavated, Pit B, was 1.3 m in depth. Again, soil was evident above the fluvial material, and below the slide debris. This is the area in which recent flowing of the slide debris has buried the original failed mass. The flow debris (sandstone and shale) is completely disaggregated. Sufficient time has elapsed between the two events to permit the growth of grass. The buried vegetation indicates that flowing has occurred relatively recently, as some of the buried twigs still have a green core.

The third pit, Pit C, identified the crack that extended downward from the exposed scarp. This crack continued at depth and was inclined similarly to that of the scarp.

Sc1 is an excellent example of a compound slide with a dominant rotational component as seen by the tilted blocks at the foot (Figure 4.45) and head of the failure, and by the concentric nature of the scarp and mass cracks. The translational component is evident from the graben structure at the head of the failure (Figure 4.46). This failure has a low-curvature surface of rupture. Stepped blocks and remnant pinnacles mark the graben area. The distortion of the debris at the toe (Figure 4.47) is possibly indicative of a transitory stage between slide and flow.

Sc2

Three pits were excavated at Sc2 along the base of the slide (Figure 4.21). Additional sections were examined along the gully walls where erosion has cut into the failed mass. Pit A, in the centre of the slide, was only excavated to 0.9 m because of the nature of the debris, a mass of indurated sandstone, clay, and ironstone nodules. The heterogeneous composition indicates that during failure this portion of the slide was subjected to internal turbulence. Pit A showed the slide debris was overlain by 0.61 m of fluvial sands. This observation was confirmed by a cutbank section (Section 1) exposed just east of the pit. Here the slide debris is overlain by 0.65 m of fluvial deposits (Figure 4.48). The debris extends downward for 1.0 m and overlies

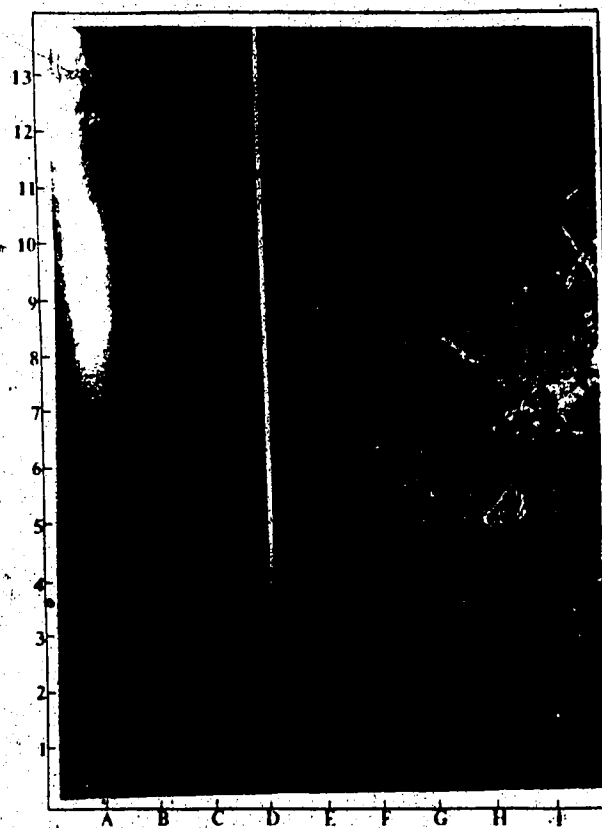


Figure 4.44 Pit A at Scl - 0.71 m of slide debris overlying the buried soil and vegetation layer (at knife - D9). Kyla at base for scale.

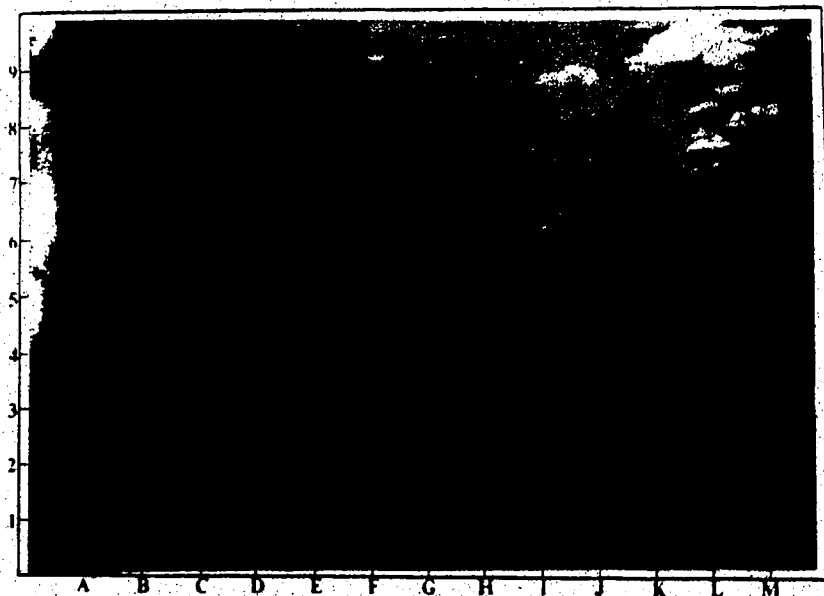


Figure 4.45 Tilted blocks at the west foot area of Scl.



Figure 4.46 Graben at the head of Scl and associated remnant blocks and pinnacles.

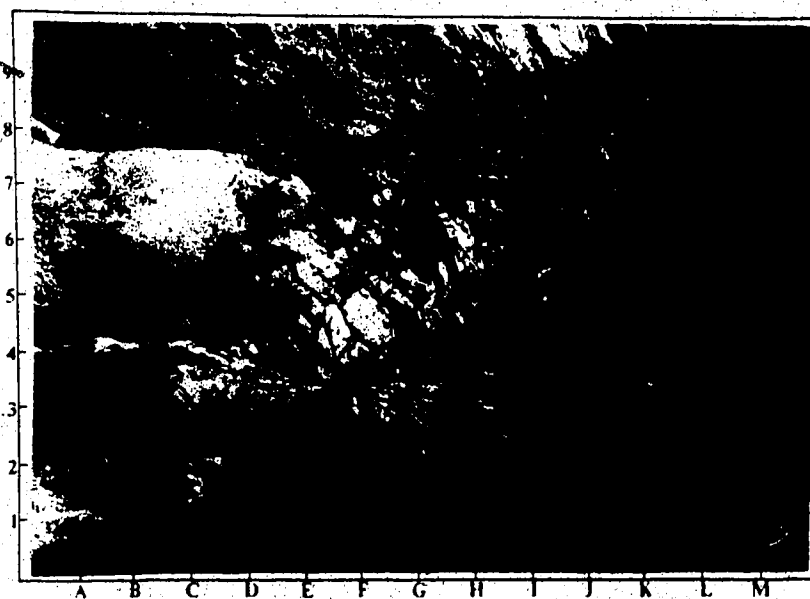


Figure 4.47 Distortion of debris at the toe of Sc1. Note also the water in the foreground. P. Nielsen at Pit A for scale (K3).

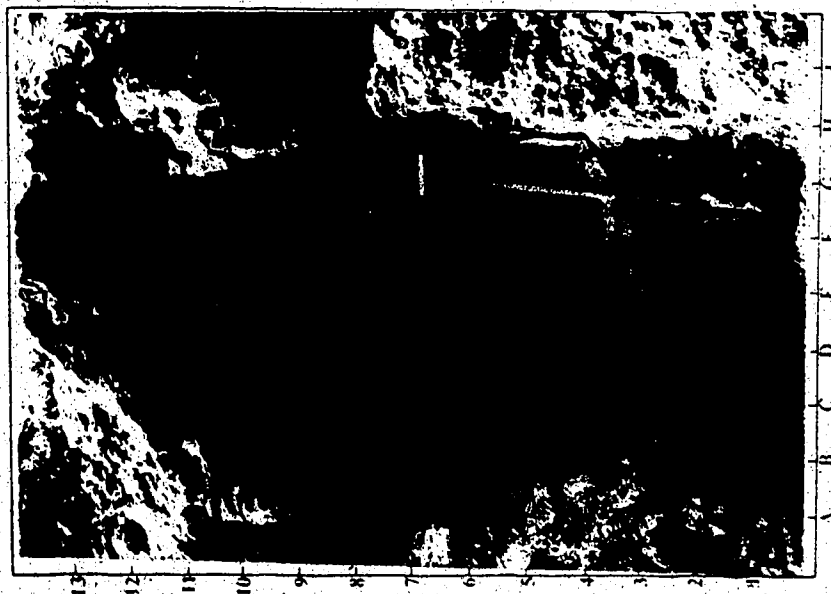


Figure 4.48 Section 1 at Sc2 - 0.65 m of weathered fluvial sands overlies 1.0 m of slide debris (F12).

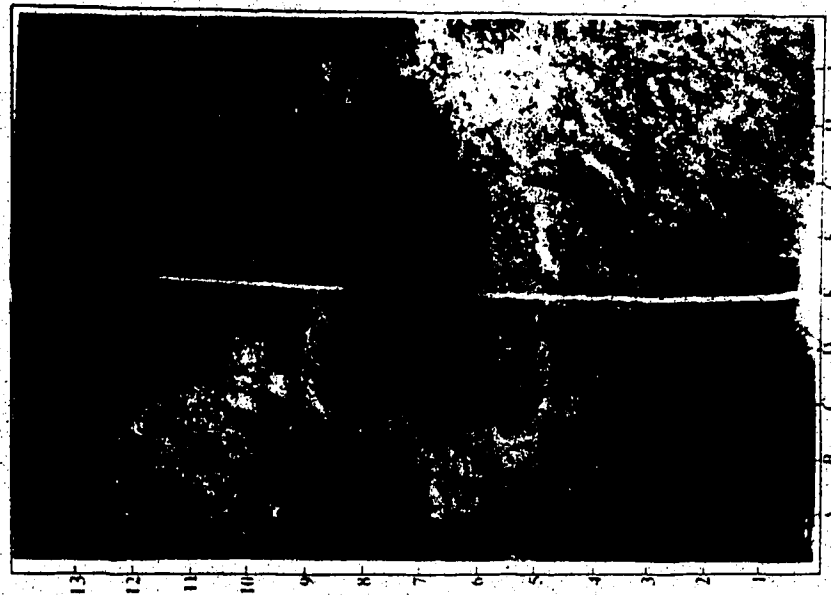


Figure 4.49 Section 2 at Sc2. 0.59 m of debris has buried a 0.21 m soil layer (E6). The underlying material is fluvially derived.

other fluvial deposits. At a cutbank further north, however (Section 2), there was no fluvial deposition evident on the slide debris. Instead, there was a buried soil and vegetation layer (Figure 4.49). The absence of a second fluvial unit and the development of a soil profile below the slide debris indicate that the north part of this failure occurred at a later date than did the southern part. The absence of the overlying fluvial deposits is confirmed by the test pits B and C, which are also located further north. A separation layer at a depth of 0.36 m, and running parallel to the surface, shows the possible creeping of the surficial weathered material over the debris mass (Figure 4.50).

Sc3

Two test pits were excavated at Sc3 (Figure 4.22). The sandstone part of the failure debris has remained as a coherent mass, while the large shale unit at the base of the slope has become disaggregated. Because of the depth of this disaggregation (greater than 0.85 m), it is likely that the material largely became distorted during failure. From the tilted bedding at the toe of the failure (Figure 4.13), the rotational component is evident. The distinct lithological units beyond the slide and within the failed mass clearly show the amount of displacement.

Sc4

Three pits were excavated at Sc4, two along the toe of the slide (A and B to determine the extent of the failure) and one within the slide mass along a gully (C) (Figure 4.23). At site A the slide mass terminated at the upper pit location (a), while at site B the debris extended into the lower pit location (b). The debris exposed in both pits A and B was sandstone blocks (gravel to boulder size) in a distorted matrix of fragmented shale and sands. A 0.17 m thick soil has developed on the failed debris at site A. Pit C, excavated within the slide mass, showed that the till and overlying materials were intact, indicating that this portion moved as a unit. In this area soil is forming on a 0.2 m layer of loess which buried the original soil. This buried profile is underlain by till. Because of the more distorted nature of the debris at the foot of the failure

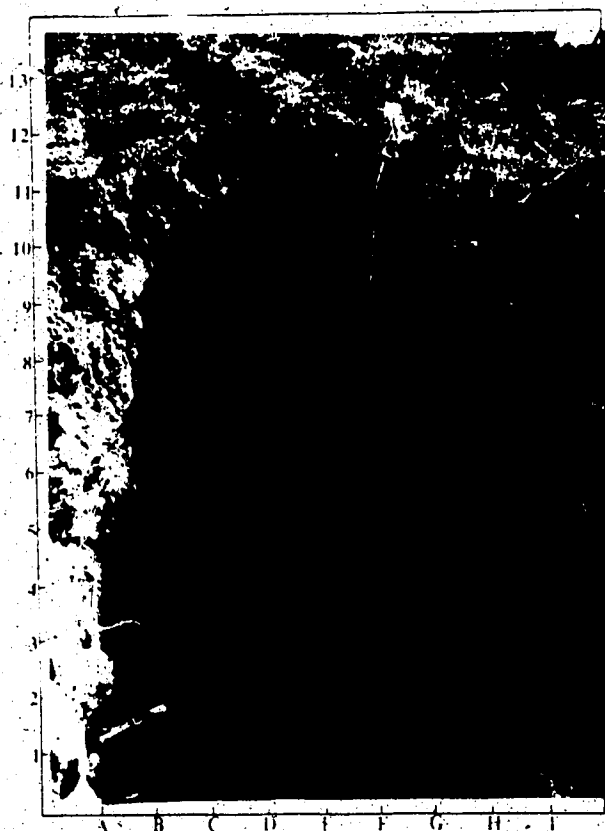


Figure 4.50 Pit C at Sc2 - evidence of creep of weathered debris as seen by separation layer (C10-F10) running parallel to the surface at a depth of 0.36 m. Knife at debris/fluvial contact (E5).

the distinct loess layer is not evident. Consequently, the soil development at pits A and B has taken place since failure, which occurred subsequent to the aeolian depositional period which is believed to be c.5,400 B.P. (Bryan *et al.*, 1987).

Sr²

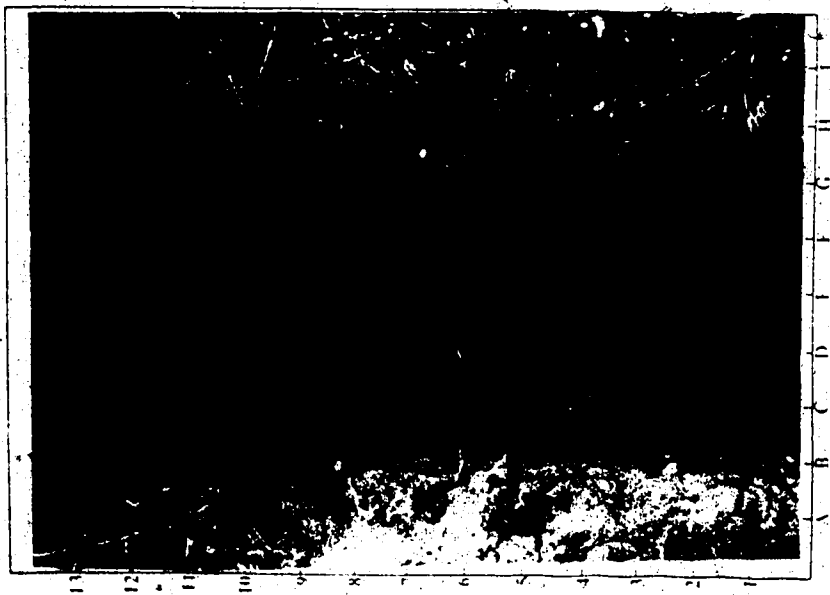
At the reactivated slide (Sr²) three pits were excavated, one along the current toe (A), one through the toe bulge (B), and one thought to be along the former toe (C) (Figure 4.24). Pit A revealed a possible failure zone (Figure 4.51). At a depth of 1.45 m, a 0.15 m thick deposit consisted of very friable and fragmented material. The material seemed similar to the till units above and below, which in comparison were much harder and more competent. Overlying the upper till layer is a 0.65 m-thick soil profile.

In order to verify the location of the failure plane, and to monitor any movement, four vertical lines of nails were placed through the possible failure plane (Figure 4.51). The three walls (north, east, and south) of the pit were staked so that movement in any direction would be detected. On August 2, 1987, one year after the installation of the nails, there had been no apparent movement.

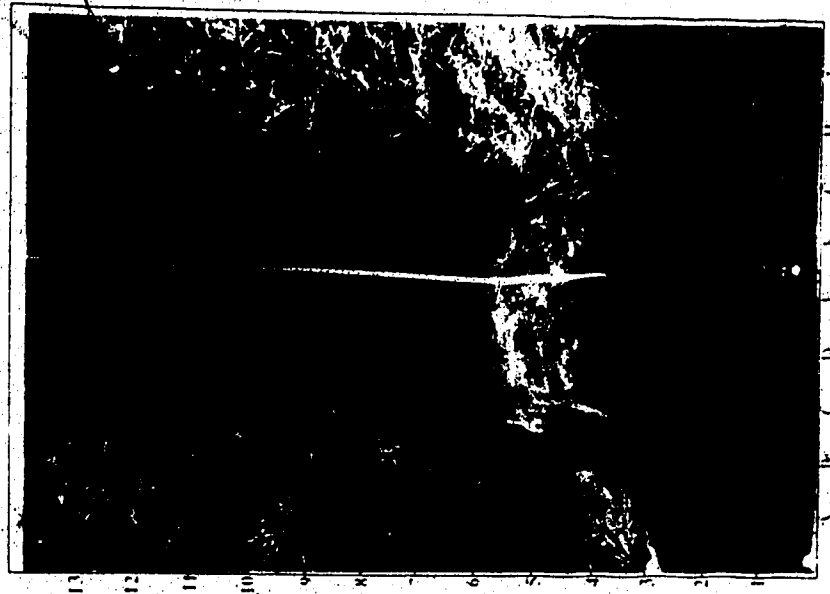
Pit B, through the toe at the centre of the slide, revealed a thin, friable layer of loose material at a depth of 0.25 m (Figure 4.51). This thin layer dipped slightly downward (approximately 4°) into the failed mass. Again, the till at this location, both above and below this sheared surface, was hard and consolidated. The third pit (C), proved to be beyond the slide mass as it was comprised entirely of fluvial material.

St1

At the translational slide, St1, three test pits were excavated, two at the toe of the failure (A and C) and one above the toe, in the slide mass (B) (Figure 4.25). At the interface between the slide debris and the channel deposits of pit A green grass was uncovered (Figure 4.52). This grass was at a depth of 1.3 m and was 0.6 m back from the debris front. The



Pit A - possible failure plane (D7)



Pit B - possible failure plane (knife - F11)

Figure 4.51 Pits A and B at Sr² - possible failure plane. The material in this zone is more loose and friable than the surrounding till. The vertical lines (B7, D8, G5, and G2) are stacked through this zone.

surface debris was largely homogeneous shale with some ironstone inclusions. The shale had been reworked and was entirely fragmented. Immediately overlying the vegetation was a thin (0.03 m) layer of very wet clay. This firm wet clay was also evident at pit B at a depth of 0.72 m. The surficial debris at this location also consisted of broken ironstone fragments in the disaggregated shale debris. With the information from these two test pits, and the surficial cracking evident (Figure 4.53), it appears as though the upper layer of weathered disaggregated shale is moving over the lower, stiffer clay layer. This conclusion is supported by the progressive burial of vegetation at the failure margin (Figure 4.54). Apart from a minor crack along the base of the scarp, there appears to be no corresponding displacement at the head of the slide area. Thus, the current movement in the toe area is surficial and localized.

Pit C along the north flank of S11 consisted of an upper and a lower part. The slide debris consists of both intact sandstone and ironstone blocks and disaggregated material. This debris extends downward for 0.84 m and overlies an alluvial deposit that also forms the upper portion (0.43 m) of the lower pit. The interface between the debris and alluvial units consists of organics and reworked shale, delineating the pre-failure surface (Figure 4.55).

S/F1

Two pits were excavated at the first complex failure, S/F1 (Figure 4.26). One pit (A) was located at the north toe of the flow and the other (B) at the base of the back scarp. Pit A was excavated to a depth of 1.45 m before the undisturbed fluvial base was encountered. Above this contact at a depth of about 1.21 m, rip-up structures were evident. The flow debris is completely disaggregated, and consists primarily of shale with sandstone and ironstone fragments and glacial erratics scattered throughout.

In addition to the seepage area north of the failure (Figure 4.38), throughflow was evident from the presence of extensive pipes, especially along the northern perimeter. The flow morphology shows that relatively large intact blocks, which moved independently of one another, were transported in a more fluid medium. Because sagebrush is evident on virtually all

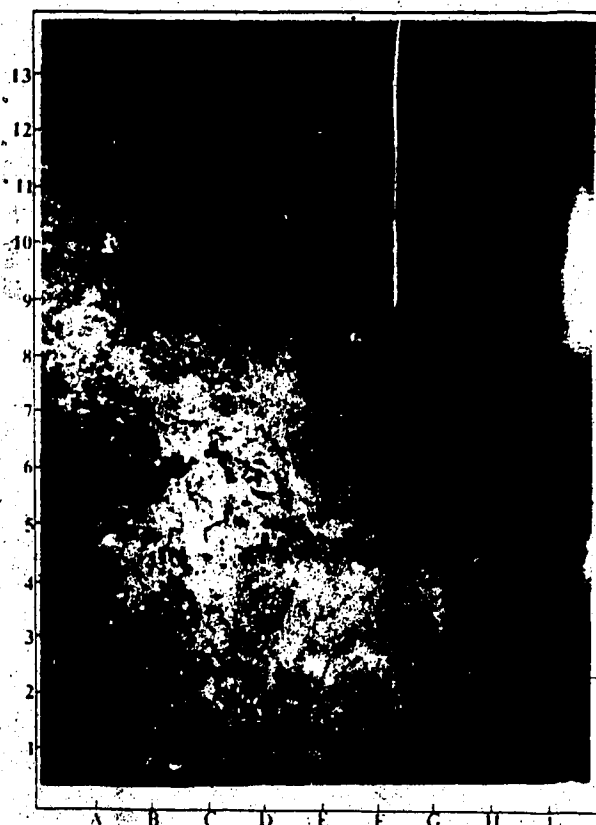


Figure 4.52 Buried grass at the base of St1 (knife - F5) at a depth of 1.3 m.

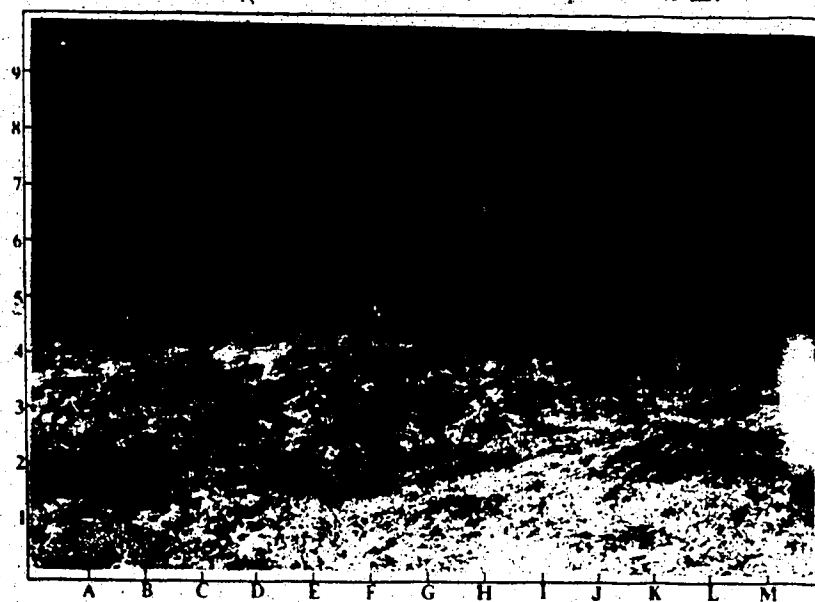


Figure 4.53 Surficial cracking at the foot of St1 running both perpendicular and parallel (toward the cottonwood tree) to the direction of movement.

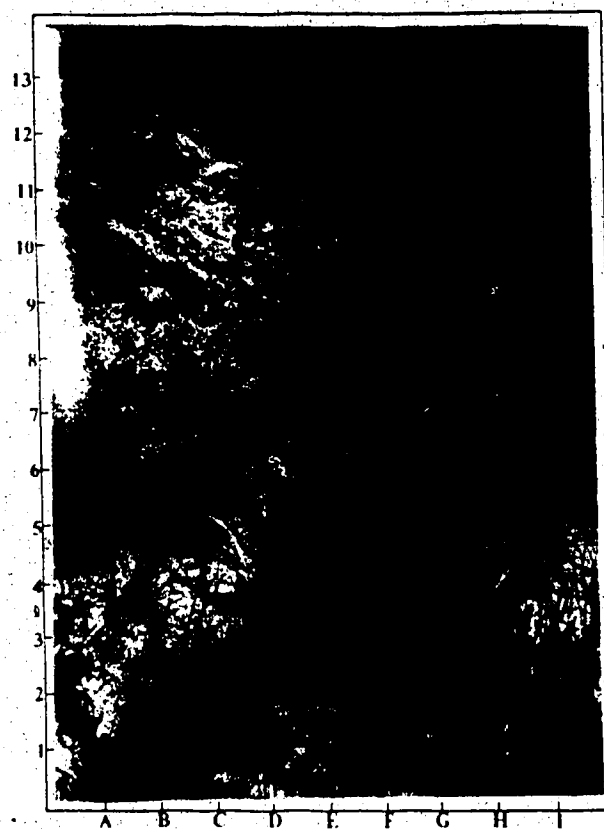


Figure 4.54 Progressive burial of vegetation at St1. Debris lobe overriding new growth (still green).

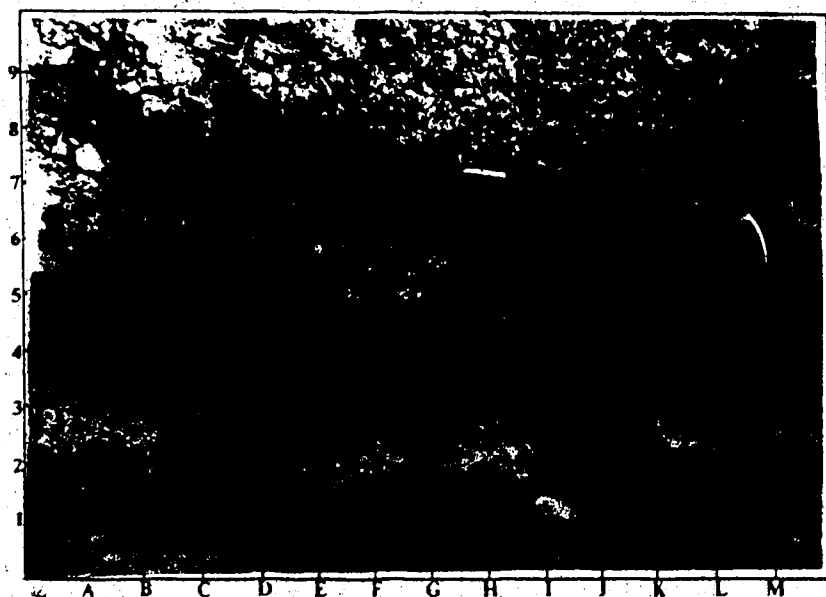


Figure 4.55 Organic interface between debris and alluvium delineating the pre-failure surface.

of these remnant blocks, vegetation established prior to failure partially helped to stabilize the debris.

S/F2

Two pits were excavated on the second slide/flow combination (S/F2) (Figure 4.27). Pit A was used to delineate the failure boundary. The failed mass did not extend to this point. Pit B was located on the centre lobe of the flow. A 0.40 m layer of reworked till covered 0.62 m of debris, which consisted primarily of shale with sandstone blocks and ironstone fragments incorporated. At the interface between the till unit and the underlying debris was a distinct organic layer. In addition to the roots and grasses, a shallow soil horizon (0.03 m) was evident (Figure 4.56). It is likely that the slide and flow components of this failure occurred successively in time. After the initial slide, sufficient time elapsed to permit the development of a shallow soil layer before the flow portion of the failure buried it.

The intact nature of the slide is made particularly evident by the distinct vegetation pattern at the contact between the displaced prairie surface and the failure debris (Figure 4.57). Tilted bedding at the base of the slide are inclined at an angle of 28°, contiguous with that of the displaced prairie surface, indicating that at least that portion of the failure moved as a unit

P/F1

Three pits were excavated at P/F1 (Figure 4.28). Pits A and C were located within the failure mass while Pit B was along the toe. The debris exposed at Pits A and C showed that the shale has been completely disaggregated (Figure 4.58). In both pits there were also some coal and ironstone pieces. Pit B, at the toe of the flow exposed the shale debris, and the underlying fluvial sands.

The slide and surrounding area were marked with many piping features. The east and west boundaries both had extensive, fused (connected) pipe networks (Figure 4.59). There are also several large piping channels within the failure mass. Along the eastern scarp there was an

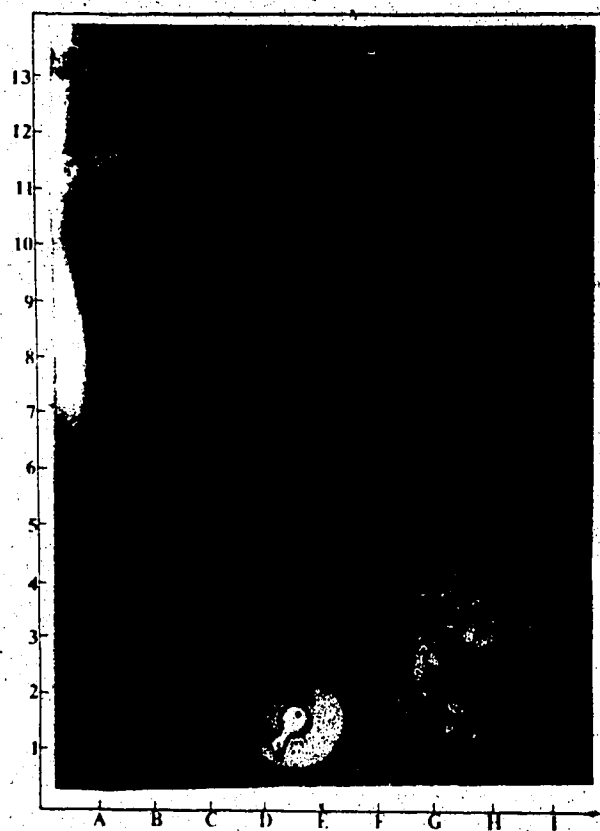


Figure 4.56 Soil and vegetation interface (knife - G8) at Pit B - S/F2, showing successive development of failure. Kyla in front of the earlier failure.

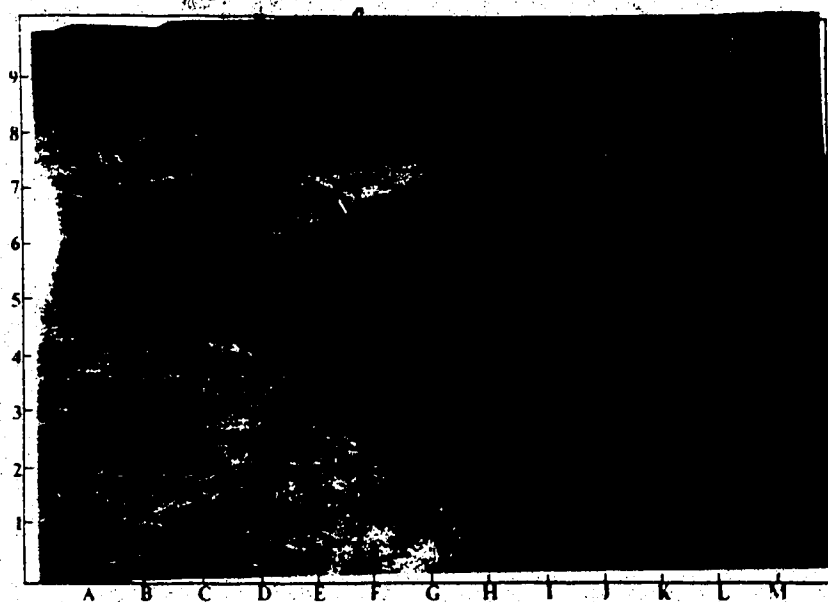


Figure 4.57 Change in vegetation showing the contact between displaced prairie surface and debris.

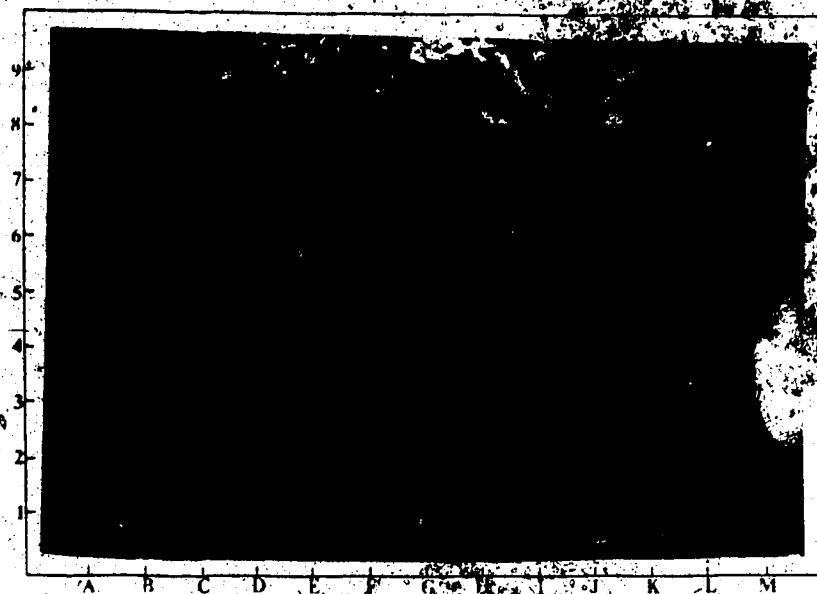


Figure 4.58 Fragmented shale debris exposed at points A and C - P/F1. Size of shards is approximately 3 cm (long axis).

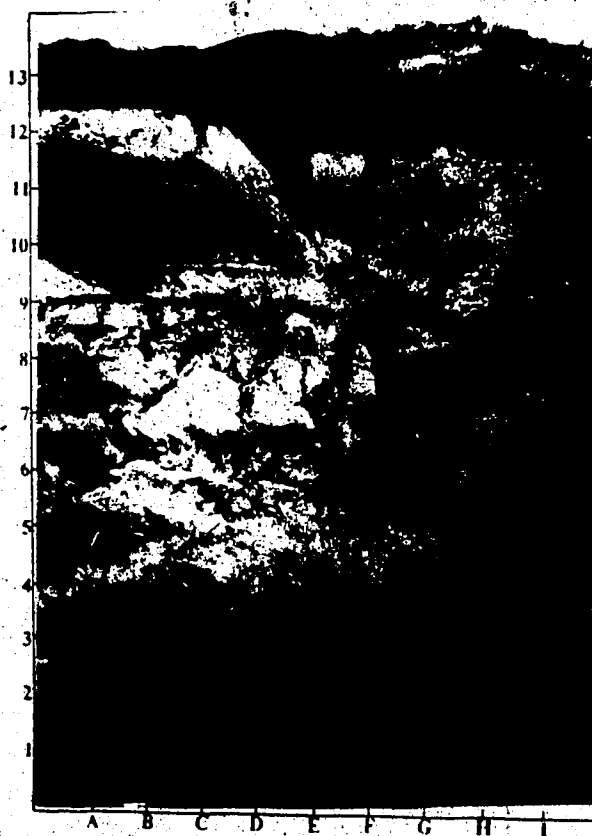


Figure 4.59 Pipes (F5,7) along east wall of failure, typical of extensive piping at P/F1.

additional piping channel with several tension cracks also evident.

Although at the two pit locations (A and C) the flow debris extended beyond 1.10 m, in places this debris was thin. The shale at the toe of the failure is evidently flowing over the more resistant underlying sandstone layer. Sloughing appears to be ongoing as weathering processes further decrease the remoulded strength of the shale debris.

In summary, through the analysis of these 9 failures several trends are apparent. The material involved and the nature of movement significantly affect the morphology of the failed mass. With an increase in shale and water content, the slope fails as a flow, producing disaggregated debris. Conversely, sandstone tends to fail as individual blocks and, depending on the degree of induration, remains relatively intact for some time.

Pipes were evident at or near seven of the nine failures, the exceptions being Sc4 and Sr². These channels act similarly to tension cracks and often occur in association with them. When located above the head of the failure or within the mass, pipes facilitate the entry of water, increasing stress - especially in the case of closed pipes.

4.2.4 Dating the nine mass movements

It was impossible to accurately date the nine failures. However, the morphology and vegetation cover, together with the aerial photographs, provided sufficient information to classify of failures as either new (within the last 10 years), intermediate (within the last 100 years), or old (within the last 10,000 years). Accordingly, the nine failures were classified as follows:

Table 4.5 - Relative age classification

New	Intermediate	Old
Sc1	Sc3	Sc2
Sr ² (reactivated)	S/F1	Sc4
St1	P/F1	Sr ² (original)
		S/F2

New failures had a minimal vegetation cover, no soil development, and distinct slope components with sharp angular breaks. The reactivated portion of Sr^2 began movement in the early summer of 1986. According to the air photographs and local information, $St1$ occurred between 1983 and 1985. The green vegetation uncovered at the base of the failure is indicative of continued surficial flowing since the initial failure. From photographic evidence, $Sc1$ is slightly older, forming between 1973 - 1977.

The intermediate failures, $Sc3$, $S/F1$, and $P/F1$, still have a distinct form. Their scarps are clearly defined and unvegetated. Grasses and small shrubs only have developed on the debris. These three failures occurred prior to 1949 (the year of the first aerial photographs). However, a light tone (lack of vegetation) suggests that the west end of $Sc3$ had experienced a recent flow (just prior to 1949). By 1949 piping was already well established on $P/F1$, indicating an even earlier date of occurrence.

The failures classified as old, ($Sc2$, $Sc4$, Sr^1 , and $S/F2$), have a well rounded form and are extensively vegetated. $Sc4$ and Sr^1 have well established shrubs and trees at the base of the backscarp. Because of the similarity in form, three of these failures (excluding $Sc2$) may have originally occurred at roughly the same time. $Sc2$ is more angular and less vegetated, suggesting a relatively more contemporary date of occurrence. Also, as indicated by the light tone on the 1968 air photographs, the south end of $Sc2$ appears to have been recently reactivated, possibly by stream erosion. Fluvial deposits were found above the debris at some locations in this slide. This further supports the idea that the river was at some time migrating laterally into the toe of the failed slope. $Sc4$ is the slide in which the loess layer at the head of the failure is not evident at the toe. Consequently, this failure must have occurred after aeolian deposition (c. 5,400 BP). The soil profile at the toe has developed since the failure, as has the soil profile on the loess layer at the head of the slide. Because the upper portion of the slide remained intact, the loess was moved as a unit, and was therefore preserved. The original failure of Sr^1 (prior to the current reactivation), is clearly old, and probably related to the extensive slumping evident along the entire western reach of Little Sandhill Creek (Figure 4.60). The main portion of $S/F2$

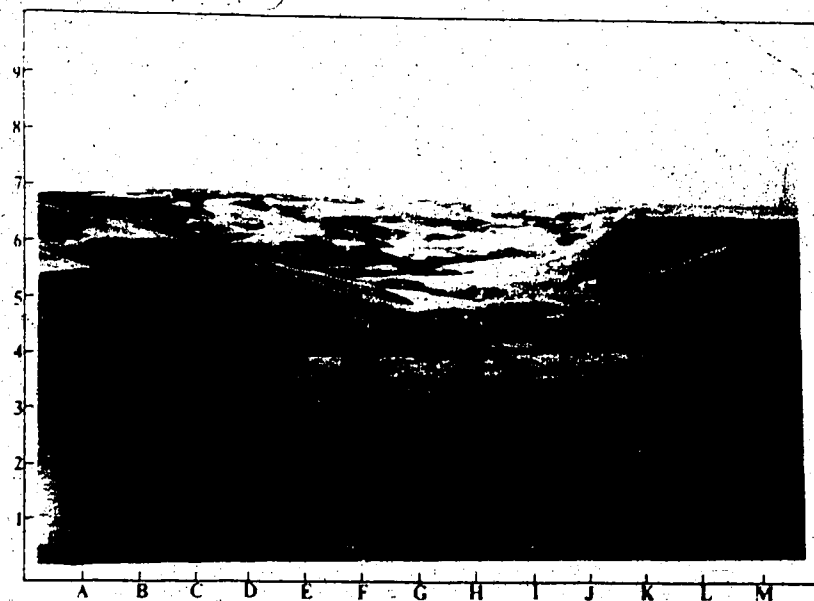


Figure 4.60 View westward along Little Sandhill Creek showing extensive failures, particularly along the south (north-facing) wall. Sr^2 (C6) is located at the beginning of this sequence of multiple failures.

is old but it is likely that the flow portion occurred at a later date, as evidenced by the buried soil layer.

Of the three wood samples subjected to ^{14}C dating, two were from Sc2, one from pit C and the other from the exposed gully section. These two samples (AECV # 401C, 402C) were found to be modern (1950 A.D.). Because flowing occurred in 1968 (according to the photographic evidence)* it seems likely the dated material was buried then, and not by the initial massive failure. The third wood sample taken from pit A at Sr², was ^{14}C dated at 130 ± 100 years B.P. (AECV # 400C). Accordingly, Sr² could have occurred at any time after 1756.

Precipitation records were used to more accurately date the two failures (Sc1 and St1) dated by the aerial photographs. The monthly precipitation in excess of the norm (based on the 30 year average) was recorded for the period between the two consecutive aerial photographs, prior to and when the failure was first identified. Consequently, data were collected from 1973 to 1977 for Sc1, and from 1983 to 1985 for St1. Sc1 probably occurred in the early summer months (May or June) of 1975. The February to June period of 1975 had a total of 17.20 cm greater than the norm, with the majority (9.83 cm) falling in May.

St1 probably occurred in April, 1985. The preceeding winter had a heavy accumulation of snow (181 percent of the norm), and April had rains 307 percent of the norm. The seasonal snowmelt in conjunction with the excessive precipitation would likely induce failure. Thus, assuming that increased slope activity can be directly correlated with excessive amounts of precipitation, Sc1 possibly occurred in the early summer of 1975 and St1 during the same season in 1985.

4.2.5 Laboratory analysis

Because in preparation for the Atterberg test the samples were oven dried, it was necessary to determine a correction factor in order to correlate the results with air dried data. From the dual preparation methods it was found that the liquid limit (LL) for the air dried

samples was, on an average, 4 percent higher than the corresponding oven dried sample. Peterson (1954) established the same relationship but found a much larger difference between the air and oven dried preparation methods (30 percent). He attributed the lower liquid limit with oven drying to the amount of organics in the sample. In most of the shale samples tested here, this trend was either negligible or reversed. The liquid limit of some shales (probably especially those rich in bentonite) increased when oven dried. If these samples are not incorporated in the calculation of the average difference, a somewhat higher value results. In this case, air dried non-shale samples have, on an average, a liquid limit value 13 percent higher than do the oven dried samples. Similarly, Peterson (1954) found that bentonitic shales were plastic enough to "overshadow" the effects of organics, and that the liquid limit did not decrease with oven drying.

There was minimal variation in the plastic limit of the samples as a result of the different preparation methods. This again corresponds to Peterson's (1954) analysis. He found that the plastic limit is less affected by the method of preparation. Nevertheless, because of the generally higher liquid limit values for air dried samples, the plasticity index tends also to be higher for the air dried samples, than for the oven dried samples. Based on this information, a correction factor of 13 percent was added to the non-shale samples only. In this manner, both oven and air dried values were determined, permitting comparison with analogous studies.

The materials tested fell under one of 4 broad categories - glacial lake sediments, till, sandstones, or shales. These groups were then broken into sub-classes based on their colour according to the Munsell colour system (Table 4.6). Table 4.7 is a compilation of the 55 test results (Appendix B). Because of the significant range of results for each sediment type, it was deemed necessary to present the entire spectrum.

In comparing these test results with those obtained by other researchers (Table 4.8), one primary and consistent difference becomes evident. In virtually all of the documented cases, both the liquid limit and the corresponding plasticity index are substantially higher. The exception is provided by the Hardy and Associates (1974) study of the Horseshoe Canyon

Table 4.6 - A local example of sediment sizes for different lithological units.

Material	Sediment Size %sand	%silt	%clay	Source
lake				Sr ²
till				Sr ² , Sc2
brown sandstone	59-60	25-30	3-16	Sc1, Sc2, Sc4
grey sandstone				Sc1, S/F2
dark shales	15-20	15	65-71	St1, P/F1
brown shales				Sc1, Sc3, Sc4, Sc5, Sr ² , S/F1
grey shales	14-18	24-46	40-57	Sc1, Sc2, Sc3, St1, S/F1, S/F2, P/F1
yellow shales	9-18	29-50	41-54	Sc4, St1

Note: These sediment size values are from Campbell (1987b) for a basin in the Dinosaur badlands. Because of the large variation with each material type, these values should be considered site-specific and only indicative of the possible sand, silt, and clay proportions.

Table 4.7 - Atterberg test results

Material	Natural water content(%)	Oven dried results(%)			Correction applied (13%)	
		LL	LP	IP	LL	IP
lake	2	23	20	3	26	6
till	3-9	27-36	13-18	9-23	31-41	5-24
brown sandstone	4-12	21-50	17-23	9-31	24-57	7-34
grey sandstone	4-11	25-69	13-21	12-48	28-78	15-57
dark shale	15-31	70-71	22-48	22-49	-	-
brown shale	3-18	27-69	16-34	7-35	-	-
grey shale	1-37	20-89	14-47	8-64	-	-
yellow shale	1-7	25-33	18-22	3-15	-	-

Table 4.8 - Atterberg values from analogous studies; determined for the fine grained, soft sedimentary Upper Cretaceous bedrock of Alberta.

Material	Nat. water content(%)	LL	LP	IP(%water)
lake	20-40	60-70	20-25	42
till	10-20	10-40	18-40	10-25
sandstone	4	25	24	1
siltstone	12-21	55-70		31-42
shale	10-45	40-220	18-45	24-92
bentonite	50-70	180-260	60	

Note: data from Thomson (1970,1071a,b), Hardy and Associates (1974), Thomson and Yacyshyn (1977), Thomson and Tweedie (1978), Thomson and Morgenstern (1979).

Formation. In this case, the liquid limit and plasticity index values are comparable. In contrast, it is worth noting that the plastic limit (versus the liquid limit) is, generally, more consistently similar to those values obtained by other authors. The application of the correction factor raises the liquid limit and plasticity index somewhat, but not substantially so. This suggests that the preparation method used for these samples does not necessarily have a significant affect on the final plasticity values.

The strength parameters varied significantly, not only between different lithological units but also within the same unit type. Table 4.9 is a summation of these values as a range of the data presented by the various authors. Although sandstone is not categorically referenced, its strength parameters would likely be comparable to those of siltstone. It is evident that bentonite is the weakest of the bedrock units. Therefore, as the bentonite content increases as an admixture to the sandstone and shale units, both strength parameters (C' and θ') would be reduced. Of the residual parameters, cohesion is the most drastically reduced. From the analogous studies, it seems that in most cases the residual value of cohesion is nil, so that the residual strength is based entirely on the residual internal angle of friction. As well as a decrease in strength with the presence of bentonite, apparently as sediment size decreases, there is a corresponding decrease in material strength, confirming the importance of the depositional history of a sediment.

Table 4.9 - Strength values from analogous studies; determined for the fine grained, soft sedimentary Upper Cretaceous bedrock of Alberta.

Material	Peak C'(kN/m ²)	θ' (°)	Residual Cr(kN/m ²)	θ_r (°)
lake	0-19	24-35	-	-
till	5-35	24-27	0	12-23
siltstone	140-420	20-40	70-385	20-25
shale	38-65	14-25	0	8-17
bentonite	38-42	14	0	5-10

Note: data from Thomson (1970, 1971a,b), Hardy and Associates (1974), Thomson and Yacyshyn (1977), and Thomson and Morgenstern (1979).

5. Discussion and Conclusions

5.1 Discussion

Several relationships between slope failures and the four attributes (location, aspect, slope geometry, and lithology) become apparent. Most failures occur along the prairie perimeter where slopes tend to be longer and steeper. Being peripheral to the badlands this area is the zone of extension where the slopes are actively retreating and where concentrated drainage of the prairie surface can be an important water source. A self-propagating cycle exists; the steep slopes tend to lead to failure resulting in over-steepened portions (particularly along the backscarp) which will then have a tendency for further failure. This process will continue until the over-steepened portions have been eliminated and a state of quasi-equilibrium is attained.

Mass movements, whether they occur as catastrophic events or as more frequent smaller magnitude events, affect the rate of slope retreat. It is widely believed that large magnitude, infrequent events are most effective in the denudation of the earth's surface (Wolman and Miller, 1960). The magnitude/frequency relationship of the different failure types ranges from low magnitude and high frequency (dry flows) to medium-high magnitude and low frequency (complex failures) (Table 5.1 and Figure 5.1). In this case the frequent, but small scale events (flows), move much less material ($23,800 \text{ m}^3$) than do the larger, more catastrophic complex failures ($284,315 \text{ m}^3$).

Most failures occur along the coulee walls, indicating the effect of basal fluvial erosion on slope stability. Although failures frequently occur along the entire length of the coulee, their magnitude decreases with increasing distance from the badlands. With other parameters assumed to be equal this difference could be due in part to the greater hydraulic gradient at the terminus of the coulee, and to the relative age difference between the advancing head and the coulee outlet.

Table 5.1 - Magnitude/Frequency relationship of failure types evident in the Dinosaur Badlands.

Failure type	Failure character	symbol	Magnitude	Frequency	Figure
Falls	rock	Fr	low-med.	high	2.3
Topple	rock	Tr	low-med.	low-med.	2.4
	debris	Td	low-med.	low-med.	
Flow	creep(lg)	Flc1	med.	low	2.9
	creep(small)	Flc2	low	high	
	dry	Fld	low	very high	2.10
	wet	Flw	low-med.	low	
Pipes	all	P	low-med.	high	2.11
Slides	trans.dom.	Sct	med-high	med.	2.7
(compound)	rot.dom.	Scr	med-high	low	2.8
Complex	slide/flow	S/F	med-high	low	
	pipng/flow	P/F	med-high	low	

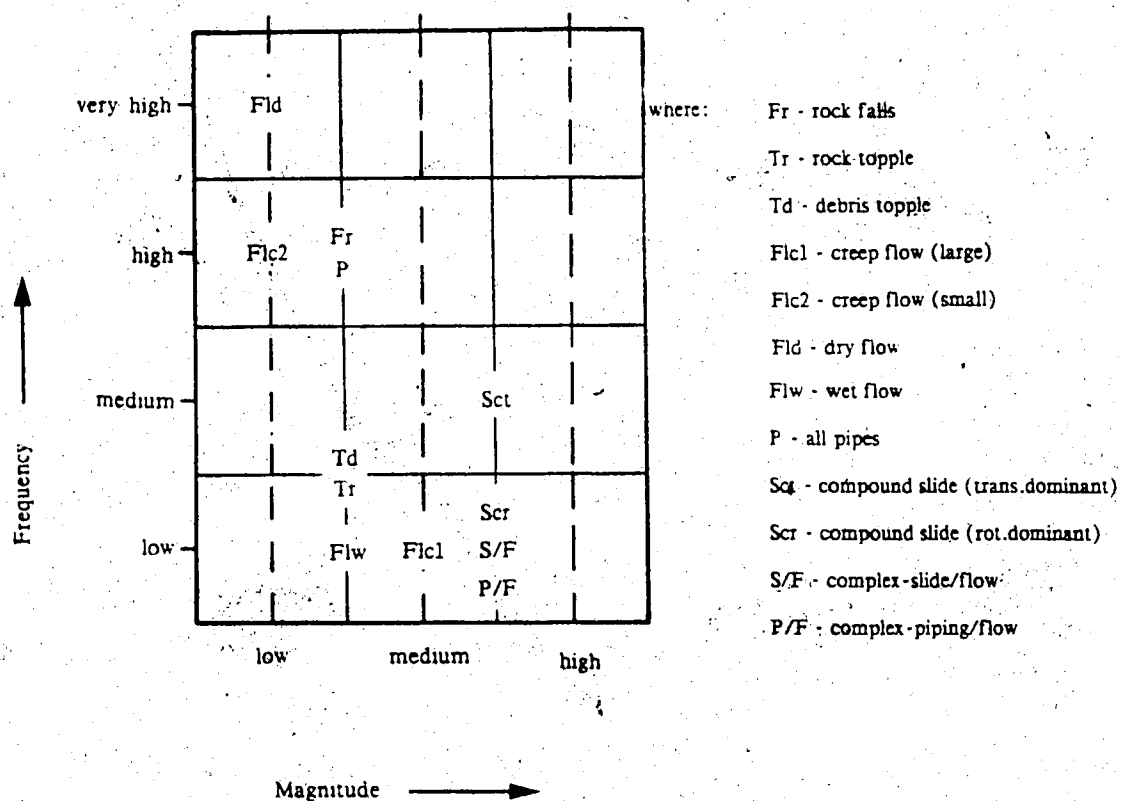


Figure 5.1 Magnitude/Frequency relationship of failure types evident in the Dinosaur Badlands.

The aspect analysis showed a significant difference (at the 0.05 significance level) in failure frequency according to slope orientation. There is statistically a greater tendency for failures to occur on slopes with a northerly aspect (northwest to northeast). However, because of the dominant coulee orientation (north - south), this observation is somewhat restricted, as most slope aspects are oriented in east and west directions. If all orientations were represented equally there would be an even greater disparity between failures on different slopes, as east - west orientated coulees would define the northerly and southerly slopes more precisely. Consequently, if no restrictive coulee orientation existed, an entirely different and more representative trend might become apparent. Furthermore, before any definitive statements can be made regarding aspect, it is important to have an idea of the concentration of slope orientations. However, relative observations are valid. As Churchill (1981) found, smaller magnitude and higher frequency failures occur extensively on all available slope orientations. However, larger scale, less frequent failures occur more consistently on the shaded northerly slopes.

The geometric analysis showed that the mean slope length for the different failure types, ranged from 76 m to 107 m. There was less variation with the slope inclination, which had an overall mean angle of 45° with only a 2° deviation to either side. Although these values are necessarily limited by the available slope lengths and inclinations, a general trend is evident. The larger failure types (slides and complex failures) tend to occur on slopes that are longer and less steep while smaller failures (falls, topples, and dry flows) generally occur on shorter steeper slopes. Although this pattern exists it is important to realize that slope height and inclination are related variables. Since short slopes tend to be steeper, it is not surprising that larger movements (slides and complex failures) will also tend to be on flatter slopes. A less steep slope would not result in immediate failure (topples and falls), but would permit the development of progressive failure, often resulting in a relatively high magnitude mass movement.

Because till is present at varying depths virtually everywhere most failures involved both till and bedrock units, although topples and falls tended to occur in bedrock. Failures that occurred in the till only were small circular slides high in the valley wall. The failure interface in these cases is the till/bedrock contact, and is probably a result of differential permeability and basal sapping at the contact.

In areas where there was a deep and extensive till layer (Little Sandhill Coulee and Waterfall Coulee) multiple slides were prevalent. These are primarily relic features that are likely a product of the wet (and possibly saturated) conditions, and the rapid glacio-fluvial incision during the immediate post-glacial period.

Atterberg testing showed that with an increase in the percentage of fines there was an increase in the plasticity. Because shale units occur at all of the failures sampled, each mass movement was characterized by at least one highly plastic unit. If the water content in these (and other) units increased to a point at which cohesion was reduced to zero (the liquid limit), the shear strength would be greatly reduced, and failure would likely ensue. Because plasticity increases and strength decreases with an increase in the percentage of fines, the depositional history is of great importance. All the failures in this study occur in the deltaic Judith River Formation, which is considered less susceptible to failure than the marine Bearpaw Formation (Thomson and Morgenstern, 1977; Thomson and Bruce, 1978).

In the assessment of the nine case failures no single factor can be deemed responsible for initiating movement. Although the preparatory, triggering and controlling factors are interrelated an attempt will be made to isolate the possible causative factors.

At Sc1, the pre-1949 irrigation ditch is probably the main cause of failure. Seepage from the unlined ditch would increase the pore pressures and reduce the factor of safety. This would be further aggravated by the periodic fluvial erosion undermining the base of the slope. Recent flowing at the eastern side of the failure is likely a response to over-steepening caused by the initial failure (1973-1977). These minor flows will continue until an equilibrium state

has been attained.

Because at Sc2 the slide debris is overlain by thick, topographically high, fluvial deposits, it is likely that this failure is very old. This is further substantiated by the development of a deep soil profile on the slide debris. The proximity of the current channel, and the fact that water at some time traversed across the slide mass, suggest that fluvial activity was at least in part responsible for triggering the failure. Because the northern portion of the slide mass was not overlain by fluvial material, it may have occurred considerably later than did the southern portion.

Sc3, the smallest slide failure, occurred prior to 1949 and was likely triggered by basal erosion. An ephemeral stream is currently eroding the toe of the slide mass, indicating that the original flow path may have been disrupted by the failure.

Sc4 is one of the many failures along the south wall of Waterfall Coulee. Virtually all (with the exception of one - Figure 2.7) of the larger failures in this coulee are along the north-facing slope, indicating that they might be aspect - related. Because the many large failures in this area have the same morphology it is possible that they were triggered by the same factor. The till along these coulee walls is relatively thick, and during the immediate post-glacial period may have been saturated. Possible saturation, in conjunction with the rapid post-glacial downcutting, created very unstable conditions and probably caused extensive slope failures, particularly along the moister north-facing slopes.

Sr², along Little Sandhill Coulee, should be assessed in two parts - the original failure, and the reactivated failure. The 14C date obtained from this failure can be liberally used to represent all of the relic failures in the area that have a similar morphology. If this date is accurate, these failures occurred no more than 250 years ago, well after deglaciation (12,000 - 14,000 B.P.). Consequently, these relic mass movements may reflect delayed response to valley rebound (breaking of bonds). If the 14C date is correct, it is possible that the initial failure occurred in the immediate post-glacial period and that the wood uncovered was actually buried by a part of a much later slide.

The prevalence of till and multiple failures along this valley suggests a relationship between the two. Furthermore, the vast majority of failures along this east - west orientated coulee, have a northerly aspect. In this localized area, the meso-scale geology and morphological processes would be similar, isolating the controlling influence of aspect.

The reactivation of Sr^2 appears to involve the entire mass of the earlier failure. Because this is a secondary failure residual strength values are being mobilized. The angle of internal friction has been reduced and cohesion is likely approaching zero. This reactivation is a result of the cumulative increase in pore water pressures that occurred prior to and during the summer of 1986. Three factors contributed simultaneously toward the water increases; the meltwater from the snow of the preceding season, the above normal precipitation in the early summer months (May and June), and, the excessive amount of pivot and ditch irrigation at the prairie surface above the failure. At the first signs of failure (June, 1986), Mr. Daryl Owen stopped irrigating the land in the vicinity of the slide, and after a lag of about two months movement had virtually ceased. A state of quasi-equilibrium had developed and subsequent movement was minor. The movement that did occur was towards the west and was rotational in nature, with a drop at the head and a rise at the toe. There was also a pivoting of the mass as the eastern portion of the slide was moving away from the scarp and the western portion was moving into it. It is probable that this movement is largely controlled by the ditch along the western perimeter of the slide mass. Because the visible displacement at the head of the failure was not matched by that at the toe it is assumed that the displacement has been absorbed within the slide mass, which has temporarily stabilized. It is also possible that the tilting of the debris backward into the slope has also contributed to the current state of quasi-equilibrium.

The vegetation ring above $St1$ surrounds a depression which possibly represents a seepage area. If so, the increased infiltration of water would lead to greater positive pore water pressures and a subsequent decrease in slope strength. The current surficial movement at the base of the slope may be a response to sub-surface sealing. The deeper, less weathered shale will seal when swelling exceeds fissuring, creating a surface of weakness and initiating a flow.

A seep at the base of S/F1 appears to control slope stability, depending primarily on where the source is. It is interesting to note that both slide/flow complex failures were the only failures with seeps evident. This suggests that a water source is necessary to initiate a flow-type failure. Piping channels, especially if blocked, may have also contributed to unstable slope conditions.

S/F2 also has a seep and piping channels, possibly indicating a mode of development similar to that of S/F1. Many failures occur along the same valley wall and adjacent to S/F2 (including the large translational slide in Figure 4.2). The aspect of most of these failures is northeast. In contrast, the opposite wall (facing southwest) has no large-scale failures, but has numerous more minor failures. This reflects nature of mass movements along Irishman's Coulee; virtually all large-scale failures are located along the west wall. The geology and geomorphic processes on both sides of the coulee are analogous, so both slopes should have a similar morphology. Because this is not the case, it is likely that another parameter - perhaps aspect, is responsible for the slope failures.

The many pipes neighbouring P/F1 must affect slope stability. Pre-failure piping probably removed enough of the supporting matrix to lead to the slope collapse. Subsequent piping is extensive, and, via both matrix removal and increased infiltration of water, the strength of the failed material (already at its residual value) is further reduced.

From those nine examples four different causes of failure are defined: 1) fluvial erosion, 2) pore water pressure increases, 3) post-glacial rebound, and, 4) piping; the first two being the most common. It appears as though, in the past, post-glacial rebound had a dominant destabilizing effect. More recently, however, lateral channel migration seems to have the most significant role on slope instability.

Piping is evident at seven of the nine failures, the exceptions being Sc4 and Sr'. Pipes generally reduce stability but may, in some cases, actually reduce the stress within the slope. If the pipes are open and water can flow freely through them they act to reduce excess pore pressures. Simultaneously, however, an open pipe would facilitate the removal of sediments,

reducing the supportive framework of the slope. Once the void area of the piping channel reaches a threshold value, slope collapse follows. If the pipe were closed the entrapped water would dissipate into the surrounding matrix, increasing pore pressures there. Furthermore, the standing water in the pipe, as Pierson (1983) suggests, can exert outward pressures of considerable magnitude.

5.2 Conclusions

There is a full range of failure types in the badlands; falls, flows, topples, and slides. Few failures are of one type, most are complex, generally with a dominant slide component. As would be expected, those failures with the highest frequency have the lowest magnitude. This includes falls, topples, and dry flows, with flows being the most common. These failure types are evident on virtually all slopes with no apparent preferred orientation, and have a tendency to occur on shorter, steeper slopes. They are responsible for the more gradual and continual slope retreat.

The lower frequency but higher magnitude events were either slides or complex failures. Compound slides generally had a dominant translational component rather than rotational. This corresponds to the type of movement found to occur in similar bedrock formations (Thomson and Morgenstern, 1977; Thomson and Bruce, 1978; Mollard and James, 1984; Bolduc *et al.*, 1987). Consequently, these failures are characterized by a planar rupture surface rather than a curved one. As with the analogous studies (Bjerrum, 1967; Hayley, 1968; Thomson, 1971b; Hardy and Associates, 1974; Thomson and Morgenstern, 1977, 1979; Thomson and Yacyshyn, 1977; Thomson and Bruce, 1978) failures most commonly occur in poorly cemented, overconsolidated clay shales and sandstones with nearly horizontal bedding. This largely accounts for the lateral movement. These failure types occurred most commonly on northerly orientated slopes. Aspect observations are qualified by the dominant coulee orientation (north - south). In contrast to the smaller failure types these failures tend to occur on longer, less steep slopes.

The smaller mass movements (falls, topples, and dry flows) are the dominant present failure types. It is likely that they have occurred continuously but evidence of earlier ones has been eradicated, as the weak bedrock is readily broken down and removed. Most of the large-scale failures (slide and complex failures) are old, and probably occurred in the early post-glacial period. These failures reflect immediate post-glacial conditions occurring in response to either; 1) rebound (progressive failure), 2) an increase in the hydrostatic pressures created by the rapid drawdown of the groundwater as it attempted to match the initial extremely rapid rates of incision, 3) the saturated conditions, and the corresponding excessive positive pore water pressures associated with the thawing ground, or, as a combination of all three. Because many of these failures have a similar morphology they are, probably contemporaneous. More recent mass movements are often reactivations of older failures, either in part or in entirety. Two recent failures, Scl and St1, are examples of first-time failures.

It is difficult to isolate precisely the causative factors controlling stability. However, several preparatory and two triggering factors evidently affect slope stability. Although the role of these factors varies considerably with each failure, in general and in descending order of importance, the main preparatory factors are: local geology, rebound (breaking of bonds), weathering, aspect, and slope steepness. This supports observations made elsewhere (Scott and Brooker, 1968; Beaty, 1971b; Hardy and Associates, 1974 Thomson and Morgenstern, 1977, 1979; Thomson and Bruce, 1978; Thomson and Tweedie, 1978; Mollard and Janes, 1984; Thomson and Kjartanson, 1984; Bolduc *et al.*, 1987; Taylor and Cripps, 1987). Pipes and previous failure activity also affect slope stability.

Geology has a major role in slope stability. All of the nine failures examined have alternating layers of sandstone and shale, with a pervious till layer overlying an impervious layer (generally shale). Such alternating layers of permeable and impermeable materials affect the internal drainage of a slope, and are therefore highly susceptible to failure (Rib and Ta Liang, 1978). The consistency of this sequence at each of the failures strongly suggests that a correlation exists between the two.

Rebound, associated with deglaciation and rapid incision, was clearly of greater consequence in the past than it is today. Delayed failures, however, can be attributed to the equilibration of pore water pressures which is a function of the rate of swelling (dependent on the bond strength) as a result of unloading.

Weathering processes decrease the shear strength of a material and permit greater infiltration of water, and in that sense are largely responsible for surficial failures. The less fissured material at depth often seals (becoming impermeable) before the surface. A theory of threshold crack density can be developed, stating that at some depth fissure density will have decreased to a point at which swelling is dominant (over crack density), sealing that surface and negating further infiltration.

Slope geometry and orientation also affect stability. Long, steep slopes occur ubiquitously in the badlands. Consequently, most slopes are already in an unstable state.

In terms of aspect all directions are not sufficiently represented to allow a definitive conclusion. However, along either side of several coulees, in which most other parameters (geology, slope geometry, and geomorphic processes) are at least similar, there is a distinct difference in failure occurrence. This suggests that aspect is responsible for these differences.

Piping, depending on its extent and location may also significantly affect slope stability. Pipes are common and weaken the slope structure, often leading to its collapse.

Two triggering factors that most commonly cause failures are ground water increases (and the subsequent pore water pressure increases) and fluvial erosion, with the former apparently more dominant. This is in direct contrast to what was found in analogous studies. Most authors found that fluvial erosion was the dominant triggering mechanism (Thomson, 1971; Hardy and Associates, 1974; Thomson and Yacyshyn, 1977; Thomson and Morgenstern, 1977; Thomson and Bruce, 1978; Bolduc *et al.*, 1987) and ground water fluctuations were secondary (Beaty, 1971; Thomson and Morgenstern, 1979; Thomson and Kjartanson, 1984; Bolduc *et al.*, 1987). Ground water levels are increased primarily by excessive irrigation, or above normal amounts of precipitation. Irrigation in arid and semi-arid regions will

significantly elevate the ground water table. In addition to increasing the pore water pressures the strength of the material is reduced if water soluble cementing agents (salts and calcium carbonate) are leached. Gypsum, present in the shales, is less soluble but is readily removed if there is adequate water. The removal of these components results in deflocculation of the clays, leading to a reduction in the structural strength.

Two stabilizing factors occur; terraces and pre-glacial channels. Terraces are very localized features along segments of the Red Deer River and a few tributary valleys. Pre-glacial channels are also very localized features, only affecting a small area. These channels were not mapped but can be recognized by the till thickness. One such channel was noted north of St1.

The factors, both preparatory and triggering, presented herein are not exclusive. They are considered to be several of the more prevalent factors affecting slope stability. Also, more than one factor is usually responsible for inducing slope failures. The immediate cause is only the trigger that sets in motion a slope that is already on the verge of failure.

To conclude, the failures most common to the Dinosaur badlands are the small dry flows, occurring on virtually all of the valley walls. However, due to the nature of dry flows very little material is moved (4 percent) in terms of total volume. Slides occur less frequently but contribute a substantial volume of failed material (95 percent of the total volume of badland material moved). Consequently, slide failures locally influence badland development to a greater extent than do the more common dry flows. Nevertheless, all four failure types have an important role, especially cumulatively, in badland development.

6. References

- Baker, R., 1981. Tensile strength, tension cracks, and stability of slopes. *Soils and Foundations* 21, 2, 1-17.
- Beaty, C.B., 1956. Landslides and slope exposure. *Journal of Geology* 64, 70-74.
- Beaty, C.B., 1971. Geographical distribution of post-glacial slumping in southern Alberta. *Canadian Geotechnical Journal* 9, 219-224.
- Beaty, C.B., 1975. Coulee alignment and wind in southern Alberta. *Geological Society of America Bulletin* 86, 119-128.
- Beaty, C.B., 1976. *Landscapes of Southern Alberta - A Regional Geomorphology*, University of Lethbridge, 95pp.
- Beaty, C.B., and Barendregt, R.W., 1987. The Milk River Canyon, Alberta: Superposition and piping in a semi-arid environment. *Geological Society of America Centennial Field Guide - Rocky Mountain Section*, 29-32.
- Berg, T.E., and McPherson, R.A., 1973. Surficial Geology of Medicine Hat, Alberta Research Council, Map NTS 72L.
- Bjerrum, L., 1967. Progressive failure in slopes of overconsolidated plastic clay and clay shales. *Journal of Soil Mechanics and Foundations Division, ASCE*, 93, SM5, 1-49.
- Blong, R.J., 1973. Relationships between morphometric attributes of landslides. *Zeitschrift für Geomorphologie Supplementband* 18, 65-77.
- Blyth, F.G., and de Freitas, M.H., 1979, *A Geology for Engineers*, London: Edward Arnold.
- Bolduc, J., Cruden, D., Leung, S., and Thomson, S., 1987. Landslide Incidence in Alberta South of 54°N. Alberta Environment, RMD 84/22, Depts. of Civil Engineering and Geology, Univ. of Alberta, 1-44.
- Broker, E.W., 1970. Riverbank stability at the University of Alberta, Edmonton. discussion *Canadian Geotechnical Journal* 7, 2, 170-172.
- Brunsdon, D., 1979. Mass movements. *Process in Geomorphology*, ed. C. Embleton and J. Thomas, London: Edward Arnold, 130-186.
- Bryan, R.B., and Campbell, I.A., 1980. Sediment entrainment and transport during local rainstorms in the Steveville badlands, Alberta. *Catena* 7, 51-65.
- Bryan, R.B., and Campbell, I.A., 1986. Runoff and sediment discharge in a semiarid ephemeral drainage basin. *Zeitschrift für Geomorphologie N.F. Supplement Band* 58, 121-143.
- Bryan, R.B., Campbell, I.A., and Yair, A., 1987. Postglacial geomorphic development of the Dinosaur Provincial Park badlands, Alberta. *Canadian Journal of Earth Sciences* 24, 135-146.

- Bryan, R.B., Yair, A., and Hodges, W.K., 1978. Factors controlling the initiation of runoff and piping in Dinosaur Provincial Park badlands, Alberta, Canada. *Zeitschrift für Geomorphologie Supplement Band 29*, 151-168.
- Campbell, I.A., 1970. Erosion rates in the Steepleville Badlands, Alberta. *Canadian Geographer* 14, 202-216.
- Campbell, I.A., 1974. Measurement of erosion on badlands surfaces. *Zeitschrift für Geomorphologie Supplement Band 21*, 122-137.
- Campbell, I.A., 1981. Spatial and temporal variations in erosion measurements. *Erosion and Sediment transport measurements* (Proceedings of the Florence Symposium, June 1981), IAHS Publication 133, 447-456.
- Campbell, I.A., 1987. Personal communication.
- Campbell, I.A., 1987a. Badlands of Dinosaur Provincial Park, Alberta. *The Canadian Geographer* 31, 1, 82-87.
- Campbell, I.A., 1987b. Infiltration characteristics of badlands surfaces and storm runoff. *Proceedings, International Conference on Infiltration Development and Application*, University of Hawaii, Honolulu, 251-260.
- Carson, M.A., 1975. Threshold and characteristic angles of straight slopes. *Mass Wasting: 4th Guelph Symposium on Geomorphology, 1975*, eds. E. Yatsu, A.J. Ward, and F. Adams, Geographical Publication 4, Dept. of Geography, Univ. of Guelph, 19-34.
- Carson, M.A., and Kirkby, M.J., 1972. *Hillslope Form and Process*, Cambridge: The University Press, 1-475.
- Casagrande, A., 1949. Notes on swelling characteristics of clay shales. Cambridge: Harvard University, 1-16.
- Chandler, R.J., 1972. Lias Clay: weathering processes and their effect on shear strength. *Geotechnique* 22, 403-431.
- Churchill, R.R., 1981. Aspect - related differences in badlands slope morphology. *Annals of the Association of American Geographers* 71, 3, 374-388.
- Costa, J.E., 1984. Physical geomorphology of debris flows. in *Developments and Applications of Geomorphology*, eds. J.E. Costa, and P.J. Fleisher, 268-317.
- Crozier, M.J., 1973. Techniques for the morphometric analysis of landslips. *Zeitschrift für Geomorphologie N.F.* 17, 1, 78-101.
- Crozier, M.J., 1986. Causes of instability. in *Landslides; Causes, Consequences, and Environment*, Beckenham: Crom Helm Ltd., 32-110.
- Crozier, M.J., Eyles, R.J., Marx, S.L., McCondie, J.A., and Owen, R.C., 1980. Distribution of landslips in the Wairarapa hill county. *New Zealand Journal of Geology and Geophysics* 23 (5-6), 575-586.
- Cruden, D.M., 1975. The influence of discontinuities on the stability of rock slopes. *Mass Wasting: 4th Guelph Symposium on Geomorphology, 1975*, eds. E. Yatsu, A.J. Ward,

- F. Adams, Geographical Publication 4, Dept. of Geography, Univ. of Guelph, 57-67.
- Dackombe, R.V., and Gardiner, V., 1983. Slope Processes. in *Geomorphological Field Manual*, London: George Allen and Unwin, 201-215.
- Day, M.J., 1980. Rock hardness: Field Assessment and Geomorphic Importance. *Professional Geographer* 32(1): 72-81.
- Deere, D.U., and Patton, F.D., 1971. Slope stability in residual soils. *Proceedings of the 4th Pan-American Conference on Soil Mechanics and Foundation Engineering, ASCE* 1, 87-170.
- de Freitas, M.H., and Watters, R.J., 1973. Some field examples of toppling failure. *Geotechnique* 23, 4, 495-514.
- de Lugt, J., 1986. Side valley evolution and the role of piping erosion. *The Albertan Geographer*, 22, 3-26.
- Dodson, P., 1971. Sedimentology and taphonomy of the Oldman Formation (Campanian); Dinosaur Provincial Park, Alberta (Canada). *Palaeogeography, Palaeoclimatology, and Palaeoecology* 10, 21-74.
- Duncan, J.M., and Dunlop, P., 1969. Slopes in stiff fissured clays and shales. *Journal of Soil Mechanics and Foundation Engineering Div., ASCE* 95, 467-492.
- Grim, R.E., and Guven, N., 1978. *Bentonites: Geology, Mineralogy, Properties, and Uses*. New York: Elsevier Scientific Publishing Co., 1-256.
- Hansen, W.R., 1965. Effects of Earthquake of March 27, 1964, at Anchorage Alaska. *US Geological Survey, Professional Paper* 542-A, 1-68.
- Hardy, R.M. and Associates Ltd., 1974. Whitemud Creek Bank Stability Study, Dept. of Environment, Prov. of Alberta, E-2758.
- Harty, K.M., 1984. The geomorphic role of snow in a badland watershed. Unpublished M.Sc. thesis, Dept. of Geography, Univ. of Alberta, Edmonton.
- Hayley, D.W., 1968. Progressive failure of a clay shale slope in Northern Alberta: Unpublished M.Sc. thesis, Dept. of Civil Engineering, Univ. of Alberta, Edmonton.
- Hodges, W.K., and Bryan, R.B., 1982. The influence of material behaviour on runoff initiation in the Dinosaur Badlands, Canada. In *Badland Geomorphology and Piping*, eds. R.B. Bryan and A. Yair, Norwich: Geo Books.
- Hoek, E., 1982. Analysis of slope stability in very heavily jointed or weathered rock masses. In *Stability in surface mining*, ed. C.O. Brawner, Ann Arbor: Edward Brothers Inc.
- Hogg, S.E., 1978. The near surface hydrology of the Steepleville Badlands, Alberta. unpublished M.Sc. thesis, Dept. of Geography, Univ. of Alberta, Edmonton.
- Hutchinson, J.D., 1968. Mass movement. in *The Encyclopedia of Geomorphology*, ed. R.W. Fairbridge, New York: Reinhold Book Corp., 688-696.
- Iverson, N.L., 1970. Riverbank stability study at the University of Alberta, Edmonton:

- Discussion. *Canadian Geotechnical Journal* 7, 2, 169-170.
- Jones, F.O., Embody, D.R., and Peterson, W.L., 1961. Landslides along the Columbia River Valley, Northeastern Washington. *US Geological Survey Professional Paper*, 367, 1-98.
- Jones, J.A., 1981. The nature of soil piping a review of research. *British Geomorphological Research Group, Research Monograph* 3, 1-301.
- Kenney, T.C., 1967. The influence of mineral composition on the residual strength of natural soils. *Proceedings of the Geotechnical Conference, Oslo*, 1, 123-130.
- Kenney, T.C., 1975. Weathering and changes in strength as related to landslides. in *Mass Wasting: 4th Guelph Symposium on Geomorphology, 1975*, eds. E. Yatsu, A.J. Ward, F. Adams, Geographical Publication 4, Dept. of Geography, Univ. of Guelph, 69-78.
- Kirkland, J.T. and Armstrong, J.C., 1982. Slope movements related to expansive soils on the Blackland Prairie, North Central Texas, in *Applied Geomorphology*, eds. R.G. Craig and J.L. Craft, London: George Allen and Unwin Ltd., 85-93.
- Koster, E.H., 1983. Sedimentology of the Upper Cretaceous Judith River (Belly River) Formation, Dinosaur Provincial Park, Alberta. *Field Trip Guide Book, Alberta Research Council*, Edmonton, 1-121.
- Koster, E.H., 1984. *Sedimentology of a Foreland Coastal Plain: Upper Cretaceous Judith River Formation at Dinosaur Provincial Park, Alberta*. Research Council, Edmonton.
- Koster, E.H. and Currie, P.J., 1987. Upper Cretaceous coastal plain sediments at Dinosaur Provincial Park, southeast Alberta. *Geological Society of America Centennial Field Guide - Rocky Mountain Section*, 9-14.
- Law, K.T. and Lumb, P., 1976. A equilibrium analysis of progressive failure in the stability of slopes. *Canadian Geotechnical Journal* 15, 113-122.
- Locker, J.G., 1973. Petrographic and engineering properties of fine-grained rocks of Central Alberta. *Research Council Bulletin* 30, Edmonton, Alberta, 1-144.
- McCalpin, J., 1984. Preliminary age classification of landslides for inventory mapping. *Proceedings 21st Annual Symposium on Engineering Geology and Soils Engineering*, Pocatello, ID.
- McKay, G.A., 1970. Problems of measuring and evaluating snow-cover. *Proceedings of the Workshop Seminar on Snow Hydrology*, Queen's Printer of Canada, 42-62.
- McPherson, H.J., 1968. Historical development of the lower Red Deer Valley, Alberta. *Canadian Geographer*, 12, 227-240.
- Matheson, D.S. and Thomson, S., 1973. Geological implications of valley rebound. *Canadian Journal of Earth Science* 10, 961-978.
- May, R.W. and Thomson, S., 1978. The geology and geotechnical properties of till and related deposits in the Edmonton, Alberta, area. *Canadian Geotechnical Journal* 15, 362-370.
- Mielenz, R.C. and King, M.E., 1955. Physical chemical properties and engineering performance of clays. *California Division of Mines Geological Bulletin* 169, 196-254.

- Mollard, J.D. and Janes, J.R., 1984. Slope Movements. *Air photo interpretation and the Canadian Landscape*, Ministry of Supply and Service, Canada, 57-74.
- Nasmith, H., 1964. Landslides and Pleistocene deposits in the Meilke River Valley of Northern Alberta. *Canadian Geotechnical Journal* 1, 3, 155-166.
- Nemcok, A., Pasek, J., and Rybar, J., 1972. Classification of landslides and other mass movements. *Rock Mechanics* 4, 71-78.
- O'Hara, S.L., 1986. Postglacial geomorphic evolution and alluvial chronology of a valley in the Dinosaur Badlands, Alberta. unpublished M.Sc. thesis, Dept. of Geography, Univ. of Alberta, Edmonton.
- Parker, G., 1963. Piping, a geomorphic agent in landform development of the drylands. *International Association of Scientific Hydrology Publication* 65, 103-113.
- Peterson, R., 1954. Studies of Bearpaw Shale at a damsite in Saskatchewan. *Proceedings of the American Society of Civil Engineers* 80, 476.
- Peterson, R., 1958. Rebound in the Bearpaw shale in Western Canada. *Geological Society of America Bulletin* 69, 1113-1123.
- Pierson, T.C., 1983. Soil pipes and slope stability. *Quarterly Journal of Engineering Geology* 16, 1-11.
- Piteau, D.R. and Martin, D.C., 1982. Mechanics of rock slope failure. In *Stability in Surface Mining*, The American Institute of Mining, Metallurgical, and Petroleum Engineers, Inc., Ann Arbor: Edward Brothers Inc., 113-169.
- Prior, D.B. and Ho, C., 1970. Bentonite Landslides. *Science* 167, 1014-1015.
- Public Works Department Hongkong, 1979. *Geotechnical Manual For Slopes*, Geotechnical Control Office.
- Quigley, R.M., 1975. Weathering changes in strength of glacial till. In *Mass Wasting: 4th Guelph Symposium on Geomorphology, 1975*, eds. E. Yatsu, A.J. Ward, and F. Adams, Univ. of Guelph, Geographical Publication 4, Dept. of Geography, Univ. of Guelph, 117-131.
- Rib, H.T. and Ta Liang, 1978. Recognition and Identification. Chapter 3 in *Landslides Analysis and Control - Special Report 176*, Transportation Research Board, eds. R.L. Schuster and R.J. Krizek, Washington, D.C., 34-80.
- Ross, J.S., 1964. *Bentonites in Canada*, Monograph 873, Dept. of Mines and Technical Surveys, Ottawa, 1-61.
- Rouse, C. and Reading, A., 1985. Soil mechanics and natural slope stability. In *Geomorphology and Soils*, British Geomorphological Research Group, London: George Allen and Unwin Ltd., 159-179.
- Russell, D.A., 1977. *A Vanished World: The Dinosaurs of Western Canada*, Ottawa: National Museums of Canada.

- Rutter, N.W., 1980. Geology in Urban Areas of Canada and its Relation to Landsliding. *Special Publication 1*, paper given at Canadian Geotechnical Society Conference, April, 1980, National Research Council, Toronto.
- Samuels, S.G., 1950. The effect of base exchange on the engineering properties of soils. *Building Research Station*, note.C176.
- Schumm, S.A., 1956. The role of creep and rainwash on the retreat of badland slopes. *American Journal of Science*
- Schweger, C., Haggood, T. and Hickman, M., 1981. Late glacial - Holocene climate changes of Alberta: a record from lake sediment studies. in *The Impacts of Climate Fluctuations on Alberta's Resources and Environment*, Report WAES 1-81, Edmonton: Atmospheric Environment, Services, 47-60.
- Scott, J.S., 1965. Landslide investigations, Saskatchewan and Alberta. *Geological Survey of Canada, Paper 65-1*, 85-87.
- Scott, J.S. and Brooker, E.W., 1968. Geological and Engineering Aspects of Upper Cretaceous Shales in Western Canada. *Geological Survey of Canada*, paper 66-37.
- Selby, M.J., 1970. *Slopes and Slope Processes*, Publ. 1, Hamilton: New Zealand Geographical Society.
- Sharpe, C.F.S., 1938. *Landslides and Related Phenomena: A Study of Mass Movement of Soil and Rock*, New York: Columbia Univ. Press, 1-137.
- Skempton, A.W., 1964. Long-term stability of clay slopes. *Geotechnique* 14, 2, 77-102.
- Skempton, A.W. and Hutchinson, J.N., 1969. Stability of Natural Slopes and Embankment Foundations. *Proc. 7th International Conference on Soil Mechanics and Foundation Engineering*, State-of-the-Art Volume, 291-340.
- Som, N., 1980. Properties of materials relevant to landslide studies. *Third New Dehli International Symposium on Landslides, Proceedings* 2, 7-11.
- Sowers, G.F. and Royster, D.L., 1978. Field Investigation, in *Landslides Analysis and Control - Special Report 176*, eds. R.L. Schuster and R.J. Krizek, Washington, D.C., 81-111.
- Spence, D.H., 1972. Relationship between slope and aspect in an area of hummocky moraine, south central Alberta. Unpublished M.Sc. thesis, Dept. of Geography, Univ. of Alberta.
- Stalker, A. MacS., 1960. Buried Valleys in Central and Southern Alberta. in *Geological Survey of Canada, paper 60-32*.
- Stelck, C.R., 1967. The record of the rocks. In *Alberta - A Natural History*, ed. W.G. Hardy, Evergreen Press, 21-57.
- Strahler, A.N., 1956. Quantitative slope analysis. In *Bulletin of the Geological Society of America* 67, 571-596.
- Taylor, R.K. and Cripps, J.C., 1987. Weathering effects: slopes in mudrocks and over-consolidated clays. in *Slope Stability*, eds. M.G. Anderson and K.S. Richards, New York: Wiley, 405-445.

- Terzaghi, K., 1944. *Ends and Means of Soil Mechanics*. Grad. Sch. Eng., Publication 402, Columbia: Harvard University.
- Terzaghi, K., 1950. Mechanism of Landslides. *Geological Society of America Berkley Volume*, 83-123.
- Terzaghi, K. and Peck, R.B., 1967. *Soil Mechanics in Engineering Practice*, 2nd edition, New York: John Wiley, 566 p.
- Thomson, S., 1970. Riverbank stability study at the University of Alberta. *Canadian Geotechnical Journal* 7, 2, 157-168.
- Thomson, S., 1971a. Analysis of a failed slope. *Canadian Geotechnical Journal* 8, 596-599.
- Thomson, S., 1971b. The Lesuer Landslide. A failure in Upper Cretaceous clay shale. *Proceedings Ninth Annual Symposium on Engineering Geology and Soil Engineering*, Boise, Idaho, 44 p.
- Thomson, S. and Bruce, I., 1978. An air photo study of landslides along the North Saskatchewan River in Central Alberta, Canada. *Sixteenth Symposium on Engineering Geology and Soils Engineering*, Boise, Idaho, 85-110.
- Thomson, S. and Kjartansson, B.H., 1984. A study of delayed failure in a cut slope in stiff clay. *Proceedings 37th Canadian Geotechnical Conference*, Canadian Geotechnical Society, 195-207.
- Thomson, S. and Morgenstern, N.R., 1977. Factors affecting distribution of landslides along rivers in Southern Alberta. *Canadian Geotechnical Journal* 14, 4, 508-523.
- Thomson, S. and Morgenstern, N.R., 1979. Landslides in argillaceous rock, Prairie Provinces, Canada. In *Rockslides and Avalanches 2*, Developments in Geotechnical Engineering, 14B, New York: Elsevier Scientific Publishing, 515-540.
- Thomson, S. and Townsend, D.L., 1979. River erosion and bank stabilization - North Saskatchewan River, Edmonton, Alta., *Canadian Geotechnical Journal* 16, 567-576.
- Thomson, S. and Tweedie, R.W., 1978. The Edgerton Landslide. *Canadian Geotechnical Journal* 15, 510-521.
- Thomson, S. and Yacyshyn, R., 1977. Slope instability in the City of Edmonton. *Canadian Geotechnical Journal* 14, 1, 1-16.
- Toy, T.J., 1977. Hillside form and climate. *Geological Society of America Bulletin*, 88, 16-22.
- Varnes, D.J., 1975. Slope movements in the Western United States. in *Mass Wasting: 4th Guelph Symposium on Geomorphology, 1975*, eds. E. Yatsu, A.J. Ward, F. Adams, Geographical Publication 4, Dept. of Geography, Univ. of Guelph, 1-17.
- Varnes, D.J., 1978. Slope movement types and processes. In *Landslide Analysis and Control*, Special Report 176, eds. R.C. Schuster, and R.J. Krizek, Washington, D.C., 11-33.
- Wolman, M.G. and Miller, J.P., 1960. Magnitude and frequency of forces in geomorphic processes. In *Journal of Geology* 68, 54-74.

- Wu, T.H. and Sangrey, D.A., 1978. Strength properties and their measurement. In *Landslides Analysis and Control*, Special Report 176, eds. R.C. Schuster, and R.J. Krizek, Washington, D.C., 139-154.
- Yair, A.B., Laree, R.B. and Adar, E., 1980. Runoff and erosion rates in the Zin valley badlands, Northern Negev, Israel. *Earth Surface Processes* 5, 205-225.
- Yair, A., 1983. Hillslope hydrology, water harvesting and areal distribution of some ancient agricultural systems in the Northern Negev desert. *Journal of Arid Environments* 6, 283-301.
- Young, A., 1972. *Slopes*, Edinburgh: Oliver and Boyd.
- Zaruba, Q. and Mencl, V., 1982. *Landslides and Their Control*, New York: Elsevier Scientific Publishing Co., 1-205.
- Zischinsky, U., 1966. On the deformation of high slopes. *Proceedings 1st Congress, International Society of Rock Mechanics*, 179-185.

7. Appendices

Appendix A - Aerial photographic coverage of Dinosaur Provincial Park and area. Note-
*near-infrared; () slopes not yet failed

Year	Role No. (AS)	Flight Ln.	Print No.	Scale	Failures
1949	170	5013	19-23	1:40,000	(Sc1), Sc4, Sr ² , (St1), S/F1, P/F1.
	171	5012(s)	90-92	1:40,000	Sc2, Sc3, Sc4
1962	(72L)	5017	86-90	1:31,680	(Sc1), Sr4, Sr ² , (St1), S/F1 S/F2, P/F1
	835	5016(s)	201-206	1:31,680	Sc3, Sr ²
1968	(72L)	5012	116-119	1:31,680	(Sc1), Sc4, Sr ² , (St1), S/F1, S/F2, P/F1
	995	5016	73-75	1:31,680	Sc2, Sc3
1969	1013	5045	38-39	1:12,000	P/F1
1973	1258	15	86-89	1:31,680	(Sc1), Sc4, Sr ² , (St1), S/F1, S/F2, P/F1
	1258	14(s)	56-58	1:31,680	Sc2, Sc3
1977	1576	6	146-147	1:10,000	Sr ² , (St1), P/F1
	1576	5	116-121	1:10,000	Sr ² , (St1), P/F1
	1576	4	84-90	1:10,000	(Sc1), S/F1
	1576	3	55-56	1:10,000	Sc4, S/F2
	1576	2	29-32	1:10,000	Sc3, Sr ²
	3014	43E	283-287	1:20,000	
	3014	42E	233-237	1:20,000	
1978	1658	3	201-206	1:30,000	
	1658	2	184-187	1:30,000	
*1980	2182	3	51-60	1:10,000	Sc4, (St1)
	2182	4	77-85	1:10,000	Sr ² , P/F1
	2182	5	109-115	1:10,000	
		6	137-142	1:10,000	
1981				1:60,000	
1983	2682	1	5-13	1:10,000	Sc1, Sc4, (St1) S/F1
	2682	2	29-39	1:10,000	(St1), P/F1
	2682	3	50-69	1:10,000	Sr ²
	2682	4	103-106	1:10,000	
	2682	5	109-113	1:10,000	
	(83-2)			1:30,000	
1984	2820	1	172	1:5,000	Sr ²
	2820	1	152-161	1:10,000	Sr ² , P/F1
	2815	1	225-226	1:6,000	P/F1
	2815	1	232-233	1:15,000	Sc4, S/F1
1985	3165	2E	90-95	1:25,000	Sc4, Sr ² , St1, P/F1
		4SE	76-78	1:25,000	Sc1, Sc2, Sc3, S/F1, S/F2
1986	3423	1L	12	1:40,000	
	3343	1	3-6	1:40,000	Sr ² , S/F1

Appendix B - Atterberg test results.

<u>Sample</u>	<u>Water content(%)</u>	<u>Liquid limit(LL)</u>	<u>Plastic limit(LP)</u>	<u>Plasticity index(IP)</u>	<u>Material classific.</u>
Sc1-A1	12	81	22	59	gr shale
Sc1-An	3	38	31	7	br shale
Sc1-B1	4	69	21	48	gr sandst.
Sc1-B2	12	57	12	45	gr shale
Sc1-B3	12	50	19	31	br sandst.
Sc1-B5	11	25	13	12	gr sandst.
Sc1-C1	5	46	19	27	gr sandst.
Sc1-C2	4	32	17	15	br sandst.
Sc2-A1	11	59	17	42	gr shale
Sc2-A2	4	26	17	9	br sandst.
Sc2-B1	8	27	18	9	br till
Sc2-C1	6	42	23	19	br sandst.
Sc2-C2	8	21	19	2	br sandst.
Sc2-C3	8	41	20	21	br sandst.
Sc3-A1	18	69	34	35	br shale
Sc3-Bn	9	47	26	21	gr shale
Sc4-A1	3	31	19	12	y shale
Sc4-Bb1	5	29	19	10	br shale
Sc4-Bn1	7	33	18	15	y shale
Sc4-C1	8	34	20	14	br sandst.
Sr ² -A1	6	32	17	15	gr till
Sr ² -A2	8	33	17	16	gr till
Sr ² -A3	9	31	17	14	gr till
Sr ² -A4	9	31	16	14	gr till
Sr ² -B1	5	27	18	9	br till
Sr ² -B2	5	27	19	8	br shale
Sr ² -lake	2	23	20	3	gr lake
Sr ² -till	3	36	13	23	gr till
St1-A1	5	70	27	43	gr shale
St1-A2	13	74	23	51	gr shale
St1-A3	49	61	25	37	gr shale
St1-A4	18	35	27	8	gr shale
St1-B1	15	71	22	49	dk shale
St1-B3	37	89	25	64	gr shale
St1-Cal	1	25	22	3	y shale
St1-Cb1	1	28	20	8	gr shale
St1-Cb2	4	41	15	26	gr shale
St1-Cb3	6	30	14	16	gr shale
S/F1-A1	7	52	17	35	br shale
S/F1-B1	6	31	18	13	gr shale
S/F2-B1	4	27	16	11	br shale
S/F2-B2	6	31	18	13	gr sandst.
S/F2-B3	14	48	22	26	gr shale
P/F1-A1	31	70	48	22	dk shale

147

P/F1-B1

14

76

47

29

gr shale

Note: dk - dark; y - yellow; br - brown; gr - grey.

THE QUALITY OF THIS MICROFICHE
IS HEAVILY DEPENDENT UPON THE
QUALITY OF THE THESIS SUBMITTED
FOR MICROFILMING.

UNFORTUNATELY THE COLOURED
ILLUSTRATIONS OF THIS THESIS
CAN ONLY YIELD DIFFERENT TONES
OF GRÉY.

LA QUALITE DE CETTE MICROFICHE
DEPEND GRANDEMENT DE LA QUALITE DE LA
THESE SOUMISE AU MICROFILMAGE.

MALHEUREUSEMENT, LES DIFFERENTES
ILLUSTRATIONS EN COULEURS DE CETTE
THESE NE PEUVENT DONNER QUE DES
TEINTES DE GRIS.



National Library
of Canada

Bibliothèque nationale
du Canada

Canadian Theses Service

Service des thèses canadiennes

Ottawa, Canada
K1A 0N4

NOTICE

The quality of this microform is heavily dependent upon the quality of the original thesis submitted for microfilming. Every effort has been made to ensure the highest quality of reproduction possible.

If pages are missing, contact the university which granted the degree.

Some pages may have indistinct print especially if the original pages were typed with a poor typewriter ribbon or if the university sent us an inferior photocopy.

Previously copyrighted materials (journal articles, published tests, etc.) are not filmed.

Reproduction in full or in part of this microform is governed by the Canadian Copyright Act, R.S.C. 1970, c. C-30.

AVIS

La qualité de cette microforme dépend grandement de la qualité de la thèse soumise au microfilmage. Nous avons tout fait pour assurer une qualité supérieure de reproduction.

S'il manque des pages, veuillez communiquer avec l'université qui a conféré le grade.

La qualité d'impression de certaines pages peut laisser à désirer, surtout si les pages originales ont été dactylographiées à l'aide d'un ruban usé ou si l'université nous a fait parvenir une photocopie de qualité inférieure.

Les documents qui font déjà l'objet d'un droit d'auteur (articles de revue, tests publiés, etc.) ne sont pas microfilmés.

La reproduction, même partielle, de cette microforme est soumise à la Loi canadienne sur le droit d'auteur, SRC 1970, c. C-30.

THE UNIVERSITY OF ALBERTA

Mass Movements in the Dinosaur Badlands

by

Jennifer S. de Lugt

A THESIS

SUBMITTED TO THE FACULTY OF GRADUATE STUDIES AND RESEARCH
IN PARTIAL FULFILMENT OF THE REQUIREMENTS FOR THE DEGREE

OF Master of Science

Department of Geography

EDMONTON, ALBERTA

Fall 1988

Permission has been granted to the National Library of Canada to microfilm this thesis and to lend or sell copies of the film.

The author (copyright owner) has reserved other publication rights, and neither the thesis nor extensive extracts from it may be printed or otherwise reproduced without his/her written permission.

L'autorisation a été accordée à la Bibliothèque nationale du Canada de microfilmer cette thèse et de prêter ou de vendre des exemplaires du film.

L'auteur (titulaire du droit d'auteur) se réserve les autres droits de publication; ni la thèse ni de longs extraits de celle-ci ne doivent être imprimés ou autrement reproduits sans son autorisation écrite.

ISBN 0-315-45501-2

THE UNIVERSITY OF ALBERTA

RELEASE FORM

NAME OF AUTHOR Jennifer S. de Lugt

TITLE OF THESIS Mass Movements in the Dinosaur Badlands

DEGREE FOR WHICH THESIS WAS PRESENTED Master of Science

YEAR THIS DEGREE GRANTED Fall 1988

Permission is hereby granted to THE UNIVERSITY OF ALBERTA LIBRARY to reproduce single copies of this thesis and to lend or sell such copies for private, scholarly or scientific research purposes only.

The author reserves other publication rights, and neither the thesis nor extensive extracts from it may be printed or otherwise reproduced without the author's written permission.

(SIGNED)

PERMANENT ADDRESS:

108 Herchmer Cr.
Kingston, Ont.
K7M 2V9

DATED Oct. 14 19 88

THE UNIVERSITY OF ALBERTA
FACULTY OF GRADUATE STUDIES AND RESEARCH

The undersigned certify that they have read, and recommend to the Faculty of Graduate Studies and Research, for acceptance, a thesis entitled Mass Movements in the Dinosaur Badlands submitted by Jennifer S. de Lugt in partial fulfilment of the requirements for the degree of Master of Science in Geomorphology.

Ken A. Campbell

Supervisor

R. B. Tanis

Date *Oct. 7. 1988*

Dedication

To my sister Lou, whose philosophy about life has been inspirational - thanks.

Abstract

Mass movements in the badlands of Dinosaur Provincial Park have been identified, mapped and evaluated. The term mass movement is used as a collective term for the different types of slope failures involving the downslope movement of materials under the influence of gravity. The types of failures are defined according to Varnes (1978), and include four main types; falls, topples, slides, and flows. A fifth category involves a combination of two or more of the main failure types and is classified as a complex failure.

There is a considerable range in mass movement magnitude and frequency. Dry flows have the greatest frequency and generally a low magnitude while complex failures have a low frequency, but a relatively high magnitude. Of the different mass movement types those that are larger and more catastrophic have a greater role in badland extension.

The smaller magnitude failures (falls, topples, and dry flows) are evident on all slopes, regardless of orientation, and tend to occur on shorter, steeper slopes. Conversely, the larger magnitude events (slides and complex failures) occur more frequently on north facing slopes, and on longer, less steep slopes.

Most of the large scale failures appear relatively old and are likely of early post-glacial age(s). Large, contemporary failures are likely often a result of increased pore water pressures, from either excessive amounts of precipitation or irrigation (or a combination of the two). The smaller failures are common on oversteepened slopes.

The long, steep and unvegetated slopes of the Dinosaur Badlands favour mass movements. Consequently, these processes contribute significantly to badland development.

Acknowledgements

This study has been completed with the help of many people. First and foremost, special thanks are due to my supervisor, Dr. Ian Campbell for his guidance and encouragement. I am also grateful to my committee members, Dr. Bruce Rains, and Dr. David Cruden for their advice and comments on the final draft of this thesis.

I wish to thank Chief Ranger Roger Benoit and his staff for permission to explore the Dinosaur Badlands, and for providing the setting for a very enjoyable summer of 1986. I also thank Lynsey, Daryl, and Jessica Owen for the use of their land, their hospitality, and for their continued friendship.

Thanks are due to members of the Department of Geography; Diana and Fran for their smiles and support, the drafting staff for their advice, and in particular, Randy Pakan for ready photographic advice and processing.

Many people gave up their spare time to help with both the field and lab work. Consequently, thanks are due to Sarah and David, Sean, Anne, Mark (Hank), Ray, and Paul. Also, Ray Nichol deserves special thanks for his help with the drafting, without which I would still have a 'Staedtler' in hand.

Finally, and perhaps most importantly, I wish to thank those who provided the support I needed during the past three years. Thanks to mom and dad, Lou, Mike, and Duncan - for always being there. Also, thanks to my mainstays Anne and Paul, and colleagues (especially Bonnie (Boo), Lauren (Lotus Blossum), Janice (Kermie), and Karen) - thanks for the memories. And, last but not least, thanks to Kyla for the many walks and comic relief I so often needed.

Table of Contents

Chapter	Page
1. Introduction	1
1.1 Study Objectives	1
1.2 Location	1
1.3 Site Description	3
1.3.1 Geology	3
1.3.2 Geological History	5
1.3.3 Climate	9
1.3.4 Vegetation	10
2. Literature Review	13
2.1 Terminology	13
2.2 Classification	14
2.2.1 Varnes Classification	14
2.2.2 General review of mass movements present in Dinosaur badlands	15
2.3 Causes of Instability	22
2.3.1 General	22
2.3.2 Factors contributing to slope failures	27
2.4 Past Research	30
2.4.1 Valley Rebound	30
2.4.2 Aspect	33
2.4.3 Analogous stability studies	34
3. Research Methodology	46
3.1 Recognition and Identification of mass movements	46
3.1.1 Nomenclature	46
3.1.2 Aerial photographic interpretation	47
3.1.3 Topographic map interpretation	49
3.1.4 Field reconnaissance	49

3.1.5 Field research	51
3.1.6 Laboratory analysis	55
3.1.7 Laboratory analysis	56
4. Results and analysis	58
4.1 Type and location of identified mass movements	58
4.1.1 General	58
4.1.2 Location analysis	60
4.1.3 Aspect analysis	60
4.1.4 Geometric analysis	63
4.1.5 Lithological analysis	69
4.2 Case studies	69
4.2.1 General	69
4.2.2 Topography	71
4.2.3 Geology	93
4.2.4 Dating the nine mass movements	118
4.2.5 Laboratory analysis	121
5. Discussion and Conclusions	126
5.1 Discussion	126
5.2 Conclusions	133
6. References	137
7. Appendices	145

List of Tables

Table	Page
1.1 Precipitation data from Brooks AHRC: 1953-1989	9
1.2 Field season (1986) climatic data	11
3.1 Derivation of the notation used for the nine case failures.	47
4.1 Slope length and inclination of different failure types	66
4.2 Summary characteristics of the nine case failures	71
4.3 Volumetric analysis of failures occurring in the Dinosaur Badlands - Case failures	86
4.4 Representative volumes of various magnitude events	87
4.5 Relative age classification	118
4.6 A local example of sediment sizes for different lithological units	123
4.7 Atterberg test results	123
4.8 Atterberg values from analogous studies; determined for the fine grained, soft sedimentary Upper Cretaceous bedrock of Alberta	124
4.9 Strength values from analogous studies; determined for the fine grained, soft sedimentary Upper Cretaceous bedrock of Alberta	125
5.1 Magnitude/Frequency relationship of failure types evident in the Dinosaur Badlands.	127

List of Figures

Figure	Page
1.1 Location of the study area	2
1.2 Bedrock geology in the vicinity of the study area - modified after McPherson, (1968)	7
2.1 Little Sandhill Coulee - looking east. Fallen debris along slope base (E4 and F8). Relief is of the order of 30 m.	16
2.2 Perched topple block along tributary valley wall (H6) (Little Sandhill Coulee). Slopes are about 15 m high.	16
2.3 A compound slide (dominantly translational) in Waterfall Coulee. Multiple scarps indicate retrogressive nature.	19
2.4 Tributary coulee of Princess Coulee - a compound slide (dominantly rotational); about 25,000 m ² in area.	19
2.5 Grassed tributary coulee of Princess Coulee - looking south. Regolith creep terracettes enhanced by animal paths (normal-I4; tear-K6).	20
2.6 Sonofabitch Coulee - looking southwest. Three adjacent failures; a dry flow (B8), fall debris (F6), and a slide (E4) (cow on prairie surface for scale).	23
2.7 Large prairie pipe (I4).	23
2.8 Resolution of forces on a potential slip surface	26
2.9 Stress-strain curves - material A is more brittle than B, resulting in a larger strength decrease after peak strength is reached - adapted after Wu and Sangrey, 1978	26
2.10 Destabilising components - adapted from Crozier (1986)	32
2.11 Schematic rebound - modified from Matheson and Thomson (1973)	32
4.1 Identified mass movements in pocket at back	
4.2 Irishman's Coulee - looking northwest. Aerial view of largest failure (137,900 m ²) in study area; a translational slide (from bottom left of photograph to I4)	59
4.3 Location Histogram	61
4.4 Aspect of all failure types	62

Figure	Page
4.5 Rose diagrams showing aspect of different failure types	64
4.6 View along Waterfall Coulee (near Sc4) - looking west. The north-facing slopes (in shadow) are clearly better vegetated and have a more uniform, longer and less steep profile than do their south-facing counterparts	65
4.7 Slope length and inclination of different failure types	67
4.8 Slope length for all failure types	68
4.9 Slope inclination for all failure types	68
4.10 Lithology of all failure types	70
4.11 Oblique aerial view of Sc1 - looking northeast. Note the structural definition of the debris and the pond at the base (E2).	72
4.12 Oblique aerial view of Sc2 - looking northwest. Note the proximity of the channel along the base.	72
4.13 Overview of Sc3 - looking north. The backward tilting and the displacement of the beds are clearly visible.	73
4.14 Overview of Sc4 - looking southeast. Car on prairie surface (K7) for scale.	73
4.15 Oblique aerial view of Sr ² - looking southwest. Note seepage areas above the visible scarp.	74
4.16 Overview of St1 - looking northeast. The upper 7 m of the exposure is till which increases in depth (A10-11) further north	74
4.17 Overview of S/F1 - looking east. Relief here is about 60 m.	75
4.18 Overview of S/F2 - looking southwest. Note flow (G4) and adjacent failures to the south.	75
4.19 Overview of P/F1 - looking south. The shale in the foreground (D3, I2, and L3) is currently flowing over the more resistant sandstone base.	76
4.20 Slope profiles and contour map of Sc1	77
4.21 Slope profiles and contour map of Sc2	78
4.22 Slope profiles and contour map of Sc3	79

Figure	Page
4.23 Slope profiles and contour map of Sc4	80
4.24 Slope profiles and contour map of Sr ¹	81
4.25 Slope profiles and contour map of St1	82
4.26 Slope profiles and contour map of S/F1	83
4.27 Slope profiles and contour map of S/F2	84
4.28 Slope profiles and contour map of P/F1	85
4.29 Vector diagram showing movement since July 1, 1986, when measurement began.	88
4.30 Scarp (mid July, 1986) of Sr ² - looking east. S. O'Hara for scale.	90
4.31 Scarp (August 2, 1987) of Sr ² - looking east. Kyla (E7) is at the same block evident in Figure 4.30 (H2).	90
4.32 Centre toe bulge (July 1, 1986) of Sr ² - looking south: For actual location see Figure 4.15 (H3)	91
4.33 Western toe bulge (August 3, 1986) of Sr ² - looking northwest. For actual location see Figure 4.15 (K5).	92
4.34 Western toe bulge (August 2, 1987) of Sr ² - looking southeast	92
4.35 Lithological sequence of slide failures	94
4.36 Lithological sequence of complex failures	95
4.37 Till failure (G7) along Irishman's Coulee - looking southeast. Note the intact bedrock below the failure(I5)	96
4.38 Seepage area north of S/F1 (D3) outlined by the denser vegetation.	98
4.39 Seepage area at south toe of S/F2 (D7). For location, see Figure 4.18 (E4)	98
4.40 Visible ring above St1 (H-J, 4-7). The vegetation inside and outside the ring is typical prairie grass while the ring itself is largely prairie lichen.	99
4.41 Debris slide (I4) (Nov. 1987) along Little Sandhill Coulee. Note the larger and older failure beyond (D5).	101

Figure	Page
4.42 Water (on sheared surface and in debris) indicated large amount present during failure. P.Nielsen for scale (L9).	101
4.43 Raised prairie perimeter (E6) due to valley rebound (Matheson and Thomson, 1973) is most evident where extensive badland development has occurred	102
4.44 Pit A at Sc1. 0.71 m of slide debris is overlying the buried soil and vegetation layer (at knife - D9). Kyla at base for scale.	104
4.45 Tilted blocks at the west foot area of Sc1	104
4.46 Graben at the head of Sc1 and associated remnant blocks and pinnacles	105
4.47 Distortion of debris at the toe of Sc1. Note also the water in the foreground. P. Nielsen at Pit A for scale (K3)	106
4.48 Section 1 at Sc2. 0.65 m of weathered fluvial sands overlying 1.0 m of slide debris (F12).	107
4.49 Section 2 at Sc2 where 0.59 m of debris has buried a 0.21 m soil layer (E6). The underlying material is fluvially derived.	107
4.50 Pit C at Sc2 - evidence of creep of weathered debris as seen by separation layer (C10-F10) running parallel to the surface at a depth of 0.36 m. Knife at debris/fluvial contact (E5).	109
4.51 Pits A and B at Sr ² - possible failure plane. The material in this zone is more loose and friable than the surrounding till. The vertical lines (B7, D8, G5, and G2) are staked through this zone (A).	111
4.52 Buried grass at the base of St1 (knife - F5), at a depth of 1.3 m.	113
4.53 Surficial cracking at the foot of St1 running both perpendicular and parallel (toward the cottonwood tree) to the direction of movement.	113
4.54 Progressive burial of vegetation at St1. Debris lobe overriding new growth (still green).	114
4.55 Organic interface between debris and alluvium delineating the pre-failure surface	114

Figure	Page
4.56 Soil and vegetation interface (knife - G8) at Pit B - S/F2, showing successive development of failure. Kyla in front of earlier failure.	116
4.57 Change in vegetation showing the contact between displaced prairie surface and debris.	116
4.58 Fragmented shale debris exposed at pits A and C - P/F1. Size of the shards is approximately 3 cm (long axis).	117
4.59 Pipes (F5,7) along east wall of failure, typical of extensive piping at P/F1	117
4.60 View westward along Little Sandhill Creek showing extensive failures, particularly along the south (north-facing) wall. Sr ² (C6) is located at the beginning of this sequence of multiple failures.	120
5.1 Magnitude/Frequency relationship of failure types evident in the Dinosaur Badlands.	127

1. Introduction

1.1 Study Objectives

The aims of this study were to: (1) locate and map the mass movements in the badlands of the Dinosaur Provincial Park area, (2) classify these mass movements, and (3) correlate the type of movement with those factors that significantly influence slope stability. These factors include location, aspect, local lithology, and slope geometry. The emphasis is primarily on the distribution and type of failure, not the mechanics.

Despite numerous studies on mass movements in the western prairies (Scott, 1965; Bjerrum, 1967; Beaty, 1971; Thomson and Morgenstern, 1974, 1977; Thomson and Bruce, 1978; Thomson and Kjartanson, 1984; Bolduc *et al.*, 1987), none have been done in Dinosaur Provincial Park. This area provides a unique opportunity to study mass failures in badlands. The long, often steep, slopes of the barren, weak bedrock influence the frequency, type of failure, and the morphology of the failed unit.

1.2 Location

Badlands line the Red Deer River between Nevis and Atlee in southeastern Alberta, for some 300 km, covering an area of approximately 800 km² (Stelck, 1967). The most extensive and spectacular badland development occurs in the 150 km² Dinosaur Provincial Park area 40 km northeast of Brooks (Figure 1.1). In places, especially on the south side of the Red Deer River, badlands extend away from the main river valley for more than 10 km. The study area of approximately 30 km² incorporates the badland region south of the Red Deer River, between the Little Sandhill Creek Coulee in the west, and Wolf Coulee in the east.

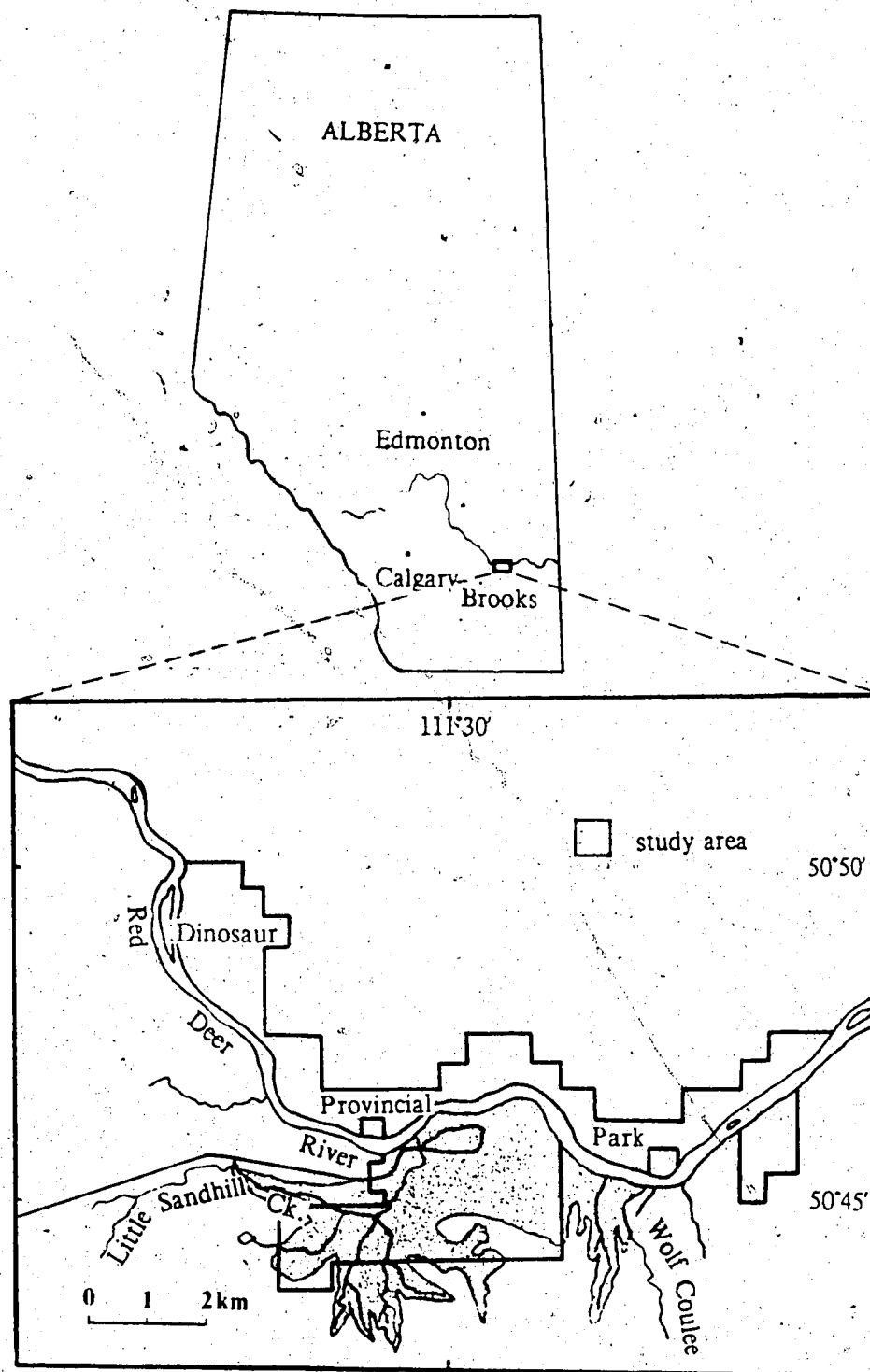


Figure 1.1 Location of the study area

1.3 Site Description

1.3.1 Geology

The badlands of Dinosaur Provincial Park have developed primarily in the Upper Cretaceous (Campanian) deposits of the Judith River Formation. This formation of nearly horizontally bedded sandstones and shales is characterized by frequent, abrupt, vertical and lateral lithological changes. Sandstones, which account for approximately 70 percent of the sediments in the Park, consist of fine-grained sands with diameters between 0.125 mm and 0.21 mm (Dodson, 1971). They are generally grey or greyish-yellow with occasional red and greyish brown units and individual beds range in thickness from less than 2.5 cm to 15 m. The finer argillaceous sediments, which are primarily soft, non-fissile shales, account for most of the remaining 30 percent of the sediments in the Park (Dodson, 1971). The shales are generally grey, or olive-grey in colour, and have a maximum unit thickness of 9 m.

These sediments are frequently interbedded with rippled muddy sandstones, iron-indurated sandstones and occasional volcanic ash layers (Koster, 1984). The shales are commonly bentonitic with a smectite content often exceeding 90 percent (Bryan *et al.*, 1984). The bentonite is likely derived from Cretaceous volcanic ash falls (Koster, 1983), carried eastward from Cordilleran eruptions. Because of the high water absorption capacity of bentonite, swelling, and subsequent contraction upon drying, results in the characteristic 'popcorn' crust observed on many shale surfaces. These surfaces seal after approximately 20 mm of precipitation, limiting infiltration and generating runoff. Although montmorillonite is the dominant clay mineral (ranging from 5-100 percent), illite can also occur in large amounts. Kaolinite is much less common, ranging from 0-30 percent (Campbell, 1987b). The amount of montmorillonite present is highly variable and is the prime control of local permeability. A pure bentonitic seam is impermeable whereas a sandstone layer with a negligible amount of bentonite may be highly permeable. Alternating layers of permeable sandstones and impermeable shales create a particularly vulnerable landform that is highly susceptible to landslides (Deere and

Patton, 1971; Rib and Ta Liang, 1978).

The diverse and complex nature of bentonitic materials have been clearly illustrated (Ross, 1964; Scott and Brooker, 1968; Grim and Gruven, 1978). The variation is dependent primarily on the type and amount of the dominant clay mineral, and the exchangeable cation present. Most of the bentonites in Alberta have calcium as a major exchangeable cation, but in the study area sodium bentonites are more prevalent. Pure bentonitic seams tend to be lenticular, thinning out horizontally, and merging with the enclosing formations. Although Ross (1964) mapped several such seams along the Red Deer River valley (near Drumheller), few pure bentonitic layers have been identified in the Park. Instead, most bentonite occurs as an admixture of the sandstones and shales.

Overconsolidated shales occur extensively in the Western provinces, and are recognized as a major cause of slope instability (Scott and Brooker, 1968). Overconsolidation occurs when loads are induced in excess of those caused by the present overburden. The transformation from a highly hydrated clayey sediment to an argillaceous rock is a function of both the magnitude of the overburden and the duration of its application. A volumetric change is associated with the escape of water as no replacement by air takes place. During consolidation a stress condition is attained that reflects the confining pressure. If the confining pressure is reduced, primarily through erosion, the sediments tend toward a new equilibrium condition in a state of reduced stress. During unloading (or rebound), the void spaces tend to increase, resulting in the influx of water and a decrease in shear strength. The extent of expansion is a function of the strain energy stored during compaction permitting the bending and compression of the clay minerals. When the load is removed, the particles tend to regain essentially their original shape, provided they were not strained beyond their elastic limit (Bjerrum, 1967). The degree and rate of expansion is varied and is restricted by the diagenetic bonds between the particles. Bonding strength depends on the consolidation pressure, constituent minerals, pore fluid temperature and time. For progressive degrees of unloading these bonds will become further stressed and will fail in increasing numbers. This time-dependent breakdown of bonds is the secondary time

effect involved in the swelling process (Bjerrum, 1967). As a result, water content depends on both the recoverable strain energy and the strength of bonds.

Unloading consists of both an elastic and a time-dependent component (Matheson and Thomson, 1973). Jointing is likely to occur as an expression of the elastic response to unloading during both uplift (glacial and tectonic) and erosion. Scott and Brooker (1968) suggested that Western Canada was subjected to two distinct and cyclic periods of loading and unloading. The first period of loading occurred with the initial deposition of sediments, followed by unloading as erosion took place during a period of uplift. Loading and unloading also occurred in response to glaciation.

The surficial geology consists primarily of glacial and glacio-lacustrine sediments (Berg and McPherson, 1973). In the vicinity of the Park, the Judith River Formation is generally overlain by 4-15 m of glacial till and lake sediments; in places these deposits are thin or absent. A well-developed prairie brown soil, 20-45 cm thick, covers the prairie and the top surfaces of the remnant mesas (O'Hara, 1986). Bryan *et al.*, (1987) suggest this soil developed on mid-Holocene loess deposits c. $5,400 \pm 800$ BP. Holocene alluvial deposits form the valley fill (O'Hara, 1986). Erratics are present in varying amounts and are scattered on both the prairie surface and within the valleys.

1.3.2 Geological History

The Judith River Formation was laid down as part of an extensive delta on the margin of the epeiric Bearpaw Sea that occupied much of central North America about 80 million years ago (Russell, 1977). Fluvial sediments derived from newly uplifted Rocky Mountains were deposited as either levee sands and silts, point bar silts and clays, floodplain vertical accretion deposits, or channel sands and bar deposits. Channel sands constitute by far the most common lithotope in the Park (Dodson, 1971). Continual channel migration resulted in the abrupt vertical and lateral discontinuities in the lithological units. Koster (1984) suggests that

deposition did not occur entirely in a freshwater environment (contradicting Dodson, 1971), but was affected by periodic tidal influences due to fluctuations in the position of the Bearpaw Sea. This variation resulted in changes in the baselevel, causing subsequent changes in the mode of deposition.

Overlying the Judith River Formation are the marine deposits of the Bearpaw Formation, that were laid down during the marine advance. Following marine regression, continental deposits accumulated for approximately 30-35 million years until about 25 million years ago. Regional uplift and tilting then occurred, and widespread denudation took place (Beatty, 1976). During the Wisconsin glacialiation (Scott and Brooker, 1968; Campbell, 1974), a veneer of till and various glacio-lacustrine and glacio-fluvial sediments were deposited. In the vicinity of Dinosaur Provincial Park, scouring by meltwater and glacial lake overflows largely removed the glacial deposits and the Bearpaw Formation, re-exposing the highly erodible Judith River Formation (Figure 1.2). Where the removal of surficial deposits was most extensive (such as along spillway margins) badlands developed.

There is evidence that spillway formation in both the Red Deer Valley and some tributary valleys was a two-stage process; an initial broad valley stage with extensive lateral scouring, followed by a period of narrow and rapid entrenchment (Bryan *et al.*, 1987). The resultant valley-in-valley form is no longer apparent in the Dinosaur Park area because of the extensive badland development. Remnants of a broad spillway extend eastward across the Park from Little Sandhill Creek to join the main Red Deer River spillway in Deadlodge Canyon (Bryan *et al.*, 1987). Once the immediate post-glacial waters were depleted, tributaries of the main Red Deer River valley began to follow the local northerly slope, channelling the drainage from the prairie surface, and thus allowing bedrock jointing to control drainage (Babcock, 1974; Koster, 1983). According to Koster (1983) the jointing pattern is a response to regional flexure over structural highs such as the Sweetgrass Arch of southern Alberta. An example of a stream affected by this jointing pattern is Little Sandhill Creek which may originally have flowed west-east through a spillway, but was later captured by tributaries eroding headward

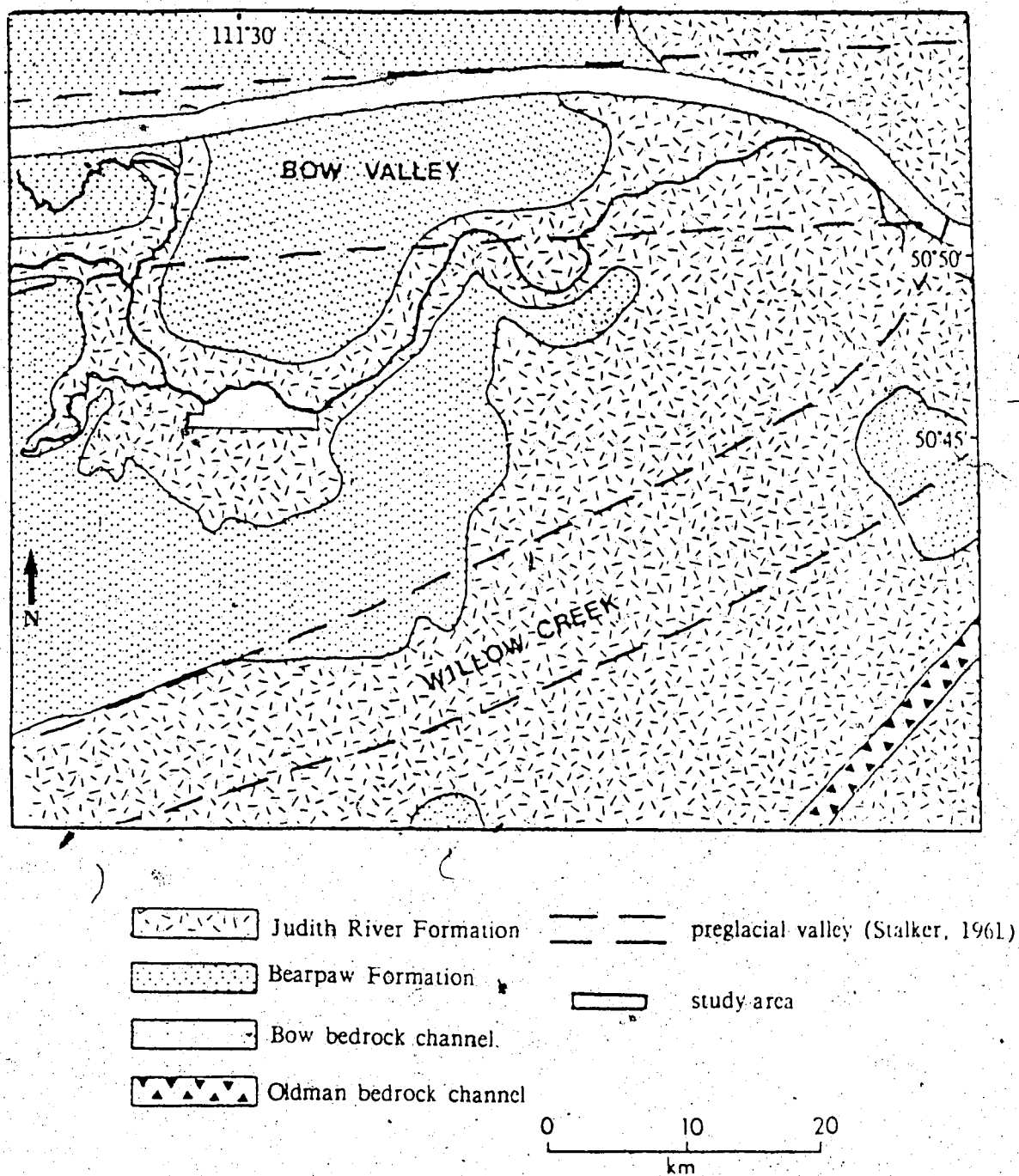


Figure 1.2 Bedrock geology in the vicinity of the study area - modified after McPherson, (1968)

along the dominant joints (Bryan *et al.*, 1987).

Erosion rates have fluctuated significantly throughout the Holocene. Bryan *et al.*, (1987) believe that within the first few hundred years following deglaciation coulee incision was generally very rapid, creating valleys 60 m in depth and several kilometers long. Following this initial extensive erosional phase there have been two primary controls on the erosion rate in the Park area; climatic variations and loess deposition. The immediate post-glacial climate was cool and moist, but became increasingly arid from c.9,000 to 5,000 BP (Schweger *et al.*, 1981). Associated aeolian activity deposited loess on the prairies and badland surfaces as the dominant north-west winds stripped the land of the fine glacio-fluvial and lacustrine sediments. Yair (1983) found that loess has a high water absorbancy as compared to the almost impermeable bedrock. This loess deposition would retard badland development. Most of the removal of the loess has occurred only within the last 2-3,000 years (Campbell, 1987a).

The warmer and dryer period was followed by a generally moister climate (with possible periods of considerable instability) that extended between c.4,000 - 2,170 BP (Schweger *et al.*, 1981). Since then, the climate has been drier and warmer, similar to that found in south-eastern Alberta today (Bryan *et al.*, 1987).

The current mean annual badland denundation rate has been calculated as c. 4.0 mm/yr (Bryan *et al.*; 1987, Campbell, 1987a). Peak rates, however, can reach 13 mm/yr (Campbell, 1974, 1981). There is considerable variation in runoff response and surface resistance (Bryan and Campbell, 1986). The weak bedrock is readily weathered and eroded at a greater rate than soil can develop, restricting plant growth. As a result of this, and the impermeable nature of the bedrock, runoff significantly alters the character of the various surfaces, producing three main types; the aggregate covered (popcorn) shale slopes, the rilled and channelled sandstone slopes, and, the pedimented-alluviated slopes (Campbell, 1987b). The slopes are generally steep, averaging 30 degrees (Campbell, 1974), and the maximum relief is 100 m. These long, steep, unvegetated slopes of generally weak material enhance denundation through both mass

movements and other erosional processes.

1.3.3 Climate

Southern Alberta has a continental climate - BSk in the Koppen system, with extreme seasonal variation in both temperature and precipitation. Precipitation data from Brooks (40 km south of the Park) provide the longest and most reliable record in the area, and show that the mean annual precipitation is approximately 335 mm/yr (Table 1.1).

Table 1.1 - Precipitation data from Brooks AHRC: 1953-1980

	Jan.	Feb.	Mar.	Apr.	May	Jun.	Jul.	Aug.	Sep.	Oct.	Nov.	Dec.	Year
Mean snow/water equiv(mm)	20.9	13.6	13.5	11.3	0.9	0	0	0	0.6	3.6	12.2	20.0	96.6
Mean rainfall(mm)	0.9	0.8	2.5	14.8	37.4	65.7	32.2	40.1	32.8	8.3	2.4	1.0	238.9
Total precip.(mm)	21.8	14.4	16.0	26.1	38.3	65.7	32.2	40.1	33.4	11.9	14.6	21.0	335.5

Data source: Canadian Climate Normals: Precipitation 1951-1980, vol.3, Environment Canada, 1982

The majority of this precipitation (about 70 percent) falls during the summer months, between May and September, often as local convective storms. These storms are relatively intense, and are generally of short duration. Typical rainstorms attain intensities of 20-30 mm/hr but peak intensities of 84 mm/hr for a 6 minute period have been recorded (Bryan and Campbell, 1980). The remaining 30 percent of the total annual precipitation falls as snow in the winter months being concentrated in December and January. Snow maximum accumulation zones are in depressions (rills and gullies) and on the lee slope bases (north, clockwise to south) (Harty, 1984). Chinook winds often result in significant mid-winter snow depletion and runoff.

The mean annual temperature is 3.9°C with a mean annual temperature range of almost 40°C. However, extreme temperatures of more than 40°C in the summer, and -48°C in the winter, have been recorded. Thus, the absolute temperature range is virtually 90°C. The

summers are short and warm, and the winters are long and cold. Winter temperatures fluctuate under the influence of frequent chinooks which can raise the temperature as much as 10°C in two hours. Because temperatures of 0°C may be experienced during eight months of the year, spring and autumn rainstorms by day may alternate with frost at night (Campbell, 1974).

Climatological data from Dinosaur Provincial Park and Brooks AHRC were collected for the field season from May until September 1986, and are summarized in Table 1.2. In comparing the Park data with that of Brooks, it is evident that during this particular season, temperatures are comparable but precipitation in the Park is, in general, considerably lower. The exceptions are the months of May, when Dinosaur Provincial Park received only 1.3 mm less precipitation than Brooks, and July when the Park received 1.4 mm more precipitation than Brooks. It is worth noting that the precipitation at Brooks for the months of May, July, and September significantly exceeds the norm (based on the 30 year average). The average precipitation for these five months exceeded the norm by 166 percent. The contrasting data for the two stations clearly show the precipitation variation that exists over a relatively short distance due to the highly localized nature of the storms that tend to dominate the summer precipitation pattern.

1.3.4 Vegetation

Vegetation in the badlands is limited by the semi-arid climate, poor soil development, highly erodible bedrock, and steep slopes. Surfaces with loess deposits tend to have a denser vegetation cover, particularly of grasses, because of greater infiltration capacity and better soil development.

The vegetation in the Park is dominated by several species of prairie grasses, xerophytic flowering plants and shrubs. Larger plants such as cottonwood trees, willow, and alder are more rare and occur in isolated clumps. O'Hara (1986) found that some species dominated certain types of surfaces; drought resistant blue grama (*Bouteloua gracilis*) and needle grass (*Stipa comata*) generally dominated dry sites. Other less frequently observed grasses are;

Table 1.2 - Field season (1986) climatic data - Dinosaur Provincial Park

	May	June	July	August	September
mean daily max.temp(C)	17	25	23	27	14
mean daily min.temp(C)	15	18	17	18	6
mean daily temp(C)	16	22	20	23	10
extreme max.temp(C)	35	35	31	36	27
extreme min.temp(C)	2	13	14	13	2
total precip.(mm)	53.0	0.0	25.1	11.5	0

Field season (1986) climatic data - Brooks

	May	June	July	August	September
mean daily max.temp(C)	19	24	23	26	14
mean daily min.temp(C)	5	10	10	9	4
mean daily temp(C)	12	17	16	18	9
extreme max.temp(C)	34	34	30	34	25
extreme min.temp(C)	-4	5	6	2	-2
total precip(mm)	54.3	30.5	62.9	12.8	140.6
% of normal	142	46	195	32	416

western wheat grass (*Agropyron smithii*), June grass (*Koeleria cristata*) and Sandberg bluegrass (*Poa secunda*). Xerophytic plants such as prickly pear (*Opuntia polyacantha*) and cushion cacti (*Mamillaria vivipara*) are commonly found in small clusters on alluvial fan and prairie surfaces. Drought resistant shrubs such as sagebush (*Artemisia cana*) and pasture sagwort (*Artemisia frigida*) are generally found in areas that probably reflect higher subsurface moisture conditions (O'Hara, 1986).

Badland slopes are largely barren. However, some vegetation covers lower angle colluvial slopes, and there is a marked increase in the amount of vegetation, particularly the

sagebush and grasses, around piping features. This is evident at both the inlet and outlet locations reflecting areas of a greater concentration of moisture. On slopes with a northerly aspect are grasses and creeping juniper bushes (*Juniperus horizontalis*), indicative of a greater amount of available water. Alder (*Alnus crispa*), thorny buffalo-berry (*Shepherdia argentea*) and occasionally willow (*Salix spp.*) dominate the depressions which act as water traps in the grabens of several of the mass movement features. (*Shepherdia argentea*) (and occasionally willow (*Salix spp.*)) dominate the depressions which act as water traps in the grabens of several of the mass movement features.

2. Literature Review

2.1 Terminology

Many terms used to describe mass movement features are ambiguous and redundant. It is therefore essential to establish a specific and consistent vocabulary.

The term landslide has been traditionally used as an all-encompassing word for slope failures. It is generally considered unsuitable (Crozier, 1973; Varnes, 1978) as the active part of the word specifically denotes sliding, thus precluding other forms of slope movements such as falls, topples, flows, and spreads. The word landslide will be retained when it is employed by cited authors, and different interpretations are not considered possible. Mass movement is currently accepted as a more refined collective term that refers to the outward or downward movement of material under the influence of gravity. This term necessarily includes gravitationally induced movement on horizontal ground, such as subsidence. Varnes (1978) has advocated the term slope movements for those mass movements restricted to slopes. In this study, since no horizontal failures are considered (except perhaps in reference to piping channels), the term mass movement refers specifically to slope movements.

Slope failure is another widely used collective term. Terzaghi (1950) restricted its use to slope movements on engineered slopes. Because engineered slopes are not included in this study, slope failure will be used synonymously with mass movement. Slope instability refers to the predisposition of a slope to mass movement.

Mass wasting is occasionally used synonymously with mass movement, but is actually a broader geomorphic concept that refers to the mass reduction of the interfluvies as opposed to degradation by channelized flow (Crozier, 1986). Mass movement processes grade imperceptibly with increasing water content into fluvial processes. Fluid mass movements often transport large-calibre debris on the surface or at the front of the failure lobe.

The nomenclature used here follows Varnes (1978).

Terms related to the sequence or repetition of movement should also be clarified. Retrogressive slide or flow failures begin in a localized area and enlarge or retreat opposite to the direction of movement. This expansion occurs either by spreading of the failure surface, successive rotational slumps, falls, or by liquefaction (Varnes, 1978). These retrogressive failures can either be multiple or successive. The term multiple refers to the development of the same mode of movement where each failure surface is tangential to a common, generally deep-seated failure surface. Hutchinson (1968) suggests that if the failures were initially rotational, an increasing number of units would change the character of the slide towards translational. Successive failures are comprised of any type of multiple movements that develop successively in time.

The term progressive has often been loosely used in reference to an advancing or retreating slide. More precisely, however, it is used to denote the process of a slow cumulative loss of strength of a material over time (Bjerrum, 1967).

2.2 Classification

2.2.1 Varnes Classification

The most widely used North American classification is by Varnes (1978). It is based largely on a previous classification by Sharpe (1938), augmented with segments from other sources, including in particular Zischinsky (1966), Zaruba and Mencl (1969), Skempton and Hutchinson (1969), Nemcok *et al.*, (1972), and de Frietas and Watters (1973).

Varnes classification is based on two criteria; the type of movement and the material involved (see figures in Varnes, 1978). There are five main types of movement: falls, topples, slides, spreads and flows. A sixth group includes all complex failures which are a combination of two or more of the aforementioned types. Most movements are complex (Varnes, 1975).

In terms of the type of material involved, two main classes are used: rock, and engineering soils. Soils can be further classified as either debris or earth. Rock is a natural

aggregate of minerals connected by strong cohesive forces whereas soil aggregates can be readily separated by agitation. Because the type of movement and material varies both spatially and temporally, any classification system should be flexible. Furthermore, an almost continuous gradation may exist in both the movement and material type, thereby negating the use of a rigid classification.

2.2.2 General review of mass movements present in Dinosaur badlands

Four main types of mass movements were present in the badlands of Dinosaur Provincial Park; falls, topples, slides, and flows (Figure 4.1 in pocket at back). The failures, especially the larger ones, were generally a combination of at least two different types. There was a large range in the magnitude of the mass movements, and a corresponding inverse relationship with frequency. The specific magnitude and frequency of each failure type provides an indication of the general nature of mass movements.

In falls, a mass of any size is detached from a steep slope along a surface on which little or no shear displacement takes place. Material descends mostly through air by either free fall, saltation or rolling. Movements of this type range from very rapid to extremely rapid (Varnes, 1978). The combination of very resistant iron-indurated sandstone overlying a significantly weaker bedrock layer of less indurated sandstone or shale inevitably leads to differential erosion. Falls occur when either fracture planes within the caprock can no longer resist the strain induced by the support removal, or when the unstable caprock becomes unbalanced. This failure type is common (Figure 2.1) and has a high frequency, but a low to medium magnitude range.

Topples involve the forward rotation of a unit (or units) around a pivot point at or near the base. They may or may not culminate in falling or sliding, and are sometimes evident as detached blocks perched precariously on a valley wall. A number of these blocks, tilted but not yet fallen, were observed (Figure 2.2). Rock and debris topples generally have a low to medium magnitude and frequency. Debris topples commonly occur in the valley fill at

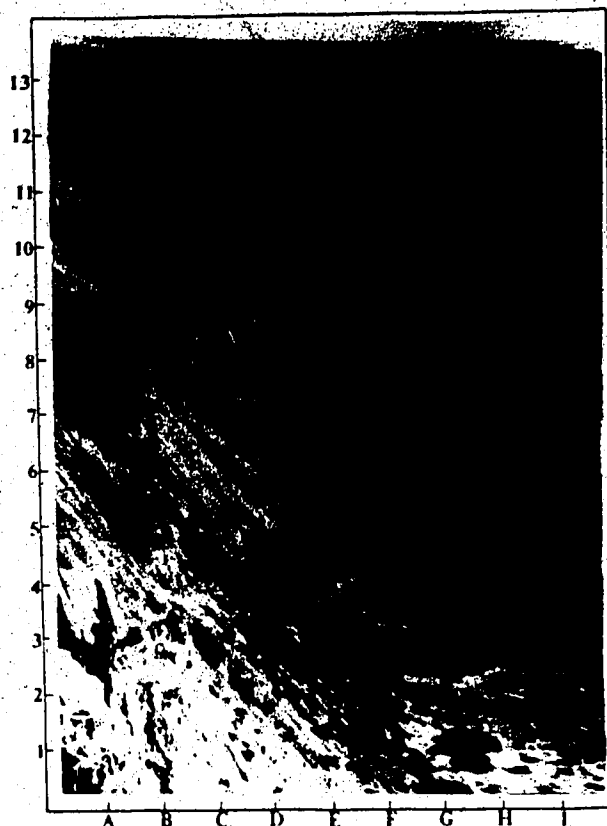


Figure 2.1 Little Sandhill Coulee - looking east. Fallen debris along slope base (E4 and F8).

Relief here is of the order of 30 m.

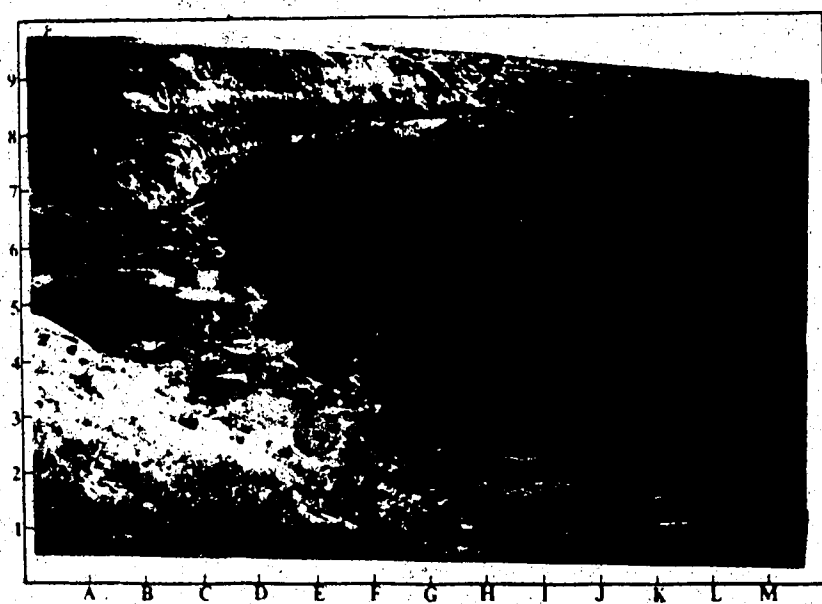


Figure 2.2 Perched topple block along tributary valley wall (H6) (Little Sandhill Coulee).

Slopes are about 15 m high.

meanders along the channels.

Slides are movements of a more or less coherent mass along one or more well defined surface(s) of rupture. The degree of deformation is indicated by the terminology used: For instance, the terms block and intact refer to slides consisting of one or a few moving units while the terms broken and disrupted refer to those consisting of many units. The latter terms are different again from the term debris slide which indicates only those slides originating in debris.

Slides are generally classified according to the form of the failure plane, of which there are two main types: translational (which has a more or less planar shear surface) and rotational (which has a failure surface curved concavely upward). Rotational slides tend to occur most frequently in homogeneous materials with uniform strength parameters (Piteau, 1982). These slides generally evolve by a process of yielding and then rotating and are often characterized by units that are tilted backward and toward the slope (see figure in Varnes, 1978). Rotational slides are commonly deep-seated and tend to increase in depth with an increase in slope angle (Skempton and Hutchinson, 1969).

Translational slides are often characterized by a graben (see figure in Hansen, 1965). The movement of a translational slide is generally controlled by surfaces of weakness such as faults, joints, or bedding planes, or by the contact between firm bedrock and overlying detritus (Varnes, 1978). In contrast to rotational slides the mass of these slides tends to be greatly deformed. In general, as water increase the slide mass develops into a flow.

There is a fundamental difference between the movement of rotational and translational slides that greatly affects the equilibrium of each. If the surface of rupture dips into the slope at the foot of the slide, the rotary movement of a rotational slide tends to restore equilibrium of the unstable mass. As a result, the driving moment during movement decreases and the slide may stop moving. A translational slide, however, may progress indefinitely if the surface on which it rests is sufficiently inclined and if the shear resistance along this surface remains lower than the driving forces (Varnes, 1978).

Compound slides having both translational and rotational components were the most common type (Figures 2.3 and 2.4). The translational component was generally dominant, but various gradations do exist. These slope failures had a medium to high magnitude range, and a medium frequency.

In spreads, the dominant mode of movement is lateral extension accommodated by either shear or tensile fractures (Varnes, 1978). This is the only group of failures in the Varnes classification scheme that was not represented.

Flows include a wide range of movements with significant variation in the velocity and water content. The main types are creep, dry flows, and viscous or fluid flows. Creep is the slow downslope movement of the regolith (and possibly rock), a deformation that continues under a constant stress. Because there is considerable disagreement concerning the geomechanical properties of creep, a more precise definition is not possible, and the use of this term is somewhat arbitrary. Nevertheless, two distinct forms of creep can be identified. This distinction is based primarily on the magnitude of each. Large-scale creep, which is the most common form, is seldom evident as it is limited to those slopes with a gentle gradient which permits soil development (Figure 2.5). Large-scale creep generally has a medium magnitude and a low frequency. In contrast, small-scale creep occurs widely, especially on shale slopes. Under the influence of weathering processes, the shale slopes readily develop a thin weathered mantle (5-10 cm thick) commonly referred to as 'popcorn' crust. This mantle has a tendency to creep down even a low angle slope. This displacement continues until stresses are induced that exceed the internal strength of the material (in particular, the cohesion between the aggregates), resulting in a more rapid failure. If the shear stresses induced by gravity are equal to the residual shear strength, the slope will experience steady slow creep, and will not lead to a slide (Bjerrum, 1967). If failure does occur, the freshly exposed surface will again be subjected to weathering. In this cyclic manner creep has a significant functional role in the denudation of the badlands (Schumm, 1956). Creep of this nature generally has a low magnitude, but a very high frequency, especially where shale slopes form the upper unit of a lithological



Figure 2.3 A compound slide (dominantly translational) in Waterfall Coulee. Multiple scarps indicate retrogressive nature.

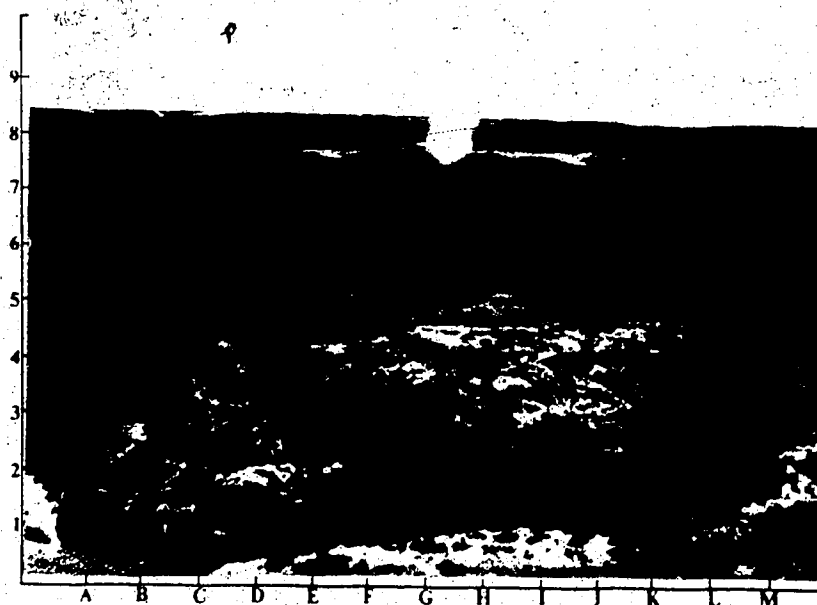


Figure 2.4 Tributary coulee of Princess Coulee - a compound slide (dominantly rotational); about 25,000 m² in area.

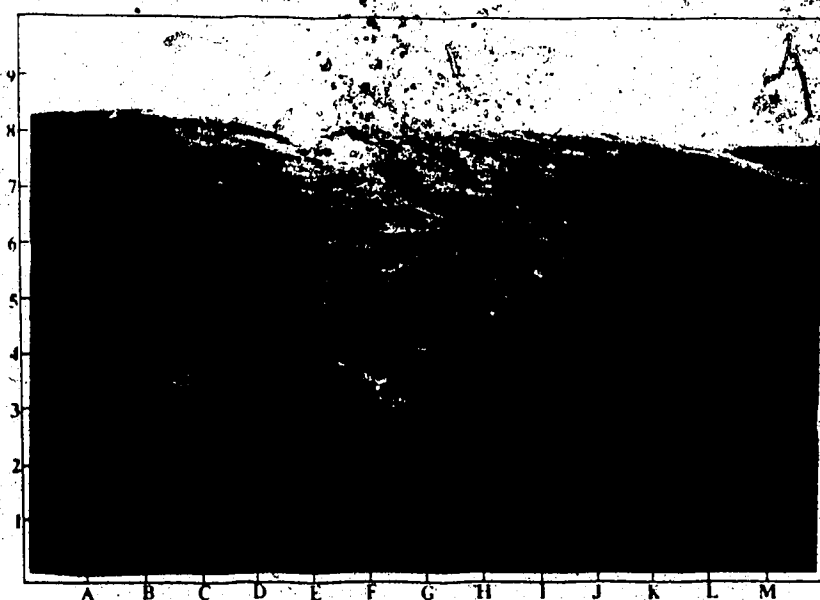


Figure 2.5 Grassed tributary coulee of Princess Coulee - looking south. Regolith creep terracettes enhanced by animal paths (normal-I4; tear-K6).

sequence.

Debris flows lack coherence throughout the mass. They often begin as either slides, falls, or as topples on steep slopes (greater than 15° - 20°), but rapidly disintegrate with the loss of coherence. Prerequisites for most debris flows include an abundant source of unconsolidated fine-grained rock and soil debris, steep slopes, a large but intermittent source of moisture, and a sparse vegetation cover (Costa, 1984). These conditions are common in the badlands. Mudflows differ from debris flows in that they consist primarily of fine grained sediments in which at least 50 percent are sand, silt, and clay-sized particles (Varnes, 1978).

The classification of flows incorporates the complete range of water content from liquid to dry (Varnes, 1978). Dry flows involve the movement of particles that are suspended in a medium of air instead of water. This flow type is due primarily to fine grained blocks falling downslope and disintegrating en route. Som (1980) distinguishes between flows and falls according to the slope angle, where flows are restricted to slopes between 27° and 29° while falls occur on slopes exceeding 35° . This distinction will not be made here. All failures (on any slope angle) that involve a falling mass which makes contact with the subjacent slope face at a point above the base, will be considered as flows. The distinction becomes evident in Figure 2.6. The failure to the left is classified as a dry flow, while fallen debris is evident in the centre of the photograph, overlying debris from a previous slide. This is the most common failure type, occurring on virtually all slopes but with a considerable variation in size. They tend to be shallow and frequently follow pre-existing drainage paths. Such failures have a low magnitude (generally) and a very high frequency.

Debris flows involving water are less common and generally occur in conjunction with other failure types (complex form). Individual debris flows therefore have a low to medium magnitude and low frequency. As a complex form, these flows have a similar magnitude, but a higher (medium) frequency.

Piping involves both erosional and mass failure characteristics. The initial surface subsidence and pending collapse are clearly forms of mass movement, but the actual formation

of the pipe is due to subsurface erosion. Pipes occur extensively along both undisturbed and failed slope units (Figure 2.7). Where they exist in conjunction with other failure types (complex form) it is difficult to determine whether they existed prior to (and therefore enhancing) the failure, or whether they have resulted subsequently. In either case, piping channels reduce slope stability by either increasing pore pressures, or by depleting the internal support of the slope. Individual or fused pipes have a low to medium magnitude and a high frequency. Complex failures involving pipes tend to have a larger magnitude, but a much lower frequency.

Slope movements mostly involve a combination of one or more of the principal types of movements. The different components of these complex slope failures either occur in various parts of the moving mass, or at different stages of development of the movements (Varnes, 1978). Numerous combinations are possible but three types were identified; (1) compound slides which are the most common and have a relatively high magnitude and a medium frequency, (2) slide/flow combinations and, (3) piping/flow combinations which both have a medium to high magnitude and a low frequency.

2.3 Causes of Instability

2.3.1 General

In all slopes there are forces which act to promote movement (shear stress) and opposing forces which resist movement (shear strength or resistance). When the disturbing forces exceed the resisting forces movement will occur (Figure 2.8). Disturbing forces, referred to as internal and external causes by Terzaghi (1950), arise primarily from a decrease in shear strength or an increase in shear stress.

Resisting forces depend on the strength of the slope material. The two primary components of this strength are cohesion and friction. Cohesion is the inherent inter-particle coherence, independent of normal stress. Effective cohesion is dependent primarily on the

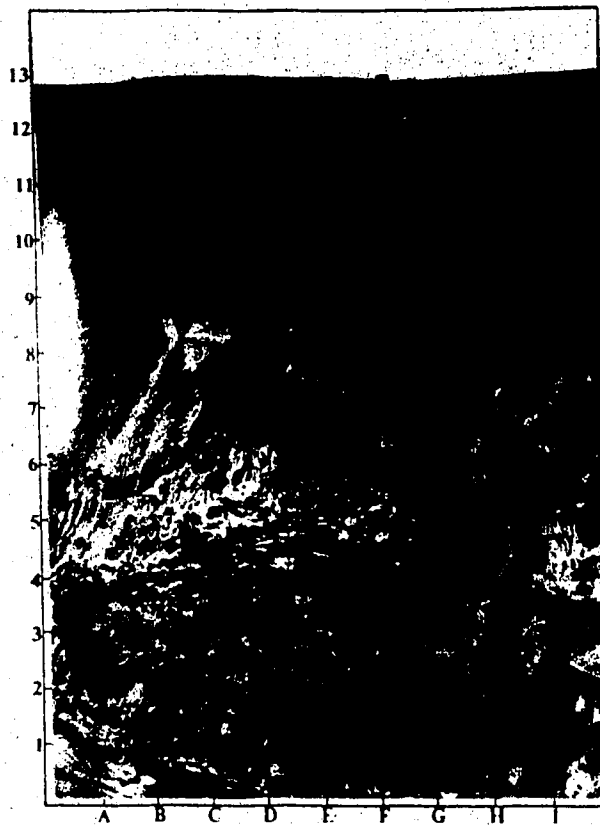


Figure 2.6 Sonofabitch Coulee-- looking southwest. Three adjacent failures: dry flow (B8), fall debris (F6), and a slide (E4) (cow on prairie surface for scale).

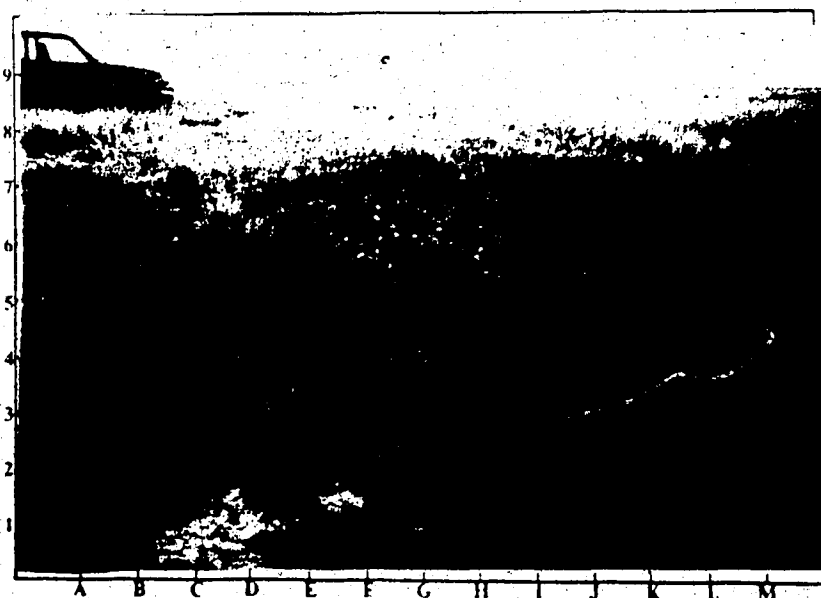


Figure 2.7 Large prairie pipe (I4).

extent of jointing and fissuring. Of subsequent importance is the strength of the material that may occupy the gaps.

Friction is directly proportional to the normal stress between the surfaces. The interlocking of asperities, under high normal stress, will result in shearing if the applied force is sufficient. Interlocking friction will therefore depend on the denseness (or packing) of the particles and high packing will result in high friction. Grain angularity is also important as rounded or platy particles do not interlock as well as angular ones.

In the assessment of the stability of a rock or soil mass, methods of limiting equilibrium are often used. In such an analysis the shear strength of the material is assumed to be fully developed along the slip surface at failure. The most widely accepted principles that govern shear strength follow the Mohr Coulomb criterion. Total shear strength is defined as follows:

$$s = c + \sigma \tan \phi \quad (1)$$

where:

- s = shear strength
- σ = normal stress on a slip surface
- c = cohesion
- ϕ = angle of internal friction

This equation, however, does not account for the significant effect of pore water pressures. These pressures consist of the hydrostatic pore pressure related to the groundwater level, and the excess pore pressure due to applied loads. This excess pore water pressure may be positive or negative, depending on the type of soil and the stresses involved. Under fully drained, long-term conditions, the excess pore pressure is zero.

Effective stress includes the force opposing normal stress by incorporating the effects of water, such that:

$$\sigma' = \sigma - u \quad (2)$$

where:

- σ' = effective normal stress
- σ = total normal stress
- u = pore pressure

Therefore, shear strength can be more accurately expressed in terms of effective stress as follows:

$$s = c' + \sigma' \tan \phi' \quad (3)$$

where: c' and ϕ' are the strength parameters for effective stress.

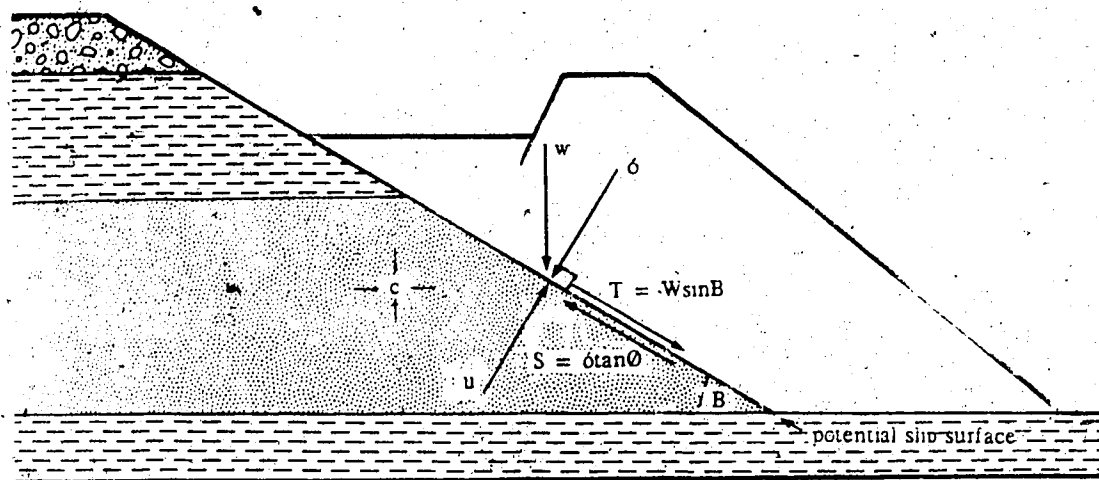
In reference to this equation, cohesion generally decreases with an increase in water. The frictional angle (ϕ') is usually very low (4° - 12°) for bentonitic shales (Mollard and James,

1984) resulting in low shear strength values or actual failures. Material deformation depends on effective stress, not total stress, as total stress can be constant, but pore pressure will naturally vary significantly. In general, the strength of a material is defined according to its peak strength, which is attained immediately prior to deformation (Figure 2.9, points a and b). When applied in a stability analysis it is assumed that the peak strength is attained simultaneously along the entire slip surface. Depending on the material and failure type, this is not necessarily the case (as in progressive failures), as some points reach peak strength before others and therefore also prior to failure. Taylor and Cripps (1987) suggest that significant displacement (of approximately 1 m) is probably required before a continuous principal slip surface is induced, possibly by the coalescence of separately growing shear surfaces and zones. Only when this surface is formed can the lowest shear strength be mobilized, probably at its residual value (secondary strength).

Many soils experience a decrease in strength once the peak strength has been reached. The magnitude of this lower limit of strength, the residual strength, is partly influenced by the ratio of plate-shaped (clay minerals) to spherical particles. Residual strength has the character of pure friction and is controlled by the pore fluid composition and the clay mineral type (Taylor and Cripps, 1987). A high percentage of plate-shaped particles leads to a low residual strength and for the formation of a continuous shear plane (Skempton, 1964). In general terms, peak and residual parameters provide the upper and lower limits of strength, with a complete range existing between the two.

A quantitative comparison between the disturbing and resisting forces is conventionally expressed by the ratio of resistance to shear stress. This ratio yields a value termed the factor of safety (F). At the moment movement occurs (the point of limiting stability), it is assumed that this value is 1.0 (when resistance equals shear stress). Values greater than unity indicate progressively more stable conditions. This method of stability assessment is known as 'limiting equilibrium analysis' (Terzaghi and Peck, 1967), and can be calculated as follows:

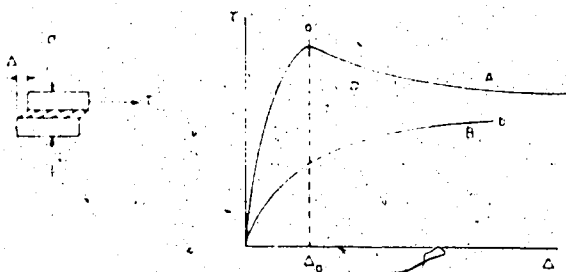
$$F = S/T \quad (4)$$



c = cohesion
 ϕ = angle of internal friction
 W = weight of a given mass
 σ = normal stress
 B = inclination of a slip surface
 u = pore water pressure

T = shear stress (disturbing forces)
 S = shear strength (resisting forces)

Figure 2.8 Resolution of forces on a potential slip surface



where: a = peak strength
 b = peak strength
 T = stress
 Δ = strain
 c = lower limit to strength (strain softened)
 ϕ = normal stress

Figure 2.9 Stress-strain curves - material A is more brittle than B, resulting in a larger strength decrease after peak strength is reached - adapted after Wu and Sangrey, 1978

where: S = shear strength (resisting forces)
 T = shear stress (disturbing forces)

This analysis can be worked in reverse ('back analysis') where known parameters and values are manipulated in order to find the unknowns. If the properties of the material are known (unit weight and shear strength), as well as the pore water pressures and the dimensions of the unstable mass, then, via the stability equation (4) the slope angle for limiting stability ($F = 1$), and the probable position of the failure plane can be determined.

2.3.2 Factors contributing to slope failures

The factors contributing to slope failures are numerous; some leading to a decrease in shear strength (internal causes), and others leading to an increase in shear stress (external causes). The division between the two is arbitrary and is only a convenient method of slope stability assessment. In general, the internal changes in the mass strength tend to be cumulative, developing over a long period of time, and are often a result of one or more external changes.

Causative factors vary temporally and can be either passive (slow-changing), transient, or active (fast-changing). Although passive factors act progressively over a long period, reducing the resistance/shear stress ratio, in almost every case a transient factor can be identified as having triggered the movement (Crozier, 1987).

Many factors affect slope stability; only a brief description of the principal ones will be given here. This subject has been covered extensively (Skempton and Hutchinson, 1969; Carson and Kirkby, 1972; Blyth and de Freitas, 1979; Brunsden, 1979; Zaruba, 1982; Mollard and James, 1984; Crozier, 1986, 1987). The factors causing a decrease in shear strength are virtually all initiated by weathering processes (Kenney, 1975; Quigley, 1975; Day, 1980; Taylor and Cripps, 1987). Physical and chemical weathering are responsible for destroying aggregates and creating surficial fissures and cracking at depth. The large variation observed in the strength of a clay is a consequence of both the random variation in water content and fissure spacing (Chandler, 1972), which generally increase with depth. Of prime importance is the increase in

infiltration of water through the weathered zone, resulting in numerous strength reduction effects; intra-particle rehydration of expandable clay minerals, an increase in pore water pressures and removal of salts (eg. Na) and cementing agents by solution and leaching. Water is therefore the agent deemed most responsible for the strength reduction of a material. Rib and Ta Liang (1978) support U.S. Federal Highway Administration findings which claim that water is the controlling, or main, contributing factor in about 95 percent of all landslides. With the addition of water, bentonitic clay minerals readily swell. The alternating expansion and contraction involved with particle hydration and dessication produces severe disruptive effects on aggregate stability. Swelling is a result of stress relief (particularly when high horizontal stresses are involved), intra-particle swelling of expandable clay minerals and inter-particle (osmotic) swelling between the clay minerals.

Taylor and Cripps (1987) found that the peak effective shear strength parameters of overconsolidated clays dropped significantly from a non-weathered to a weathered sample. The change in the degree of weathering degradation usually involved a large drop in cohesion, but a smaller change in the angle of shearing resistance. Overconsolidated clays will continue to dilate, reducing strength to the residual value.

Heavily jointed or weathered rock masses exhibit failure characteristics between those of rock and soil (Hoek, 1982). Analysis of failure mechanisms should therefore be based on the strength of the discontinuities, rather than the strength of the intact rock itself (Cruden, 1975; Pitcairn and Martin, 1982). Because of the swelling nature of the bentonite the effect of the dessication cracks is significantly reduced. Depending on the crack density, and rate of swelling, it is possible that a less dessicated layer at depth will seal before the outside layer. An impermeable layer will then form, creating a weakened zone. Prolonged periods of precipitation will cause almost complete surface sealing. Once saturation occurs mudflows may result (Yair, 1980) in a series of surges and microslumps (Bryan *et al.*, 1978).

Several factors causing an increase in the shear stresses, are as follows:

- loading (surcharge) or unloading

- removal of lateral support (such as that caused by fluvial erosion)
- undermining caused by piping or groundwater sapping
- the formation of tension cracks.

When a clay is initially unloaded it is possible that the excess pore pressures will be negative, increasing the shear strength. Subsequent swelling occurs as pore pressures increase, such that the effective shear strength will decrease in accordance with the rate of swelling. Unloading of overconsolidated shales enhances physio-chemical weathering by allowing the infiltration of greater amounts of water. According to Taylor and Cripps (1987) unloading, together with surface erosion, may have a major role in decreasing slope stability.

The removal of lateral support will result in the release of horizontal stresses, weakening the slope material. Also, both the height and gradient of the slope will be altered, increasing the degree of internal stress. The role of critical height (Dacombe and Gardiner, 1983) and critical slope angle are well known (Carson, 1975). When a slope is over-stressed, because it is either too steep or high, the clay particles necessarily shed some of their load to neighbouring elements. Terzaghi and Peck (1948) concluded that in a non-uniform stress and strain situation, shear stress distribution will develop in this manner, leading to a progressive failure.

Undermining by piping appears to have a dominant role in the badland evolution (de Lugt, 1986; Beaty and Barendregt, 1987). According to Campbell (pers. comm., 1986), stresses caused by deformation during diagenesis or unloading may have created fractures facilitating piping erosion. In general, and in decreasing order of importance, pipes most readily develop in the presence of swelling clays (especially montmorillonite); extensive dessication; seasonally high precipitation; differentially permeable layers; a steep hydraulic gradient; and where outlets are above the base level of erosion, usually appearing initially as seepage zones (Parker, 1963).

The presence of tension cracks significantly increases the shear stress of a slope by providing a ready access for water into the slope. Any water that may become trapped in these cracks, or the surrounding matrix, can exert considerable outward pressure. Baker (1981)

presented a system of formulas and charts to estimate the depth of tension cracks and their effect on slope stability.

Three stability states can be identified when assessing the causes of instability. This concept, as proposed by Crozier (1986), distinguishes the three groups of destabilizing factors on the basis of function (Figure 2.10). These groups include preparatory, triggering, and controlling factors. Preparatory factors create an environment that makes the slope susceptible to movement but does not actually initiate it. In other words, these factors tend to place the slope in a marginally stable state. Triggering factors initiate movement, shifting the slope from a marginally stable to an actively unstable state. Controlling, or perpetuating, factors dictate the conditions of movement (form, rate, and the duration of movement) as it takes place. The aforementioned internal and external causative factors may take on any of these functions, depending on the degree of activity and the margin of stability within the slope.

2.4 Past Research

2.4.1 Valley Rebound

Overconsolidation of the clay shales in Western Canada has had a marked effect on the morphology of the present landscape. Because of the extreme pressures exerted during consolidation the subsequent release during unloading resulted in distinct strain release features. During loading, when the vertical stress was increasing, the effective horizontal stress was also increasing at a rate dependent on the shear resistance properties of the clay (Bjerrum, 1967). For weak clays the induced horizontal stress would be larger than that of strong clays. During unloading the clay is able to expand vertically, but not horizontally. As a result, the changes in effective vertical stress were greater than the changes in effective horizontal stress. Therefore, excavation, such as that induced by fluvial erosion of valleys, will allow the release of these excessive horizontal stresses. As the lateral support is removed the outward expansion will likely result in slope failure (Bjerrum, 1967).

Also directly related to rebound is 'valley flexure' as defined by Matheson and Thomson (1973) in southern Alberta, Saskatchewan, and Manitoba - an area of low surficial relief, and a thin veneer of glacial deposits. This phenomenon has two distinct components: raised valley rims and a gentle anticlinal structure at the valley bottom. With the raised valley rims there is an upwarping of the beds in the valley walls. The dip of these beds increases as the valley is approached. The amount of rebound along the valley perimeter can be as much as 10 percent of the valley depth, although values of 3-5 percent seem more common (Matheson and Thomson, 1973). The resultant change in bed inclination, although minor (in the order of 1-2°), is often characterized by interbed slip. This displacement may then give rise to mylonite zones (Matheson and Thomson, 1973), which will significantly affect slope stability, especially if they are located near the base of the slope. These stress relief features of thin (0.6-1.3 cm) nearly horizontal layers of soft remoulded material tended to occur at the contacts of different lithological units, lowering the shear strength along the bedding planes.

The rebound of the valley floor (the anticlinal structure) occurs in response to both a vertical stress relief and the inward movement of the valley walls as a function of the lateral stress relief (Matheson and Thomson, 1973). Interbed slip also takes place in this area, below the centre of the valley bottom (Figure 2.11).

The extent of rebound depends primarily on the modulus of elasticity (E) of the bedrock, where (E) is the stress to strain ratio at a given stress level. For a low modulus, a change in stress by either loading or unloading will produce a relatively large strain. Accordingly, Matheson and Thomson (1973) found that there was a marked trend for larger amounts of rebound in bedrock with a low modulus of elasticity. It is important to note that the bedrock of their study area is characterized by low values of E , for both the Pierre and Bearpaw shales which have modulus in the order of 3,325 to 6,650 Pa. This and other parameters affecting the extent of rebound have been covered in detail by Thomson and Matheson (1973). In general, these rebound features are best developed in areas with low topographic relief and thin overburden, where the river valley is steep-walled and deep

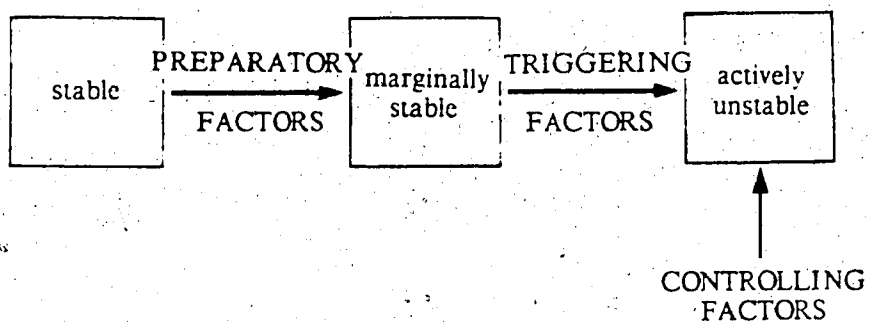


Figure 2.10 Destabilising components - modified after Crozier (1986).

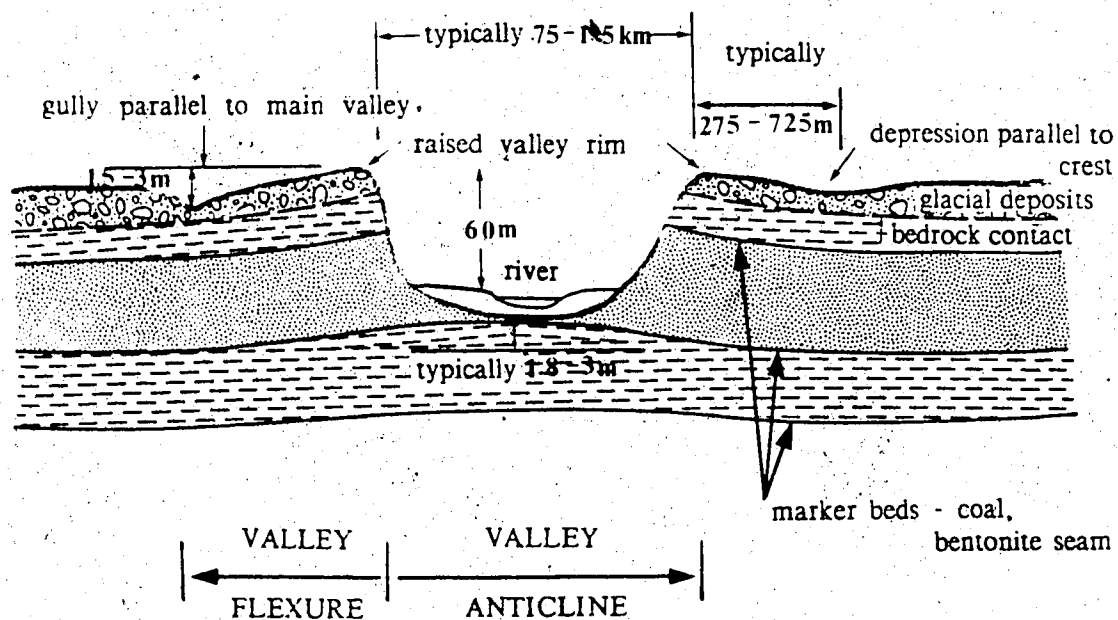


Figure 2.11 Schematic rebound - modified from Matheson and Thomson (1973)

(Matheson and Thomson, 1973). Such conditions typify the badlands.

2.4.2 Aspect

The influence of aspect, or slope orientation in terms of slope morphology and stability has been the subject of considerable debate. Many authors (Beaty, 1956, 1971; Spence, 1972; Hardy and Associates, 1974; Toy, 1977; Yair *et al.*, 1980) believe that because of the greater amount of available water on the north-facing slopes (in the northern hemisphere), weathering and erosion are enhanced. Consequently, north-facing slopes have a gentler, more undulating gradient, with a more developed regolith. Conversely, the south-facing slopes have less available soil moisture, resulting in straighter, shorter, and more rectilinear slopes. Others (eg. Rib and Ta Liang, 1978) oppose this consensus claiming that microclimate variations result in steeper north-facing slopes. This is attributed primarily to greater soil moisture retention which leads to a better vegetation cover, and less active erosion.

The differential soil moisture is a result of both macro and microclimate conditions. The high velocity winds (northwest and southwest) in the winter act to redistribute snow. As a result, maximum snow accumulation zones are on slopes oriented north, northeast, east, and southeast (Beaty, 1971; Harty, 1984). North-facing slopes often retain snow throughout the winter, while south-facing slopes are often snow-barren. Furthermore, subsurface moisture penetration is deeper under snowmelt than during rainfall, due to prolonged infiltration and sorption processes permitted by slow-melting snow packs (McKay, 1970; Harty, 1984).

Microclimatic conditions are controlled primarily by the minimum effective insolation on the north-facing slopes. Precipitation occurring equally on north- and south-facing slopes will linger longer on the north-facing slopes because of the lower amounts of insolation, and the subsequent reduction in evaporation. Beaty (1971) found that northeast slopes are most affected by both the macro and microclimates.

According to some studies slope stability is also affected by slope orientation. There is evidently a marked trend for north-facing slopes (in the northern hemisphere) to have a

significantly higher rate of slope failure (Beatty, 1956, 1971; Churchill, 1981). Churchill (1981) found that 85 percent of all observed mass movements occurred on the north-facing slopes. However, small magnitude failures occurred more frequently on the drier south-facing slopes, whereas larger slumps and flows were relatively rare. The prime causative factor affecting slope stability in these cases is the retention of water on the north-facing slopes. This increases the pore water pressures, resulting in a subsequent decrease in shear strength. Because the south-facing slopes are drier they are less susceptible to mass movement processes such as creep, slumping, and mudflows (Spence, 1972; Churchill, 1981).

While mass movements occur on both north and south orientated slopes, there are aspect - related differences in their magnitude and frequency. However, if persistent heavy rains saturate all slopes ubiquitously, failure may occur irrespective of slope aspect. This is likely the cause of the anomalous results obtained by Crozier *et al.*, (1980) for the Wairarapa hill country (New Zealand). In 1977 the slopes with most failures were sunny north-facing slopes (southern hemisphere). Tests showed that the weakest conditions occurred at the bedrock/regolith interface of the southerly slopes. Crozier *et al.*, (1980) concluded that unusual climatic conditions had prevailed in 1977, causing the north-facing undisturbed (and possibly steep) slopes to become saturated and unstable. Normally failures would tend to be more prevalent on the shaded south-facing slopes. Light to moderate rains would create differential moisture conditions, inducing aspect - related variance in slope stability.

2.4.3 Analogous stability studies

Although there has been much work concerning slope stability of the Upper Cretaceous bedrock of Western Canada, very little research has been concerned specifically with the Judith River Formation. As a result, analogous studies in other Upper Cretaceous bedrock formations will be reviewed. Slope failures in the Horseshoe Canyon, Belly River, and primarily the Bearpaw Formations have been extensively studied. These formations are comparable to the Judith River Formation in that they, too, consist of flat-lying, poorly indurated sandstones

and shales. The primary difference between these formations is their depositional environment, ranging from marine to brackish to freshwater. The Bearpaw Formation was laid down in a deep-water marine environment while the sandstones and shales of the Judith River Formation were deposited in a shallow-water deltaic environment.

The unstable nature of slopes in Western Canada has long been recognized (Bjerrum, 1967; Scott and Brooker, 1968; Beaty, 1971; Thomson and Morgenstern, 1977; Thomson and Bruce, 1978; Mollard and James, 1984). Numerous studies have emphasized large disparities in the engineering parameters (index and strength values) and in the factors deemed responsible for failure. The index values refer to the Atterberg Limits, or the liquid and plastic limits of a mass. Laboratory analysis measures the relative plasticity of sediments by defining the upper and lower limits of the plastic state. The liquid limit refers to that moisture content which defines the boundary condition between the plastic and liquid states. It is at this minimum moisture content that a soil will flow as a liquid under its own weight. The plastic limit refers to the moisture content which defines the boundary between the plastic and more rigid, solid condition. At this minimum moisture content the plastic soil begins to crumble. The plasticity index is the numerical difference between the liquid and plastic limits, indicating the range of moisture content within which the soils are in a plastic state. These parameters are often used to define the plasticity of slope materials.

The clay shales of the prairie provinces consist of weakly cemented clay-sized sediments that exhibit highly plastic characteristics when manipulated in the presence of water (Peterson, 1958). In general, fine grained rocks are characterized by high plasticity values which generally increase with the degree of weathering degradation (Taylor and Cripps, 1987). A wide variation in plasticity exists and is largely affected by the amount of clay content, the type of mineral present, and the presence of organics. Peterson (1954) found that there was a decrease in the liquid limit if an organic shale was oven dried (versus air dried). In the Bearpaw shales, however, the high plastic properties over-powered the slightly organic-related characteristics. Furthermore, he showed that varied methods of preparation (undried, air dried, or oven dried)

significantly affected the liquid limit value. For instance, the liquid limit of the moist Bearpaw shale is increased by approximately 30 percent if the clay is air dried before testing. Other authors (Casagrande, 1949; Grim and Guven, 1978) consider highly bentonitic clays, because of their variable rate of water sorption, difficult to test, often producing unreliable and inconsistent results.

Bjerrum (1967) has provided an extensive analysis of the strength parameters of the various overconsolidated plastic clays and clay shales. He claims that this recoverable strain energy is the single most influential agent capable of bringing even the hardest clays to failure. The most dangerous clays are those overconsolidated clays with strong diagenetic bonds which are subjected to gradual disintegration by weathering. The large amounts of stored energy released lead to significant lateral stresses and a pronounced tendency to expand in a direction parallel to the surface. For the same level of consolidation, the danger of progressive failure is dependent on the length and steepness of the slope, the strength of the diagenetic bonds, the degree of weathering, and the plasticity of the clay. In general, an increase in any of these parameters would significantly increase the danger of progressive failure.

As with the index values the strength parameters of the Upper Cretaceous bedrock formations are highly varied. Bjerrum (1967), Scott and Brooker (1968), Duncan and Dunlop (1969), Public Works Dept., Hongkong (1979), Kirkland and Armstrong (1982), all question the validity of using laboratory strength analysis results (from triaxial testing) as representative of field conditions. Shales in the field are fractured, jointed and slickensided. These discontinuities control the soil mass behaviour because both the shear resistance of the soil mass and the mass permeability will be a function of such local detail. Consequently, testing of intact samples in the laboratory may have little relationship to field conditions. Laboratory testing tends to over-estimate the shear strength and under-estimate the compressibility and permeability. In the Edgerton landslide (48 km northeast of Wainwright, Alberta), the peak angle of shearing resistance and cohesion proved to be much less than that determined from laboratory testing (Thomson and Tweedie, 1978).

In addition to the discrepancy between field and laboratory strength results there is also significant variation within the same stratigraphic unit. This is due in part to post-depositional weathering of the bedrock which alters the intact strength at various rates. The gradual and irregular destruction of diagenetic bonds will result in non-uniform swelling of the clay which is a function of the mineralogical composition, dependent primarily on the presence of montmorillonite (Bjerrum, 1967), which tends to be highly variable spatially.

Although there is considerable variation in the type of failures, the material involved and their possible causes, tentative conclusions can be drawn from the evidence presented. In the Upper Cretaceous shales of Western Canada failures tend to be progressive (Bjerrum, 1967; Hayley, 1968; Thomson and Morgenstern, 1977; Thomson and Tweedie, 1978; Mollard and James, 1984). The cumulative strength loss of these failures was generally from toe to head, with the exception of the Edgerton landslide of the Belly River Formation. This failure was found to progress from scarp to toe (Thomson and Tweedie, 1978) because of the development of a significant scarp (2.75 m) with no corresponding observable movement at the toe. Failures tend also to be retrogressive in nature (Scott and Brooker, 1968; Mollard and James, 1984). In several cases old slides were reactivated (Thomson and Tweedie, 1978; Thomson and Morgenstern, 1979).

The primary type of movement is translational sliding (Bjerrum, 1967; Hayley, 1968; Scott and Brooker, 1968; Thomson, 1971b; Thomson and Morgenstern, 1977; Mollard and James, 1984). Often the horizontal plane is coincident with a plane of weakness such as a bentonitic seam, a previous surface of rupture, or along an inter-bed zone that has slipped as a result of rebound.

Compound slides with a dominant translational component are also very common (Thomson and Morgenstern, 1977; Thomson and Bruce, 1978; Mollard and James, 1984; Bolduc *et al.*, 1987). In an air photo study of landslide incidence along the North Saskatchewan River, Thomson and Bruce (1978) found that 55 percent of all recognizable slope failures were

compound failures.

Rotational slides were also observed, but less frequently (Beaty, 1971; Hardy and Associates, 1974; Thomson and Morgenstern, 1977; Thomson and Bruce, 1978). In the air photo study conducted by Thomson and Bruce (1978) 30 percent of the failures were found to be rotational in nature. Almost all slides were classified as large (Mollard and James, 1984) and deep-seated (Thomson and Bruce, 1978; Bolduc *et al.*, 1987). Hardy and Associates (1974) found a correlation between the depth of the failed unit and the slope inclination. Steep slopes tended to produce shallow slides, while more gentle slopes produced deep-seated failures. This is in direct contrast to what Taylor and Cripps (1987) claim. They found that overconsolidated shale slopes with low angles (8° - 12°) tended to result in failures that were shallow and markedly non-circular. In the case of steeper slopes (approximately 30°), instability tended to occur as deep-seated rotational slides.

Falls were noted only twice in the literature (Hardy and Associates, 1974; Thomson and Bruce, 1978), as were dry flows (Thomson and Bruce, 1978; Mollard and James, 1984). Falls and dry flows combined, produced the remaining 15 percent of the slope failures noted in the Thomson and Bruce (1978) study. Piping was briefly noted by Hardy and Associates (1974), and was directly related to seepage zones consisting primarily of sand and silt-sized particles.

The most common material of the failed unit was bedrock composed primarily of overconsolidated, poorly cemented bentonitic clay shales and sandstones with nearly horizontal bedding (Bjerrum, 1967; Hayley, 1968; Thomson, 1971b; Hardy and Associates, 1974; Thomson and Morgenstern, 1977, 1979; Thomson and Yacyshyn, 1977; Thomson and Bruce, 1978). Of the 37 slides analyzed in the Horseshoe Canyon Formation by Thomson and Yacyshyn (1977), 50 percent occurred in the poorly indurated shales of the Upper Cretaceous.

In many cases the failure type was correlated with the material involved. Hardy and Associates (1974) found that rotational slumping and sliding was associated with lacustrine clays. Similarly, Thomson and Morgenstern (1977) found that largely rotational failures were

associated with Pleistocene sediments, often high in the valley wall. In contrast, bedrock tended to produce translational failures. In the air photo study (Thomson and Bruce, 1978), compound failures generally occurred in the relatively flat-lying bedrock, while the rotational slides occurred evenly in bedrock, and glacial deposits. However, of those failures occurring in glacial deposits, rotational slides are most common (Thomson and Bruce, 1978). Of the remaining slides analyzed by Thomson and Yacyshyn (1977), only a few were in glacial lake sediments. In general, water-deposited sediments, freshwater or marine, are most susceptible to landslides (Rib and Ta Liang, 1978). Beaty (1971) found that most slumps involved both the bedrock and overburden, but most occurred in the latter.

Possible causes of the slope failures can be classified as either preparatory or triggering factors. This division is somewhat arbitrary as no definitive line exists between the two. Furthermore, while preparatory factors can be more readily recognized, triggering factors act in the short term, often making identification difficult. Consequently, the majority of potential causes presented in the literature tend to be preparatory in nature.

Of the preparatory factors noted, bedrock geology appears to have the dominant influence. Beaty (1971), Thomson and Morgenstern (1977, 1979), Thomson and Bruce (1978), Mollard and James (1984), and Bolduc *et al.*, (1987), concluded that the marine shales (Bearpaw and Lea Park Formations) were clearly more unstable than freshwater deposits (Horseshoe Canyon Formation). Beaty (1971) found that most slope failures occurred in the Foremost, Judith River and Bearpaw Formations, with more than half in the Bearpaw marine shales. Marine and brackish deposits were considered most prone to failure, followed by freshwater deposits, and then clastic or deltaic deposits (Thomson and Morgenstern, 1977; 1979; Thomson and Bruce, 1978). This sequence is believed to be directly related to sediment size which reflects the depositional environment. Marine sediments are composed primarily of clay-sized particles and are therefore particularly sensitive, especially those rich in montmorillonite. Because the marine Bearpaw shales are generally more susceptible to failure

than are those of the Judith River Formation strength analysis provides an outer (lower) limit of stability for the Judith River Formation.

Bentonite, whether it be a pure seam or an admixture, significantly affects slope stability (Scott and Brooker, 1968; Thomson and Morgenstern, 1977, 1979; Thomson and Bruce, 1978). Its presence is considered to be the most important geological factor affecting shear resistance (Scott and Brooker, 1968; Thomson and Morgenstern, 1979). Not only does bentonite retard the downward flow of water but, with the addition of relatively small amounts of water, there was a marked decrease in the peak angle of internal friction (Thomson and Morgenstern, 1979). In general, Scott and Brooker (1968) found that there was no apparent preferential relationship between the incidence of slides and any particular stratigraphic section. However, bentonite seams were observed in the toe area of most slides, probably acting as the prime control on movement. The toe of the Devon slide in the Horseshoe Canyon Formation was also along a bentonitic (and coal) seam which was responsible for creating a perched water table (Thomson and Morgenstern, 1979).

Rebound, or the release of stored strain energy, has a significant effect on slope stability. The deformation created by the inter-bed slip decreases the shear resistance from peak to residual leading to a weakened zone susceptible to failure (Thomson, 1971b; Thomson and Morgenstern, 1977, 1979; Thomson and Tweedie, 1978). Diagenetic effects of the Upper Cretaceous bedrock significantly affects the rate of rebound. Strong bonds may hinder rebound substantially, increasing the disparity between the rate of erosion and the rate of strain energy release. The effect of the diagenetic bonds on slope stability can be seen in Western Canada. The strength of the Cretaceous shales in the eastern part of the prairies is mainly from compaction, while the strength of the bedrock further west is a result of cementation (Locker, 1973). Bolduc *et al.*, (1987) found a marked increase in the landslide activity in the western prairie provinces, and suggest that this is due in part to the differences in diagenesis. Bjerrum (1967) classified the Bearpaw Formation as a plastic marine shale with very strong diagenetic bonds. The gradual release of this stored strain energy weakens the material, often leading to

progressive failures. In the South Saskatchewan River Dam failure (Peterson, 1954), gravity appeared to have had a lesser role (seen by the horizontal failure plane), than did post-excavation lateral expansion induced by the significant release of horizontal stresses. In general, if the rate of excavation, either fluvial or anthropogenic, is greater than the rate of residual stress relief, instability of the valley walls will ensue (Scott and Brooker, 1968). Consequently, rapid post-glacial erosion resulted in rebound which, in conjunction with the induced slippage and a weakened zone, led to very unstable conditions (Thomson and Morgenstern, 1977, 1979; Rib and Ta Liang, 1978; Thomson and Bruce, 1978; Mollard and James, 1984; Bolduc *et al.*, 1987). The existence of a low level terrace (about 6,500 years old) near the Devon slide suggests that immediate post-glacial erosion was very rapid, resulting in many large-scale landslides. This is supported by the fact that 80 percent of the failures in that vicinity are inactive and very old (Thomson and Morgenstern, 1979).

Weathering, both physical and chemical, is noted for its role in decreasing the shear strength of a material (Thomson and Tweedie, 1978; Thomson and Kjartanson, 1984; Bolduc *et al.*, 1987; Taylor and Cripps, 1987). Physical weathering is largely responsible for the initial breakdown of the agglomerates, exposing the particles to chemical weathering. The cumulative decrease in shear strength is further enhanced if the bedrock is high in montmorillonite (Bolduc *et al.*, 1987). Weathering affects slope strength by increasing the permeability of the slope face, leading to greater infiltration which further increases the rate of weathering degradation, and the pore water pressures within the slope mass. Weathering is also considered the dominant agent responsible for destroying the cohesion of a material, even over a short period of time (Thomson and Tweedie, 1978; Thomson and Morgenstern, 1979; Thomson and Kjartanson, 1984). Thomson and Morgenstern (1979) found that in the 8 year period following the Lescur slide, cohesion had decreased toward zero, and the angle of shearing resistance along the horizontal part of the failure had decreased toward the residual value.

The effect of aspect on slope stability of the Upper Cretaceous bedrock is uncertain. Generally, aspect is not considered but in some cases it was found that the west side of river

valleys were most prone to landslide development (Scott and Brooker, 1968; Beaty, 1971b). Beaty (1971b) found that of those slides identified, 76 percent occurred on the north, northeast, and east exposures. He concluded that slumps must be significantly affected by microclimate because their occurrence would be random if the geology (Bearpaw Formation), undermining, or other elements were the main causative factors. Scott and Brooker (1968) considered slope orientation as possibly significant, especially during the initial stages of slide development, while Thomson and Bruce (1978) felt that aspect did not appear to have a major role in instability.

Slope steepness contributed to instability in several cases (Hardy and Associates, 1974; Mollard and James, 1984). The slopes along Whitemud Creek (Edmonton) of the Horseshoe Canyon Formation were generally 40°- 50°. This angle was maintained during slope retreat (induced by fluvial erosion), while the actual height increased, possibly leading to mass failure (Hardy and Associates, 1974).

In several instances, erosional processes were considered dominant in the denudation of extremely steep slopes (Scott and Brooker, 1968; Campbell, 1974). Consequently, it was felt that these slopes retreated at a constant rate rather than the periodic rate of mass movement.

Other preparatory factors affecting slope stability include the effects of ice shove (Thomson and Morgenstern, 1979), old landslide activity (Thomson and Tweedie, 1978; Thomson and Morgenstern, 1979), and surface drainage (Thomson and Morgenstern, 1979). The upper portion of the Devon slide exhibited distortions that were likely due to ice shove. The resultant effect of this strain was shearing which creates a zone of weakness.

Previous landslide activity significantly affects the current stability of a slope. Pre-existing planes of weakness created by earlier displacement will still act as weakened zones within the mass. In the Edgerton landslide, residual angles of shearing resistance were mobilized along the pre-sheared surface of an old slide (Thomson and Tweedie, 1978). Old landslides tend to be marginally stable, and surprisingly little stress relief is needed to re-activate movement (Thomson and Morgenstern, 1979).

Terraces and pre-glacial channels act as significant stabilizing agents. Terraces, especially low-level terraces, enhance stability by providing a natural toe load (Bolduc *et al.*, 1987). The Red Deer River generally has a lower incidence of slope failure in comparison with other rivers in the area (tributaries of the Red Deer, the South Saskatchewan, and St. Mary rivers) (Scott and Brooker, 1968; Bolduc *et al.*, 1987). This is due primarily to the development of terraces which decrease the shear stresses that would exist in an unbenched slope of the same height. They are also indicative of fluctuating rates of incision. Residual stresses in the valley would therefore likely be relieved at a rate more compatible with erosion, decreasing residual stress concentrations that contribute to failures in other river valleys. Conversely, destruction of these terraces enhances instability, as was the case in the Leseur slide (Thomson, 1971b; Thomson and Morgenstern, 1979).

Pre-glacial buried channels are often floored with clean free-draining sands and gravels. Consequently, they have a stabilizing effect on landslides by lowering the water table (Thomson and Morgenstern, 1977, 1979; Thomson and Bruce, 1978; Bolduc *et al.*, 1987). In general, a high ground water level tends to increase the landslide activity.

Triggering factors are more difficult to identify but fluvial erosion is clearly the prime cause of slope failure (Thomson, 1971; Hardy and Associates, 1974; Thomson and Yacyshyn, 1977; Thomson and Morgenstern, 1977; Thomson and Bruce, 1978; Bolduc *et al.*, 1987). Erosion of the toe of slopes was the dominant cause of landslides deep-seated in bedrock according to Thomson and Bruce (1978). Thomson and Morgenstern (1977) found that more than 90 percent of the landslides occur on meander bends, along the outside bank just downstream of maximum curvature. Of those slides studied by Thomson and Yacyshyn (1977), 25 percent were found to be due to lateral erosion of the North Saskatchewan River. In general, rivers with greater sinuosity will have a greater incidence of slope failure.

In many cases fluctuating ground water levels, and associated pore water pressures, have been deemed responsible for triggering failures (Beatty, 1971; Thomson and Morgenstern,

1979; Thomson and Kjartanson, 1984; Bolduc *et al.*, 1987). The high water table coincident with the spring melt often leads to a high incidence of slope failure. Thomson and Tweedie (1978) concluded that the Edgerton failure probably occurred due to the gradual loss of soil strength manifested by a disappearance of cohesion and was triggered by a spring-time rise in pore pressure. The delayed failure along the Whitemud freeway in Edmonton was largely a result of the equalization of the post excavation excess negative pore pressures, causing instability with time (Thomson and Kjartanson, 1984). Mollard and James (1984) found that as slopes in the Bearpaw shales along the South Saskatchewan River became saturated by torrential rains, mud or debris flows often resulted. These appeared to be especially prevalent in areas with prolonged dry spells followed by sudden intense precipitation. Semi-arid regions are particularly sensitive, especially if slopes are comprised mostly of fine grained materials. However, the low permeability of the bedrock, and the relatively low amounts of precipitation in the badlands, lead to reduced amounts of ground water flow which acts to stabilize the slopes in the area.

Pipes and pipe-induced slope collapses are prevalent in the badlands. It is possible that contemporary large-scale piping also accompanied the rapid cutting phase of the immediate post-glacial period. Pierson (1983) suggests that a causal link may exist between some soil pipes and slope failures. When a pipe is closed or blocked the water that may partially fill the pipe can generate pore pressures in proportion to the hydrostatic head achieved. These pore pressure increases may be sufficient to trigger slides on otherwise stable slopes.

In summary, failures are common in the Upper Cretaceous bedrock and tend to be deep-seated and primarily translational. The most common preparatory factor cited is the bedrock type with marine sediments being most sensitive. The triggering mechanism most frequently attributed to inducing mass movements is fluvial erosion. Although these causative factors have been segregated for ease of presentation, most are necessarily linked as they carry

a slope from its initial relatively stable state to one of instability, and possibly failure. Such is the case of the Leseur slide in which, a low-level terrace initially protected the slope by minimizing shear stresses. Once this toe load was removed by the lateral migration of the river, shear stresses increased. The unloading led to a decrease in the confining pressure at the toe. This resulted in swelling, an increase in the moisture content and the subsequent decrease in shear strength. The actual triggering mechanism could have either been a fluctuating water table or from the rising levels in the toe area (Thomson, 1971b). The interconnection of the factors of this sequence led to the initial failure (1969) and have continued to act, further decreasing the margin of stability. pressure at the toe. This resulted in swelling, an increase in the moisture content and the subsequent decrease in shear strength. The actual triggering mechanism could have either been a fluctuating water table or from the rising levels in the toe area (Thomson, 1971b). The interconnection of the factors of this sequence led to the initial failure (1969) and have continued to act, further decreasing the margin of stability.

3. Research Methodology

3.1 Recognition and Identification of mass movements

Recognition and identification of mass movements in the Dinosaur Park area was accomplished by the use of aerial photographs, topographic maps (supplemented by geological and pedological maps), and field reconnaissance. Mass movements were recorded and classified according to Varnes (1978) criteria. Exceptions include those indeterminate failures that were either too ancient or too small to have maintained a distinct failure form, making definitive identification impossible. Smaller-scale failures are often difficult to discern, even relatively soon after their occurrence, because the weak bedrock is readily weathered and eroded during the infrequent but effective storms. It has been suggested that landslides occurring in arid regions are usually distinct and easily recognized because of the lack of vegetation cover and slower weathering rate (Rib and Ta Liang, 1978). This, however, may be negated by the presence of weak bedrock and the rapid disappearance of the feature by erosion.

Many minor surficial movements are excluded. Creep, piping, and dry flows are the smallest-scale phenomena, and only the larger of these were recorded. An approximate minimum size was set for dry flows. The failures that warranted recording could be surficial (less than 1.5 m in depth), but should involve a minimum area of 30 m². The role of the more minor movements should not be ignored, however, as they are extremely frequent and significantly affect slope retreat in the area.

3.1.1 Nomenclature

The notation used to label these failures was based on the type of movement (Table 3.1). Each mass movement was given an upper case letter denoting the failure type, followed by a lower case letter defining the type of movement. A numerical value terminates this sequence indicating the sequential number of that particular failure type. One failure, however, does not conform exactly to this nomenclature. In this case Sr² is a reactivated rotational slide.

Table 3.1 - Derivation of the notation used for the nine case failures.

Failure type	Failure charac.	Notation
slide	compound	Sc1
slide	compound	Sc2
slide	compound	Sc3
slide	compound	Sc4
slide	reactivated rotational	Sr ²
slide	translational	St1
complex	slide/flow	S/F1
complex	slide/flow	S/F2
complex	piping/flow	P/F1

Complex failures are similarly labeled. In these cases, however, two upper case letters are used with the preceding one representing the dominant one of the two. For example, a failure with a dominant slide and a flow as a secondary component would be labeled as - S/F1. All the flow components of these complex failures were wet during movement (as seen by their lobate form).

3.1.2 Aerial photographic interpretation

Aerial photographs are a valuable tool for the identification of mass movements and the extraction of pertinent information of the failure and surrounding area. They were used primarily for preliminary reconnaissance, historical analysis, and for obtaining details such as moisture conditions (as indicated by the vegetation pattern). The use of air photo interpretation in terrain and slope analysis is a widely accepted technique. It provides a portable three-dimensional overview of the landscape from which interrelations between slope, drainage, vegetation, and human activity can be viewed and evaluated. Furthermore, historical development can often be traced, showing conditions prior to, during, and after failure. Small-scale photographs provide a regional overview, while larger-scale photographs allow for a more detailed study.

The principles of aerial photographic interpretation have been described in great detail (Rib and Ta Liang, 1978; Mollard and James, 1984). These principles basically follow the

premise that landforms developed by the same geomorphic processes, and in the same environmental setting, will have distinct patterns in aerial photographs. These patterns are comprised of several major elements that can be evaluated and aid in interpretation: they include topographic expression, drainage, erosion, surface tones and textures, vegetation, and land use. Accordingly, failures can be located and delineated by their unconforming topography. Moisture conditions can be assessed; darker surface tones and denser vegetation indicate higher moisture content. The age of slope failures can also be determined to some extent by the tone and extent of vegetation cover as relatively recent failures tend to have a lighter tone (depending on bedrock type and moisture content) where vegetation has not yet become established.

In locating the mass movements, particular attention was paid to areas considered most susceptible to failure. Typical vulnerable locations include areas of steep slopes, along fluvial channels, areas of drainage concentration, and seepage zones. Several features are considered indicative of existing failures:

1. irregular topographic outline; the presence of a graben (translational slides), or backward tilted blocks (rotational slides)
2. hillside scarps
3. broken or irregular tracks (or roadways)
4. ponding of water in depressions on a slope
5. disturbed vegetation cover.

Other features can be indicative of potential failures:

1. ponded depressions
2. seepage areas
3. diverted drainageways
4. tension cracks.

Infrared photography provides supplemental information for evaluating existing landslides and landslide-susceptible terrain. It is most useful in delineating the presence of water, and precisely locating seepage zones at or near the surface. This is clearly shown by the vigor of the vegetation cover. Consequently, tracing the surface and near surface drainage channels may be possible.

For the preliminary reconnaissance, 1983, 1:10,000 scale Panchromatic black and white photographs were used. Several possible failures were identified, and were later verified in the

field. The near-infrared photographs used were taken in 1980, and also had a 1:10,000 scale.

Tracing the historical development of failures (and other details such as channel migration) was made possible by a sequence of aerial photographs dating back to 1949. A complete list of the aerial photographic coverage for Dinosaur Park and area is given in Appendix A.

3.1.3 Topographic map interpretation

The identification of mass movements on topographic maps is restricted by the map scale and contour interval. If the scale is sufficiently large, and the contour interval small, several features may indicate slope failures; (1) distinct topographic expression with closely spaced contours at the head of a failure (steeply sloped scarp), irregular and disjointed contours in the failure mass, and possibly flow characteristics at its base, and (2) wavy contour lines, uneven or broken local tracks, roads and other artificial lineaments such as transmission lines (Rib and Ta Liang, 1978).

Photogrammetrically produced 1:10,000 scale topographic maps were used in conjunction with the aerial photographs and field reconnaissance. These maps had a contour interval of 4 m (badlands) and 2 m (prairie surface), and because of the large scale, were useful in locating and mapping the various mass failures. Slope orientation, length and inclination were measured using these maps.

3.1.4 Field reconnaissance

Because the slope failures are generally small and, given the extremely irregular topography, field reconnaissance was essential and the most accurate of the three identification methods. Furthermore, detailed field interpretation was necessary for classifying the failure type and for obtaining specific slope details.

Failures that have already taken place are generally readily recognized. Incipient failures are often preceded by the development of tension cracks, portraying instability. These

cracks can indicate the nature of the movement. Cracks above the failure surface, near its head are normal to the direction of movement, while peripheral cracks are nearly parallel to it. These en echelon cracks often delineate the failure boundary. Peripheral cracks tend to form along the lateral limits of the failure because of the differential shear between the moving mass and the adjacent intact material. The toe of the failure may be perforated with short tension cracks parallel to the direction of movement, and some crescent-shaped ones with the points oriented uphill. If the surface of rupture extends beyond the toe of the slope, distortions such as bulges, cracks, or ripples may occur well beyond the slide toe (Sowers and Royster, 1978).

In addition to movement direction the crack form can indicate the type of movement. Concentric crack patterns indicate a rotational slide. Cracks that are essentially parallel to the slope indicate a translational slide. Translational slides show dominant horizontal movement with little vertical displacement (except where a graben is formed). In addition to the prevalent graben structure the lateral movement of translational slides is also characterized by the absence of a toe bulge, indicating that the principal surface of rupture is one of low curvature. In some cases graben structures occur in rotational failures, indicating lateral movement, but along a zone of rupture having a large radius of curvature (Scott and Brooker, 1968). Rotational slides, however, are more commonly characterized by backward tilted blocks that at times trap water in the depression created.

Although the propagating mechanisms of falls and topples are different, after movement their appearances are similar. Both show accumulation of debris at the slope base that is derived neither from weathering of the underlying material, nor from erosional processes. The size of the debris is determined by the competency of the parent material, the mode of transportation, the distance from the source area, and the time elapsed since failure. The accumulation of this debris is dependent on the balance between the rate of accumulation, and the rate of removal. In the Dinosaur Park area the generally weak, fine grained bedrock is readily removed, precluding its accumulation. Consequently, and especially with smaller failures, there tends to be negligible accumulation of debris at the base of a slope, at times

making definitive identification impossible.

Dry flows are recognized as either channelized flows or broad drapings of fine, uniform sediments. These flows, except for some channelized runs, lack a well defined foot. Conversely, wet flows are most readily identified by the distinctive lobate form of their foot. Flows generally have an even gradient and a relatively uniform mass generally lacking discrete units or blocks. Viscous movements will not have a defined slip surface. Cracks tend to be absent unless the material has dried and shrinkage occurs. Distinct scarps are generally non existent with dry flows, but often occur with wet flows.

In order to locate and identify these and other failure types, the perimeter of the badlands, and some interior sections were explored by foot. Because of the steep slopes, particular attention was paid to the prairie perimeter along coulees, and to the side slopes of residual uplands. This reconnaissance took a month to accomplish, and covered land that lies within Dinosaur Provincial Park, Irwin and Owen property (west of the Park), and Eastern Irrigation District (EID) land (south of the Park). Mass movements identified through photographic interpretation were confirmed, and other failures not evident on the photographs, or that had formed since 1983, were located and identified. Finally, the framework for those failures to be studied in greater detail was established.

3.1.5 Field research

Each failure was surveyed using a theodolite and stadia reduction techniques. Numerous profiles, the number dependent on the size and complexity (distortion) of the failed mass, were taken from head to toe, roughly parallel to the direction of movement. Where the direction of movement did not coincide with the steepest slope, additional profiles were made. Where possible a profile was run through an adjacent, undisturbed slope to provide a possible indication of the original slope geometry. This, in conjunction with aerial photographs and map information, helped establish pre-failure slope conditions.

Mapping of intermediate points defined major features such as scarps, bulges, irregular topography, prominent cracks, piping channels, ponding, and seepage areas. These details provided the necessary information for the construction of contour maps for each of the nine mass movements.

The volume of material moved by each of the nine failures was determined. The post-failure areal parameters were obtained through the surveys, and the depth of failure was indicated by the pre-failure form (from adjacent slope surveys or topographic map information). Volumetric measures were then applied to a magnitude scale assigned to the identified mass movements. In this way it was possible to determine the amount of material moved by the various failures, providing an approximation of the total amount moved by all currently observable mass movements in the badlands.

One of the failures (Sr²) was found to be currently active - the reactivation of an former slide. This movement was monitored by a survey of 14 fixed points from a control point set on a slope opposite the failure and was monitored on a regular basis. When movement was first detected (June 11, 1986) the theodolite was not available so measurement began only on July 1, 1986. The location of the points was monitored every two days, and after every significant rainfall, until August 21, 1986, with subsequent measurements taken on October 11 and 12, 1986. A final survey was made on August 2, 1987. The successive positions of the monitored points were plotted, depicting the cumulative horizontal and vertical movement. A vector map was then constructed with the original position of each station as a reference point, and the subsequent vectoral movements. In addition to regular monitoring, the location and extent of the developing scarp and predominant tension cracks were staked and recorded. An adjacent slope (to the west) was staked with six points and also monitored, but as no movement was apparent this program ended on August 7, 1986.

Four tape extensometers were located at regular intervals along the back scarp. The distance between each paired member provided a measure of the increase in displacement between the slide mass and the stable ground above. Also, at each extensometer location, the

depth of the scarp was measured. Distance and depth measurements were taken approximately every week and after major storms.

Only the Judith River Formation outcrops within the study area (Koster and Currie, 1987)(Figure 1.2). The alternating sandstones and shales of the Judith River Formation are generally topped with till with the occasional glacio-lacustrine deposits. Till depth might be indicative of pre-glacial valleys which have not yet been fully defined. The depth of each lithological unit was measured and plotted against the slope profile, producing a cross-section. Where possible, distinct units (such as iron-indurated sandstone bands) were mapped on both the undisturbed slope and on the failed mass.

In addition to the geological sequence, structural details were noted. Fissure and jointing patterns, bedrock inclination, and the mass structure were recorded. Trenches were excavated at each of the nine mass movements generally along either the perimeter of the failed mass, or at its toe. The sides of these test pits were sampled, logged and photographed, providing a synopsis of the failure debris. An attempt was made to define the contact between the displaced mass and the original surface. The trenches revealed the state of the disturbed material - whether the original structure was preserved, or if it was partially or wholly remoulded. Also, a trench on the west flank of the active slide Sr² revealed evidence of a possible failure plane. Consequently, four vertical nail shafts were staked along three walls (north, east, and south) of the test pit. It was hoped that any distortion of these lines would confirm the location of the failure plane, and indicate the rate and direction of movement.

The surface characteristics of the failure and the surrounding area were mapped in greater detail than that afforded by the aerial photographs. Tension cracks, above the scarp and within the failed mass, bulges, piping channels, the vegetation type and pattern, and hydrological details were recorded for each mass movement. Evidence of surface flow (sheetwash, rills gullies), seeps, springs, undrained depressions, and permeable strata were all noted. The location of seepage zones is of prime importance. Seeps uphill from the failure serve

as a source of surface water that can infiltrate into the failed mass, contributing to instability. Conversely, if a seep is located within the failure zone, or downhill from it, the opposite is usually true. In this case, internal pressures are alleviated as water is allowed to escape. Sowers and Royster (1978) consider the total effect of springs and seeps as beneficial, rather than detrimental.

An attempt was made to date each of the nine mass movements. This was approached both qualitatively and quantitatively, the former by general morphological observations, and the latter by ^{14}C dating of buried material, aerial photographic interpretation, and information from local residents.

The morphology of a failed slope reveals its relative age, whether it is a newly developed (contemporary) or an ancient failure (relic). The current state of the failure, whether it be active, dormant, or stabilized, can also often be recognized through its morphology. These observations are based on the premise that over time denudation reduces the once angular form into one with more of a rounded, undulating form. The extent and maturity of the vegetation cover is also indicative of age, as is the depth of weathering and soil development. A recent slope failure would be notably more defined with distinctive components (scarp, toe, etc.), and would have no post-failure soil development on ruptured surfaces and negligible vegetative growth. Depending primarily on the climate and the geological conditions, the rate of change of these characteristics will vary significantly. Nevertheless, in similar settings these changes can be compared, providing a relative date for failures.

Organic material was recovered from the failure mass as it was exposed through excavation of the test pits. Bone, wood, twigs, and organic-rich soils, were collected for radiocarbon dating (^{14}C). For a number of the wood, and all of the bone and soil samples, the weight proved to be insufficient and only two wood samples and one of twigs were sent for dating to the Environmental Isotopes Section of the Alberta Environmental Centre in Vegreville, Alberta.

In addition to this attempt to absolutely date the mass movements, historical aerial photographs were also used. Photographs with varying coverage and scales (from 1:60,000 to 1:5,000) were available for a number of years between 1949 and 1986 (see Appendix A). This provided an approximate date of occurrence for several failures, and interpretation made it possible to trace the morphological changes of the failure surfaces and surrounding area. Supplemental information dating several of the slides was also obtained through discussions with local residents.

3.1.6 Laboratory analysis

Sediment samples were taken from the failed mass of each of the nine examples. The source of this material was generally from the perimeter of the test pits, which revealed either discrete units or jumbled debris, with a considerable range existing between the two. If more than one unit was evident a sample was taken from each. Using the Casagrande apparatus these samples were then tested for their liquid and plastic limits. Standard Atterberg procedures were followed where the #40 (420 micron) sieve was used to separate the fines to be tested. Sediments were oven dried prior to testing and the plasticity index was subsequently determined.

Because test results have been found to vary considerably according to the preparation method used an additional test was performed. Ten samples from a number of representative materials were both oven dried and air dried before Atterberg testing. The resultant plastic and liquid limits, and the plasticity index were then compared to determine the correction factor necessary for correlating oven and air dried data.

Direct derivation of strength parameters and stability analysis is beyond the scope of this thesis and is unnecessarily specific. Because of the large areal coverage and the more general approach, detailed geotechnical analysis is not warranted. Consequently, strength data from analogous bedrock formations (particularly the Bearpaw Fm.) are used to indicate the possible strength conditions prevailing in the Judith River Formation. As previously mentioned

(Chapter 2), the marine Bearpaw Formation is considered to have a higher sensitivity to failure than does the deltaic Judith River Formation. Therefore, in evaluating the strength of the Judith River bedrock, based on the parameters of the Bearpaw Formation, a lower strength limit will be obtained. As with all strength analyses, it is imperative to consider the validity of laboratory test results when comparing them to the actual field conditions. Nevertheless, and with these limitations in mind, strength parameters are a useful indication of the margin of stability of a given slope, failure surfaces and surrounding area. Supplemental information dating several of the slides was also obtained through discussions with local residents.

3.1.7 Laboratory analysis

Sediment samples were taken from the failed mass of each of the nine examples. The source of this material was generally from the perimeter of the test pits, which revealed either discrete units or jumbled debris, with a considerable range existing between the two. If more than one unit was evident, a sample was taken from each. Using the Casagrande apparatus these samples were then tested for their liquid and plastic limits. Sediments were oven dried prior to testing and the plasticity index was subsequently determined.

Because test results have been found to vary considerably according to the preparation method used, an additional test was performed. Ten samples from a number of representative materials were both oven dried and air dried before Atterberg testing. The resultant plastic and liquid limits, and the plasticity index were then compared to determine the correction factor necessary for correlating oven and air dried data.

Direct derivation of strength parameters and stability analysis is beyond the scope of this thesis and is unnecessarily specific. Because of the large areal coverage and the more general approach, detailed geotechnical analysis is not warranted. Consequently, strength data from analogous bedrock formations (particularly the Bearpaw Fm.) is used to indicate the possible strength conditions prevailing in the Judith River Formation. As previously mentioned (Chapter 2), the marine Bearpaw Formation is considered to have a higher sensitivity to failure

than does the deltaic Judith River Formation. Therefore, in evaluating the strength of the Judith River bedrock, based on the parameters of the Bearpaw Formation, a lower strength limit will be obtained. As with all strength analyses, it is imperative to consider the validity of laboratory test results when comparing them to the actual field conditions. Nevertheless, and with these limitations in mind, strength parameters are a useful indication of the margin of stability of a given slope.

4. Results and analysis

4.1 Type and location of identified mass movements

4.1.1 General

A location map was constructed showing the type of failure and its relative size (Figure 4.1 - in pocket at back). The centre of each symbol represents the approximate centre of each failure mass. In this manner each failure can be specifically located. This is true for all failures mapped including the nine case failures (Figures 4.20 - 4.28).

Two hundred and sixty-three mass movements were identified. Many more were not recorded as they were either smaller than the set minimum size, or were not clearly mass movements. The majority of failures (54 percent) were flows. Of these, most were dry and small, marginally within the size restriction. Slides, (translational, rotational, and compound) formed the next largest group (34 percent). Falls and topples combined contributed 9 percent of the failures, and complex failures (particularly slide/flow combinations) contributed 3 percent. The slides and the complex failures were the largest in magnitude, while dry flows, falls and topples were generally the smallest, often of the minimum size. The relative sizes of the failures were based on the largest and the smallest identified. The largest mass movement ($137,900 \text{ m}^3$) was a translational slide along the west wall of Irishman's Coulee, just south of S/F2 (Figure 4.2). The smallest failures ($c.25 \text{ m}^3$) are represented by numerous dry flows, falls and topples.

The type of mass movement can be correlated with a number of factors including its location, aspect, slope geometry, and the lithology of the failed unit. To aid in the interpretation of these relationships, histograms were drawn for each. The different failure types were classified into four main categories: 1) slides, 2) flows, 3) topples and falls, and 4) complex failures. Slides include all slide failures whether they be translational, rotational, or compound. Flows include both wet and dry flows. Falls and topples have been grouped together

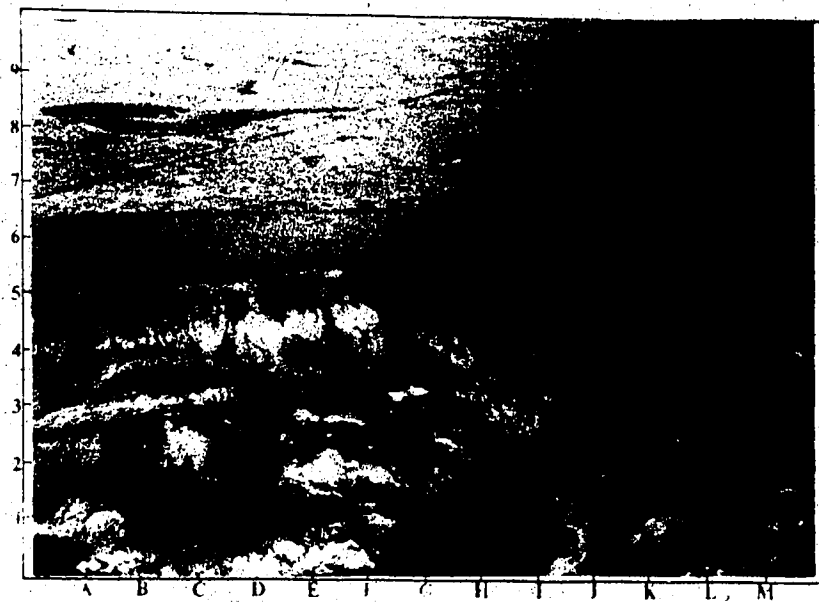


Figure 4.2 Irishman's Coulee - looking northwest. Aerial view of largest failure (137,900 m²) in study area; a translational slide (from bottom left of photograph to 14)

because of their inherent similarities and because, in their final form, it is often difficult to distinguish between the two. Complex failures include all those with two or more distinct components, particularly slide/flow combinations. The one recorded piping/flow is also included in this category.

4.1.2 Location analysis

The location of each failure is shown in Figure 4.3. The mass movements occurred in the badlands proper, along the prairie perimeter or on residual uplands. Residual uplands are isolated prairie remnants now surrounded by badland topography. Failures occurring in the badlands proper take place on surfaces that are considerably lower than the original prairie surface.

Ninety-one percent of all the slope failures occurred along the prairie perimeter. Of these, ninety percent were located along coulees, and in particular, Irishman's Coulee (22 percent). In general, the mass movements were fewer but larger nearer the junction of the coulee and the badlands proper. As distance along the coulee, and away from the badlands, increased the failures became more frequent but of a smaller scale. This suggests that as the coulees extend prairieward, more recent small-scale failures take place. Meanwhile, those at the terminus of the coulee have likely expanded retrogressively since their initiation, and are therefore larger and more stable. Many small failures were located along the entire length of Sonofabitch Coulee, a narrow steep-sided coulee near the eastern boundary of the study area. There was also a marked trend for failures to occur along side valleys, thus propagating valley extension.

4.1.3 Aspect analysis

The aspect of each failure type is shown in Figure 4.4 which summarizes the different slope orientations according to eight compass points. Aspect refers to the direction that the slope is facing, and not the actual location of that slope. The southeast direction had a slightly

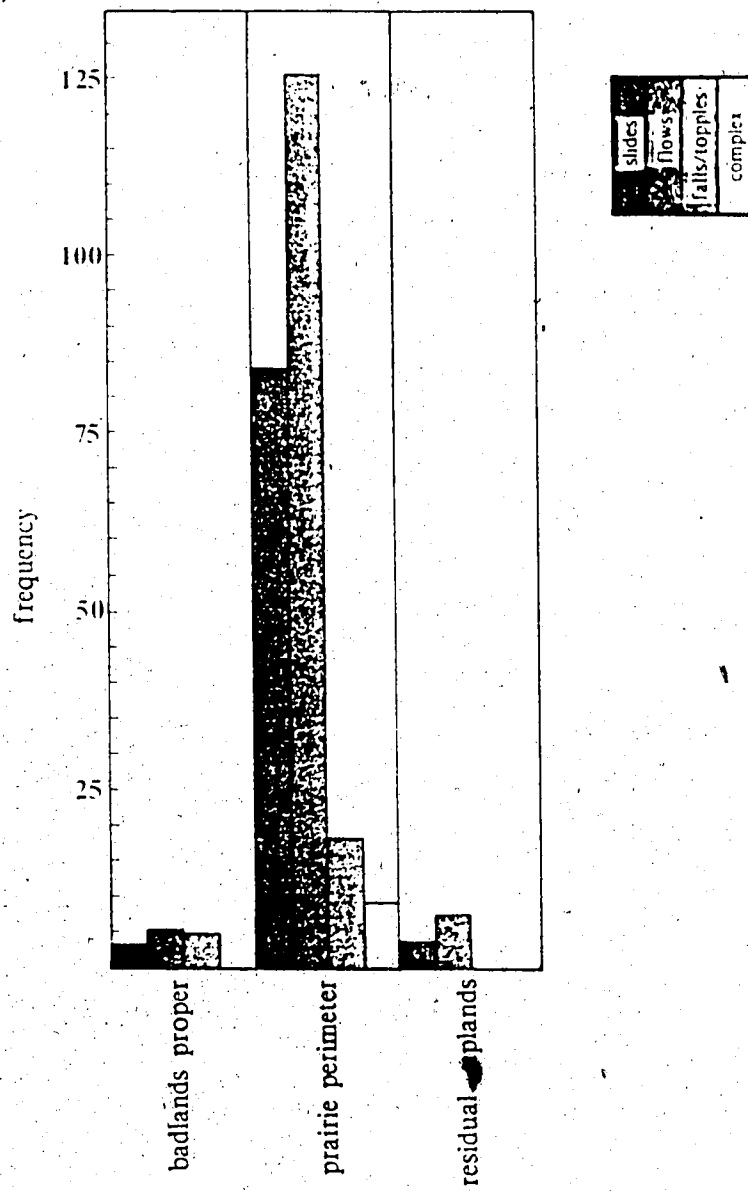


Figure 4.3 Location Histogram

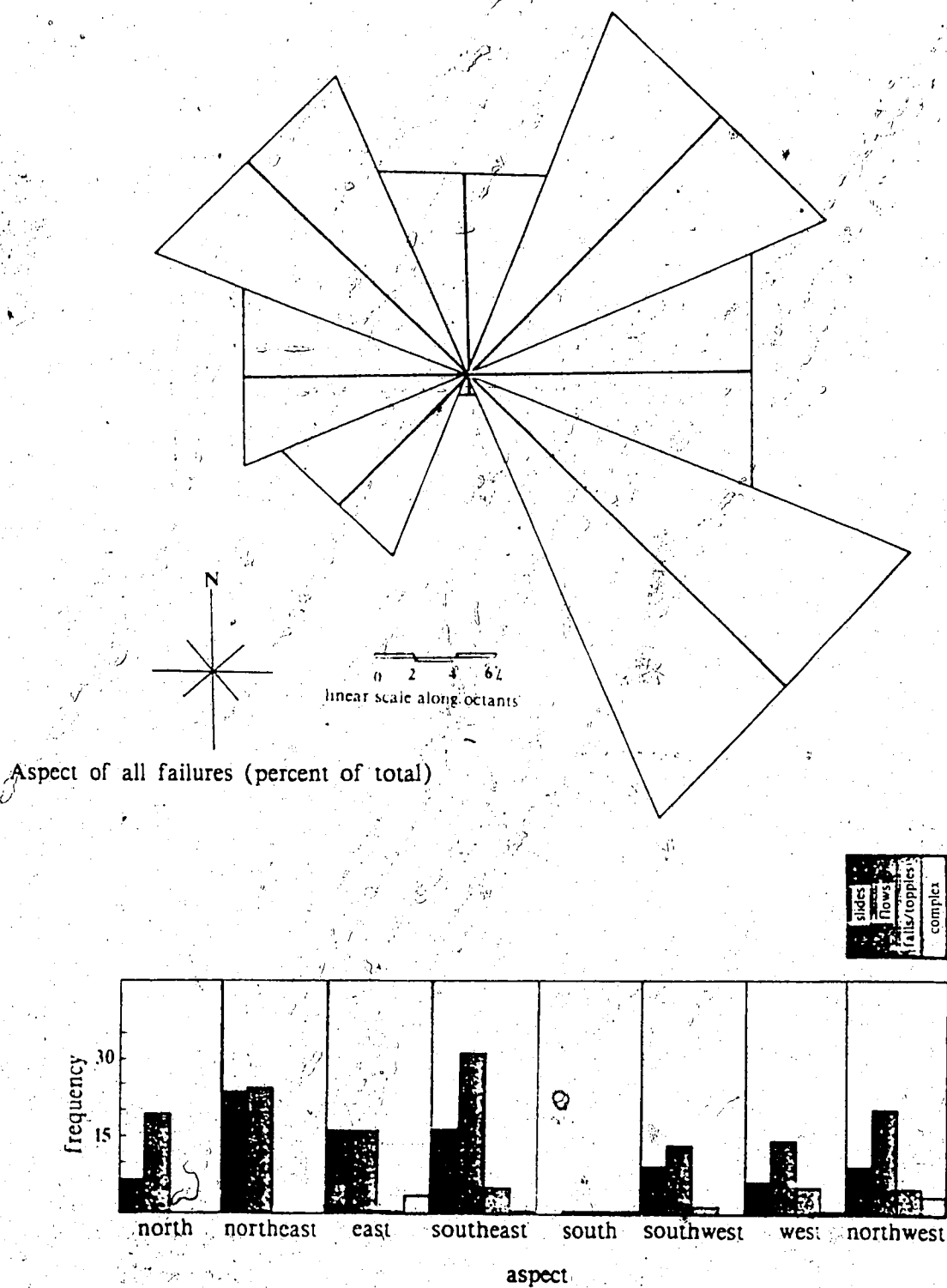


Figure 4.4 Aspect of all failure types

higher occurrence of failure (4 percent), due primarily to the large percentage of dry flows identified along northwest slopes. Cumulative data, however, show that the northern aspects (northwest - northeast) have a greater number of failures (43 percent) than do their southern counterparts (32 percent). This was significant at the 0.05 level, but not at the 0.01 level (using the Chi-square test). Furthermore, only 1 percent of all the failures occurred on slopes with a southern aspect.

Flow rose diagrams (Figure 4.5) reveal some interesting intra-failure characteristics. Most (26 percent) of the slides have occurred in a northeasterly direction, while none has occurred on south-facing slopes. This is the only failure type that conforms with the generally accepted aspect concepts. Flows (falls and topples), occur on slopes with all aspects, but dominantly so on those with a southerly orientation. Field observations show some aspect related differences in slope morphology. North-facing slopes tend to be longer, of a lower gradient, and more uniform than their south-facing counterparts (Figure 4.6). There is also a more extensive vegetation cover on the northerly orientated slopes, due to the greater retention of water and the gentler slopes present. Several locations in which these contrasts are particularly evident have been identified in Figure 4.1.

4.1.4 Geometric analysis

Slope geometry is of prime functional importance in terms of slope stability. Slope length and inclination, the predominant geometrical components, have been measured (from the 1:10,000 topographic maps) for each of the 263 recorded failures. Once the slope lengths had been calculated, 10 classes were established:

1. less than 20 m
2. 20 - 39 m
3. 40 - 59 m
4. 60 - 79 m
5. 80 - 99 m
6. 100 - 119 m
7. 120 - 139 m
8. 140 - 159 m
9. 160 - 179 m
10. greater than 179 m

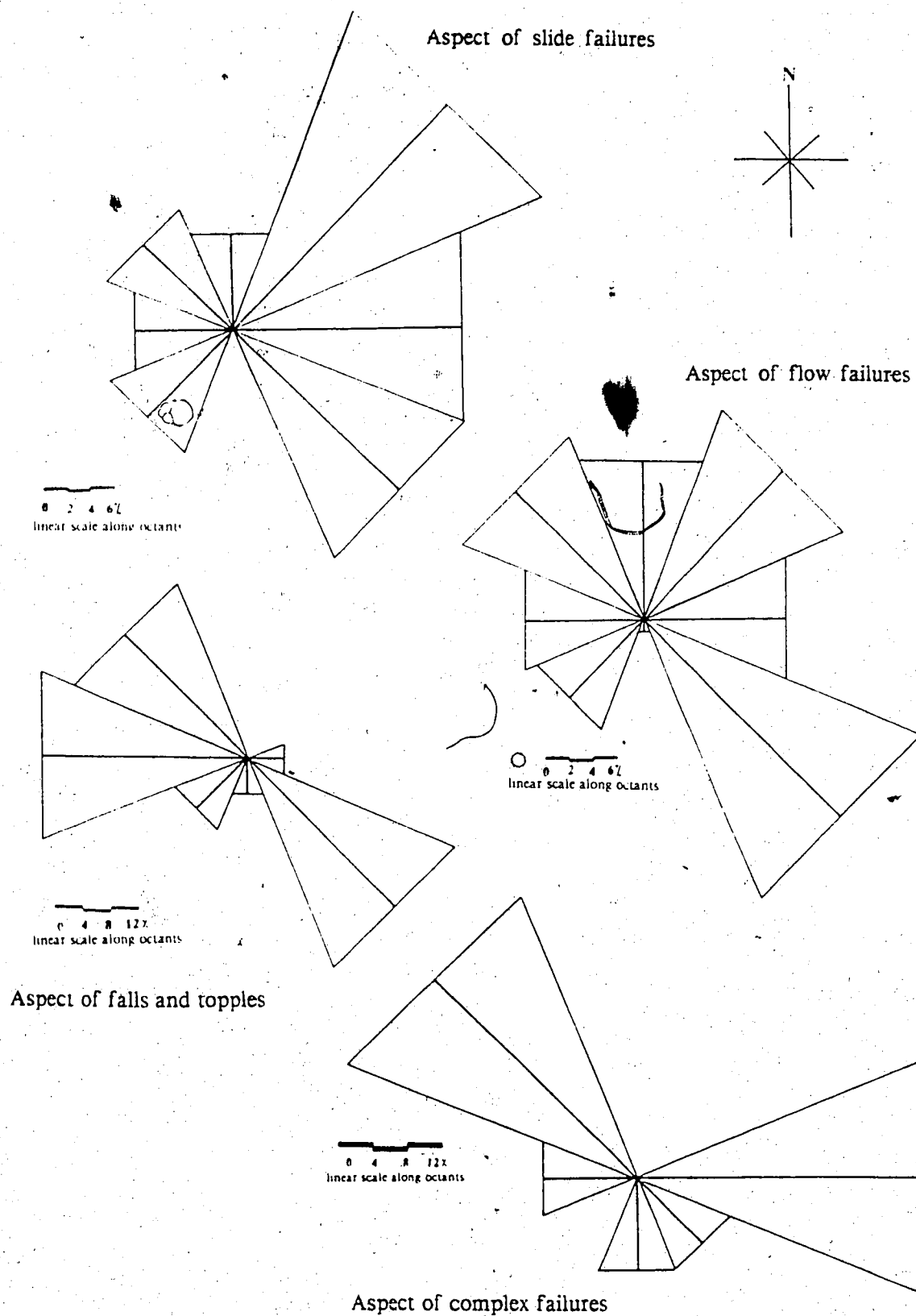


Figure 4.5 Rose diagrams showing aspect of different failure types

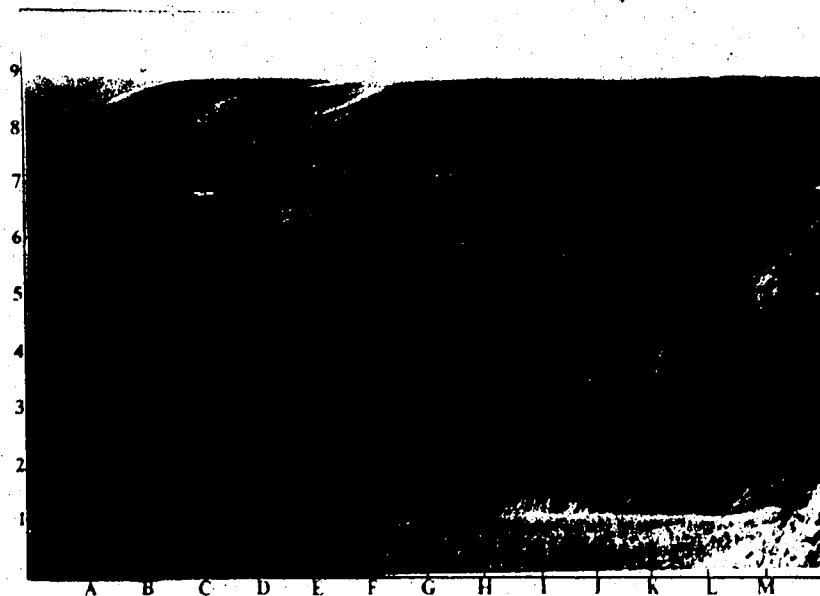


Figure 4.6 View along Waterfall Coulee (near Sc4) - looking west. The north-facing slopes (in shadow) are clearly better vegetated and have a more uniform, longer and less steep profile than do their south-facing counterparts

A similar classification system with 8 classes was established for the slope inclination:

1. less than 20°
2. 20 - 29°
3. 30 - 39°
4. 40 - 49°
5. 50 - 59°
6. 60 - 69°
7. 70 - 79°
8. greater than 79°

Figure 4.7 shows the individual histograms of the lengths and inclinations of the four failure types, while Figures 4.8 and 4.9 depict the geometric attributes for all of the failure types combined.

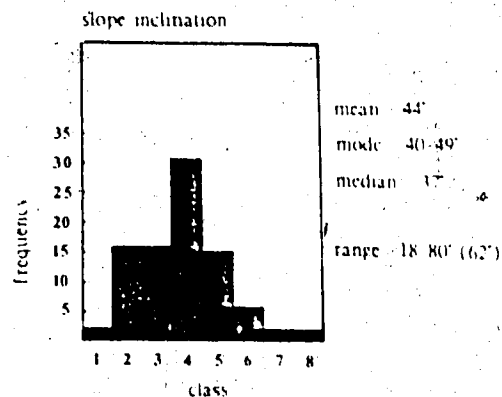
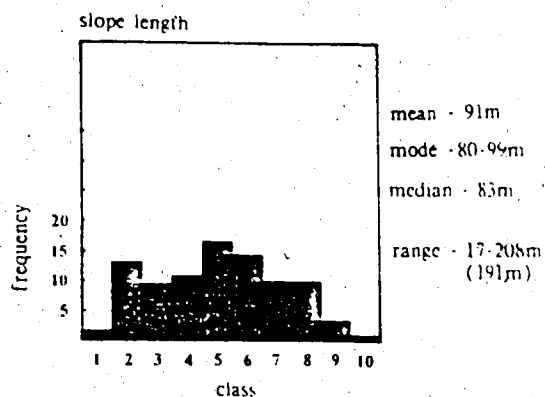
The total distribution of slope length and inclination is unimodal and skewed slightly to the left. In terms of slope length it is clear from the histogram (Figure 4.8) and Table 4.1, that most failures occur on slopes with a length between 80 and 99 m.

Table 4.1 - Slope length and inclination of the different failure types.

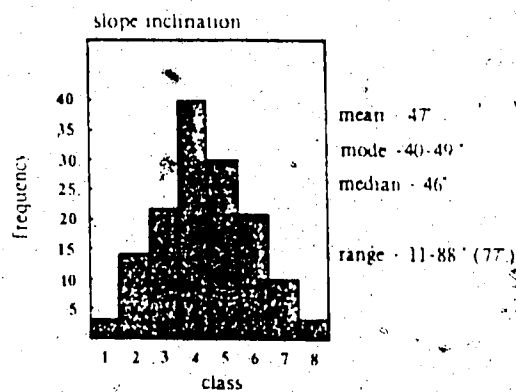
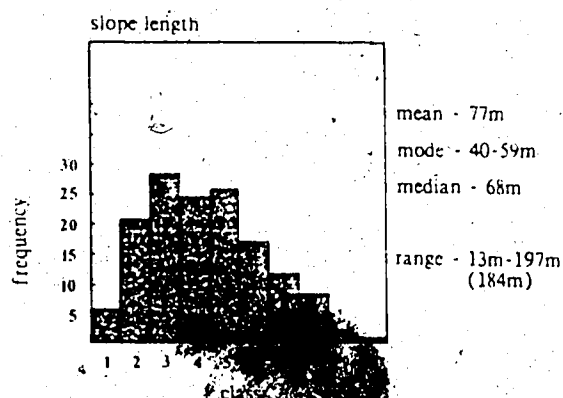
Failure type	mean(m)	Length modal class(m)	median(m)	mean(°)	Inclination modal class(°)	median(°)
slides	91	80-99	83	44	40-49	37
flows	77	40-59	68	47	40-49	46
falls and topples	76	20-39	30	44	40-49	34
complex failures	107	40-59	80	43	30-39	40

A distinct pattern of slope lengths for the different failure types becomes apparent. The mean slope length for flows (77 m) is virtually equal to that of topples and falls (76 m), while slides and complex failures had significantly higher mean values (91 m and 107 m respectively). The range in length values is comparable for all failure types although it is interesting to note that despite the small sample size, topples and falls have the largest range. The mean slope angle on which slope failures occurred was 45° (Figure 4.9) with only a slight variation from this mean.

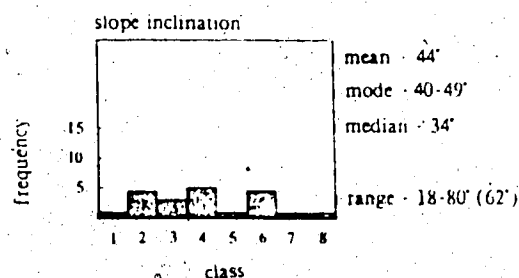
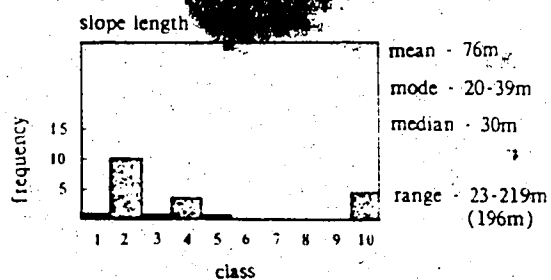
Of the four failure types flows have the most standard distribution of slope lengths. In contrast, however, flows occurred on a large range of slope inclinations (11°-88°). Because of the large sample size, this group influences considerably the distribution depicted in Figures 4.8



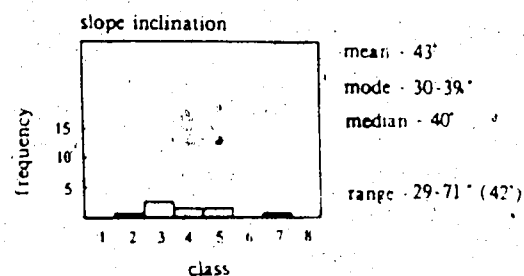
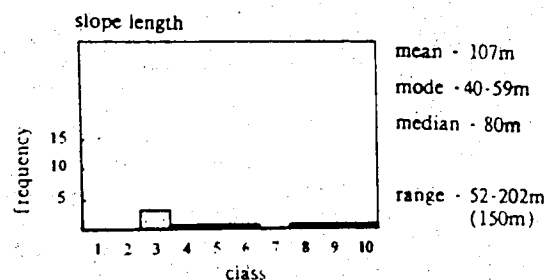
Length and inclination of slide failures



Length and inclination of falls and topples



Length and inclination of falls and topples



Length and inclination of complex failures

Figure 4.7 Slope length and inclination of different failure types.

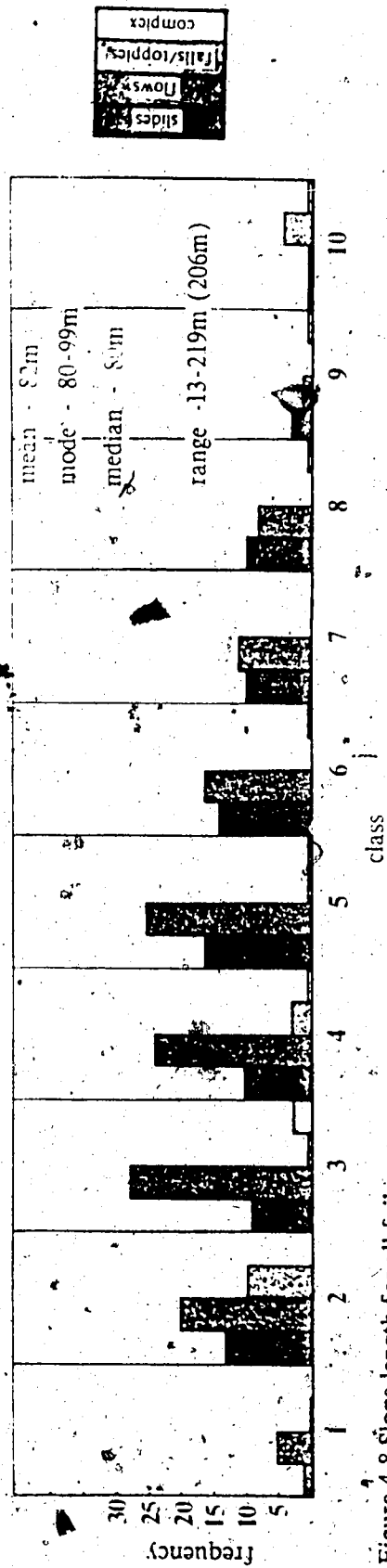


Figure 4.8 Slope length for all failure types

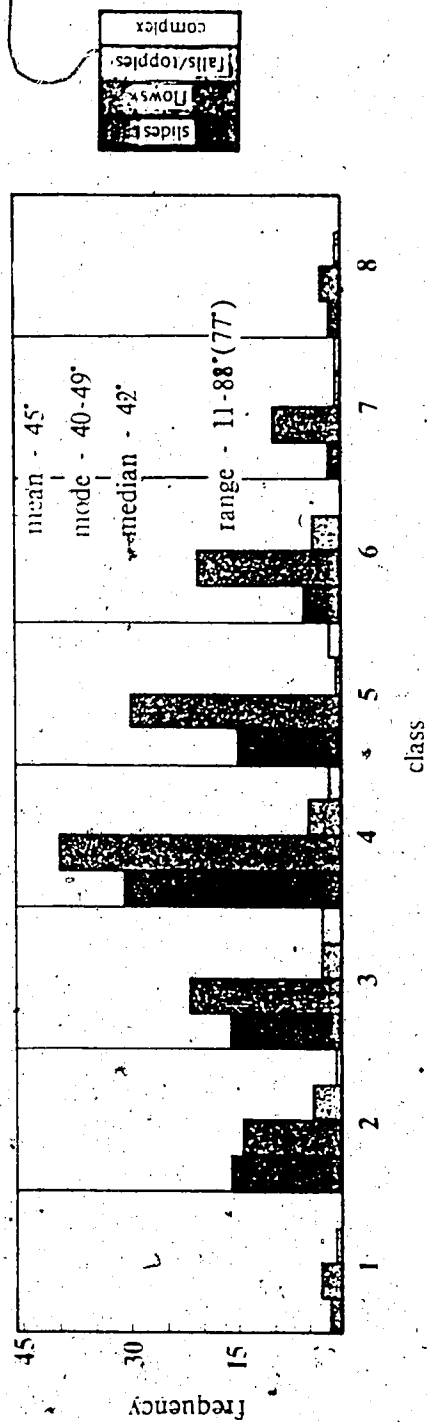


Figure 4.9 Slope inclination for all failure types

and 4.9.

4.1.5 Lithological analysis

The general lithology of each failure is shown in Figure 4.10. Because till is generally present, failures most commonly involve both till and bedrock. In some cases, however, either the till or bedrock unit was not involved. Not included in this classification are the three failures that occurred in channel deposits at meander bends. It was not always possible to identify the actual failed unit or units. Consequently, the adjacent slopes were often used to provide an indication of the pre-failure lithology.

Despite the ambiguity of some cases it is evident that most failures (71 percent) involve both bedrock and till units. The infrequency of failures occurring in till only (5 percent) could be due in part to the limited areal extent and depth of the till cover. No topples, falls, or complex failures occurred in till only.

In summary, while these trends should be interpreted with caution, they characterize the nature of mass movements occurring in the Dinosaur badlands. From these relationships the relative importance of each factor can be assessed for each failure type.

4.2 Case studies

4.2.1 General

Of the nine case failures, four were compound slides (Sc1, Sc2, Sc3, Sc4) two were singular slides (St1, Sr²), and three were complex failures (S/F1, S/F2, P/F1). Sc1 and Sc3 were compound slides with the rotational component dominant, while Sc2 and Sc4 had a dominant translational component. S/F1 and S/F2 are complex failures with a rotational slide component and a flow component. Selection was based on frequency of occurrence and persistence of form. Although falls, topples, and dry flows occurred most frequently, they were

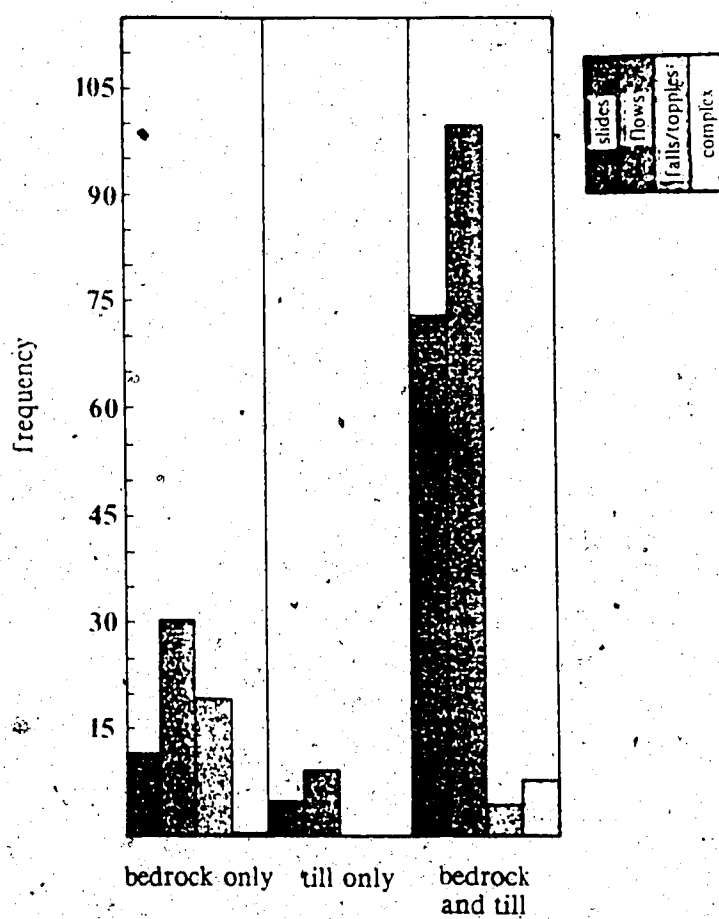


Figure 4.10 Lithology of all failure types

commonly small-scale and had often lost their form soon after failure. Compound slides with both translational and rotational components were most prevalent. Table 4.2 is a summary of the general characteristics of each failure. The area was determined by planimetry while the slope length and angle were determined by field surveys.

Table 4.2 - Summary characteristics of the nine case failures

Mass movement	Area(m ²)	Aspect	Length(m)	Slope(°)	State	Figure
Sc1	6,535	SW	55	41	dormant	4.11
Sc2	37,395	NE	109	56	dormant	4.12
Sc3	2,310	SW	23	42	dormant	4.13
Sc4	28,540	NE	89	46	relic	4.14
Sr ²	38,195	NE	169	62	re-activ.	4.15
St1	6,770	SW	128	65	active	4.16
S/F1	8,805	NW	202	59	dormant	4.17
S/F2	19,715	NE	102	56	relic	4.18
P/F1	6,850	NW	156	28	dormant	4.19

failures occurred along the prairie perimeter and in areas where till was present.

The remainder of this chapter will assess each of the nine failures individually in terms of surficial details (vegetation, hydrology, and morphology), geology, and the liquid and plastic limits.

4.2.2 Topography

Slope profiles and a contour map were constructed for each mass movement. These are shown in Figures 4.20 through 4.28. The centre (*) of these contour maps corresponds to the centre of the symbol representing that failure in Figure 4.1. Each profile is vertically exaggerated so the actual slope form has been distorted. The baseline for these profiles is as indicated on the contour maps.

The volumetric analysis of mass movements in the Dinosaur badlands (Tables 4.3 and 4.4) shows that a total of about 6,400,000 m³ has moved by all failure types. These volumes

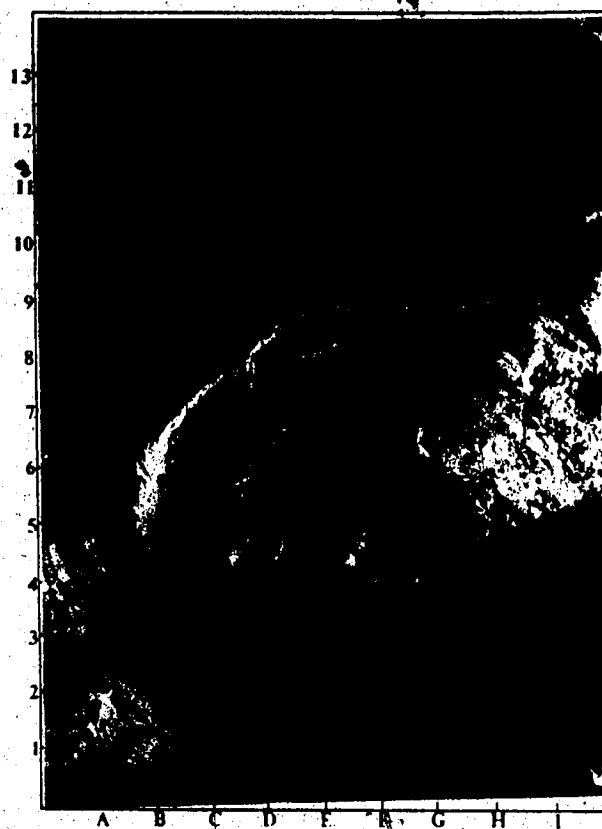


Figure 4.11 Oblique aerial view of Sc1 - looking northeast. Note the structural definition of the debris, and the pond at the base (E2).

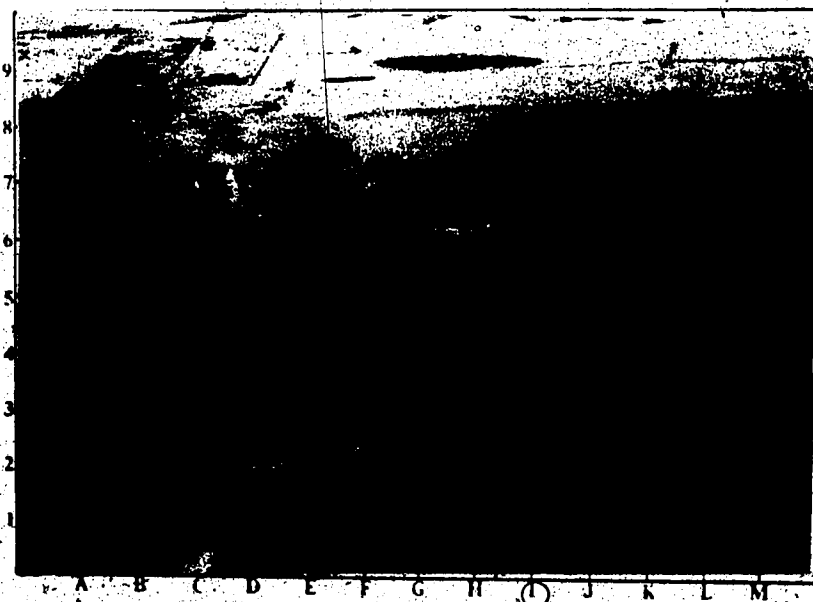


Figure 4.12 Oblique aerial view of Sc2 - looking northwest. Note the proximity of the channel along the base.

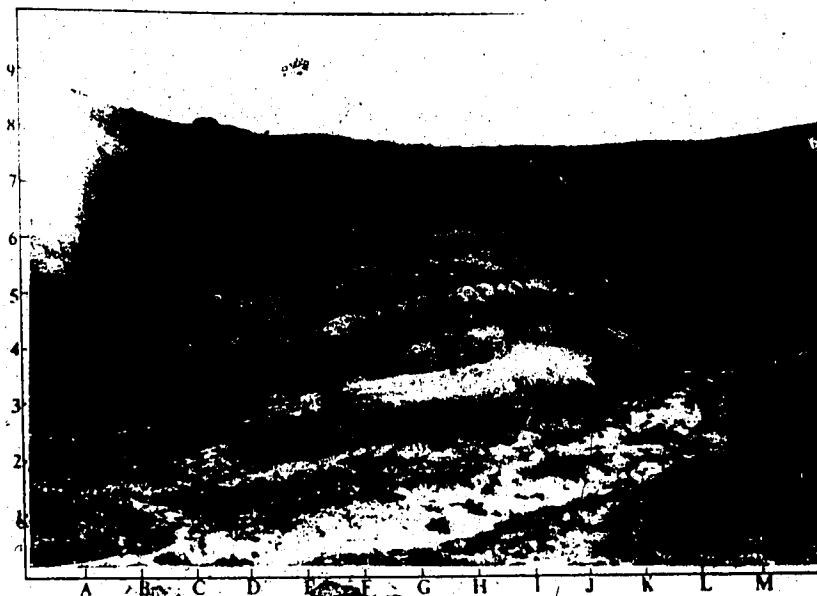


Figure 4.13 Overview of Sc3 --looking south. The backward tilting and the displacement of the beds are clearly visible.



Figure 4.14 Overview of Sc4 - looking southeast. Car on prairie surface (K7) for scale.

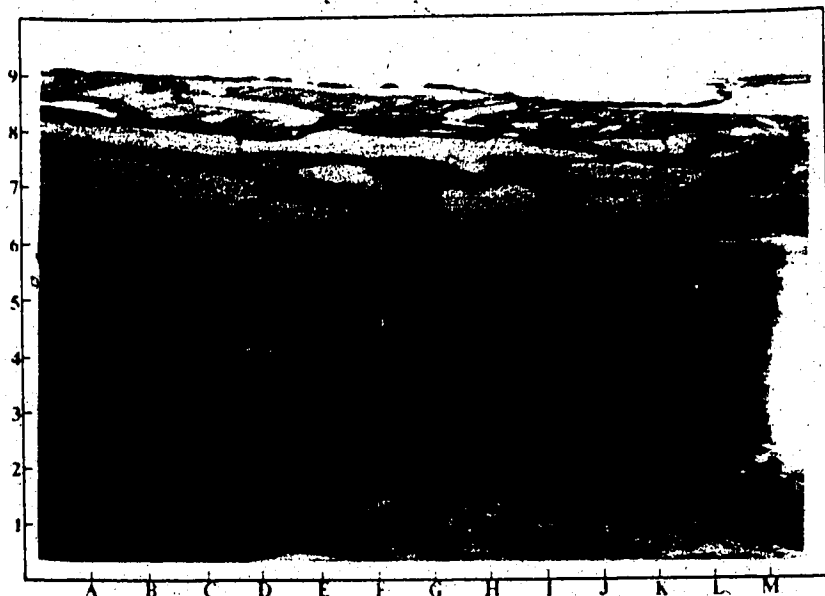


Figure 4.15 Oblique aerial view of Sr^2 - looking southwest. Note seepage areas above the visible scarp (from A5 to M6).

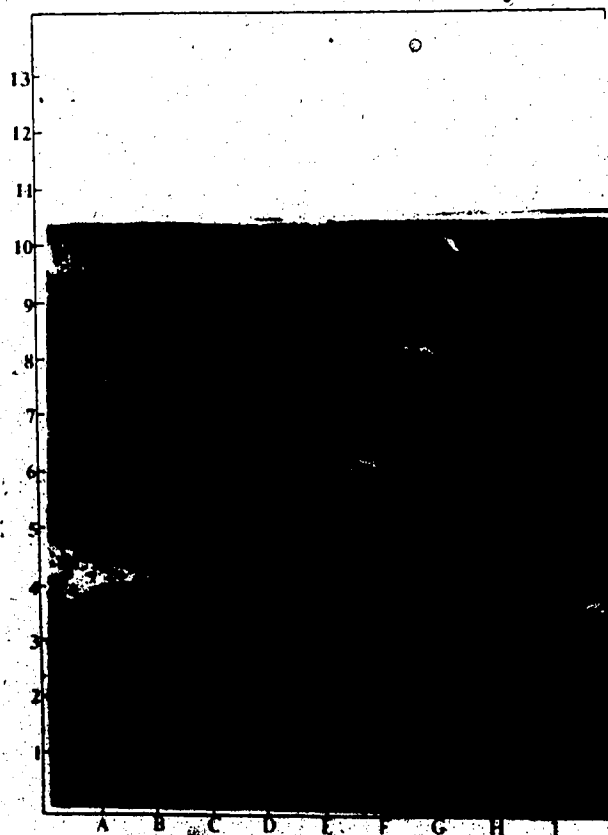


Figure 4.16 Overview of $St1$ - looking northeast. The upper 7 m of the exposure is till which increases in depth (A10-11) further north.

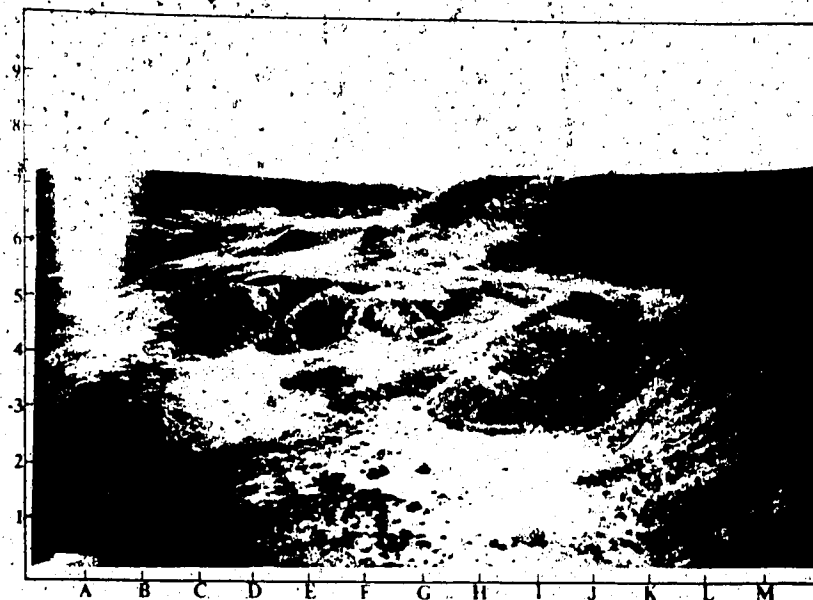


Figure 4.17 Overview of S/F1 - looking east. Relief here is about 60 m.

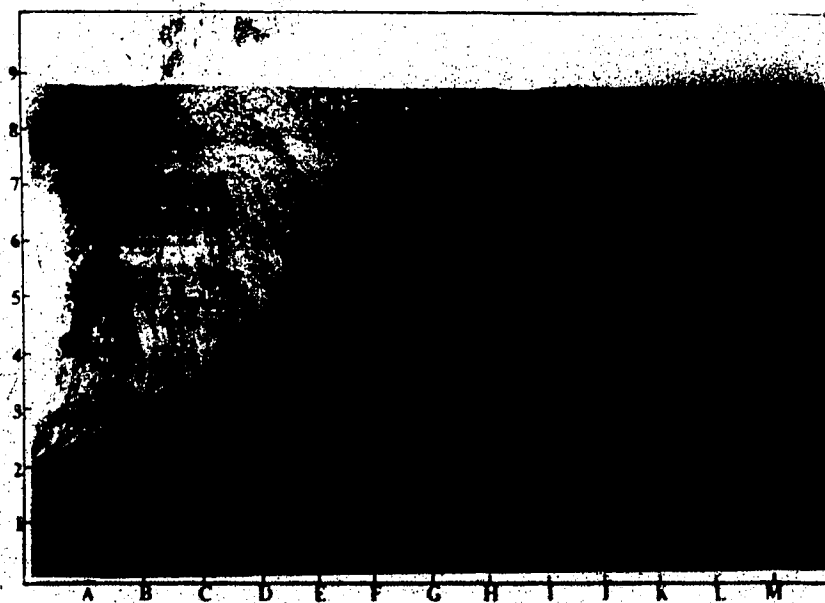


Figure 4.18 Overview of S/F2 - looking southwest. Note flow (G4) and adjacent failures to the south.

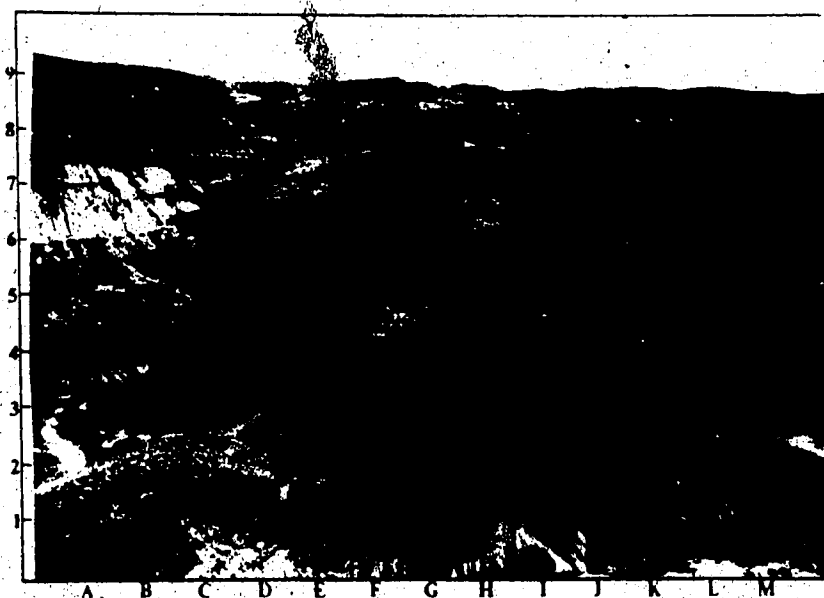
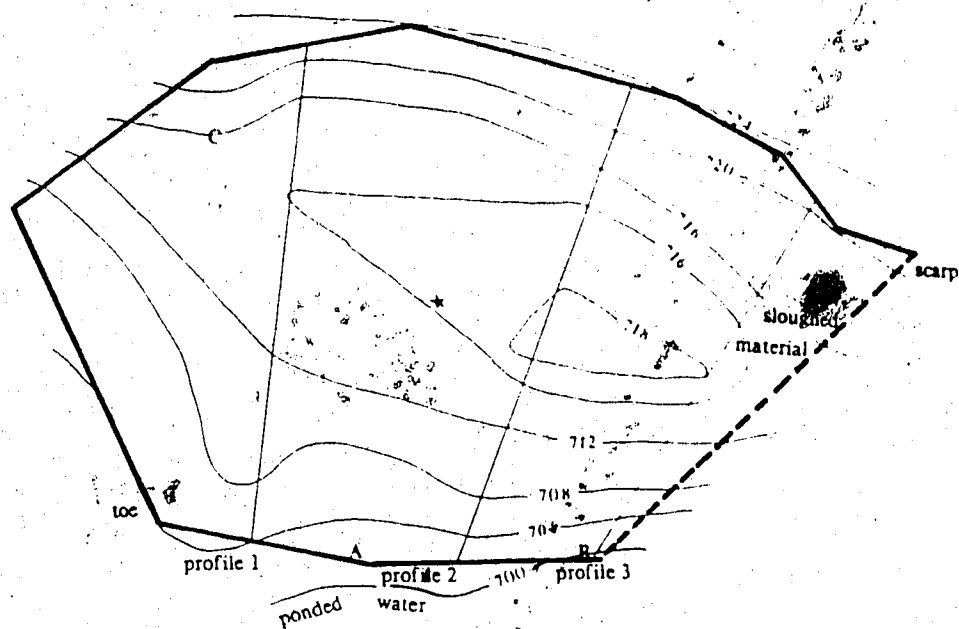


Figure 4.19 Overview of P/F1 - looking south. The shale in the foreground (D3, L2, and L3) is currently flowing over the more resistant sandstone base.



0 10 20m

scale

contour interval - 2m, 4m

--- estimated slide limit

A pit locations

* approximate centre of failure

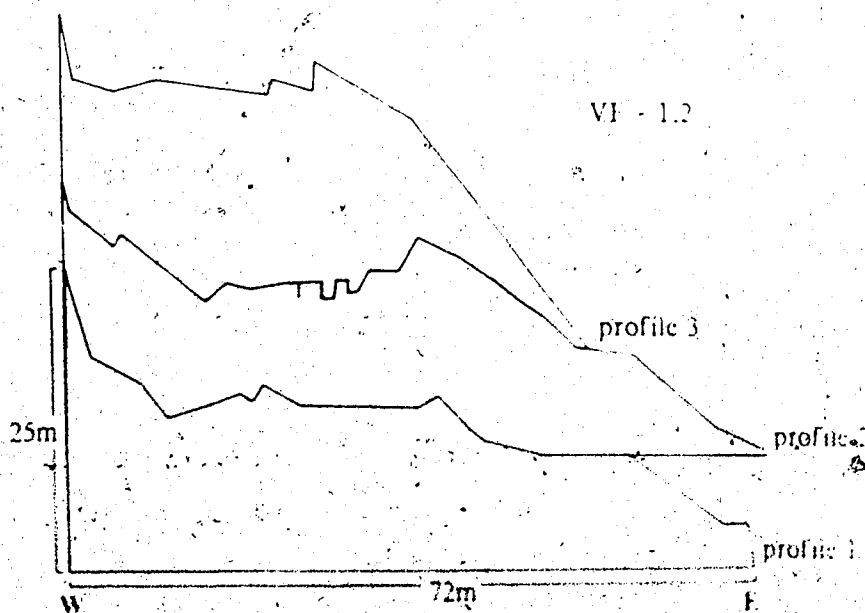


Figure 4.20 Slope profiles and contour map of Sc1

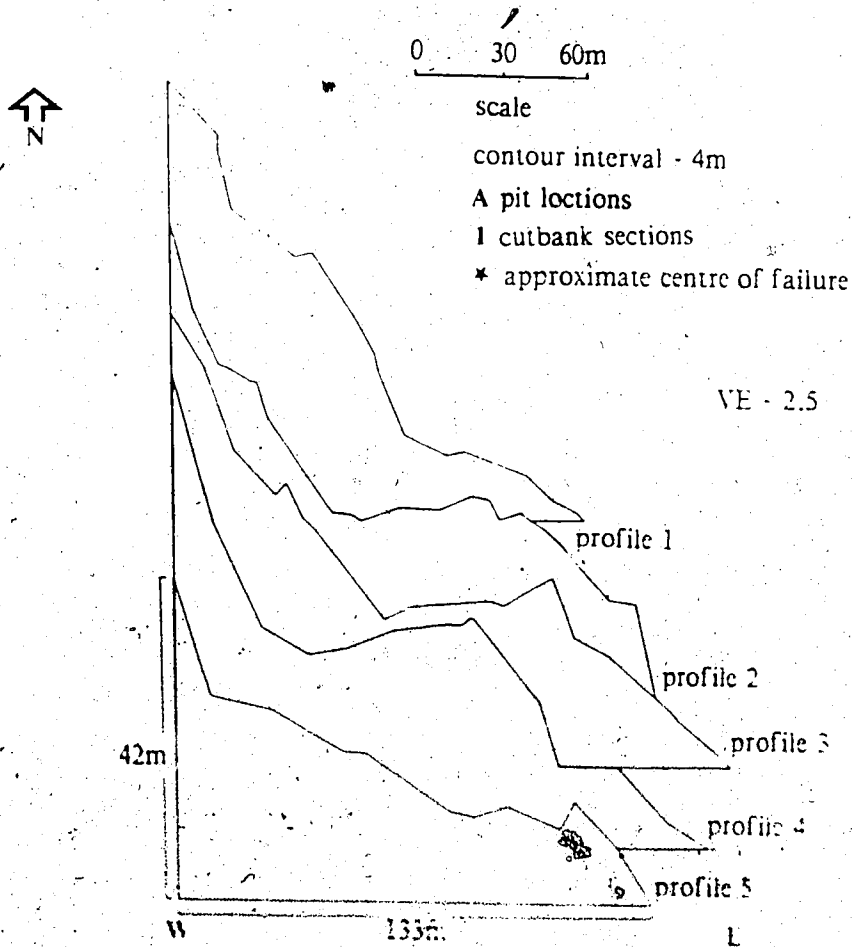
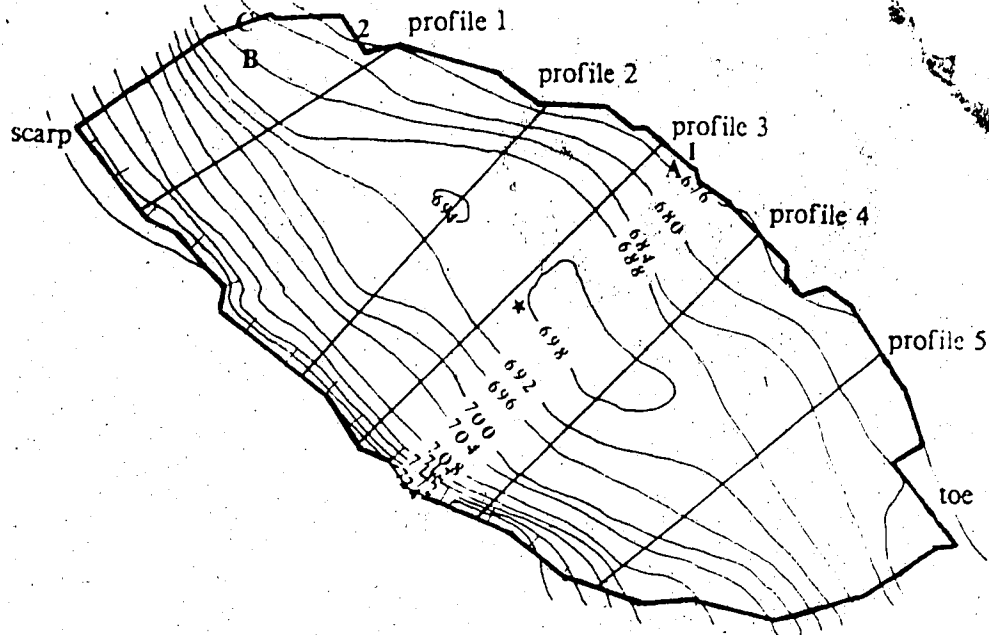
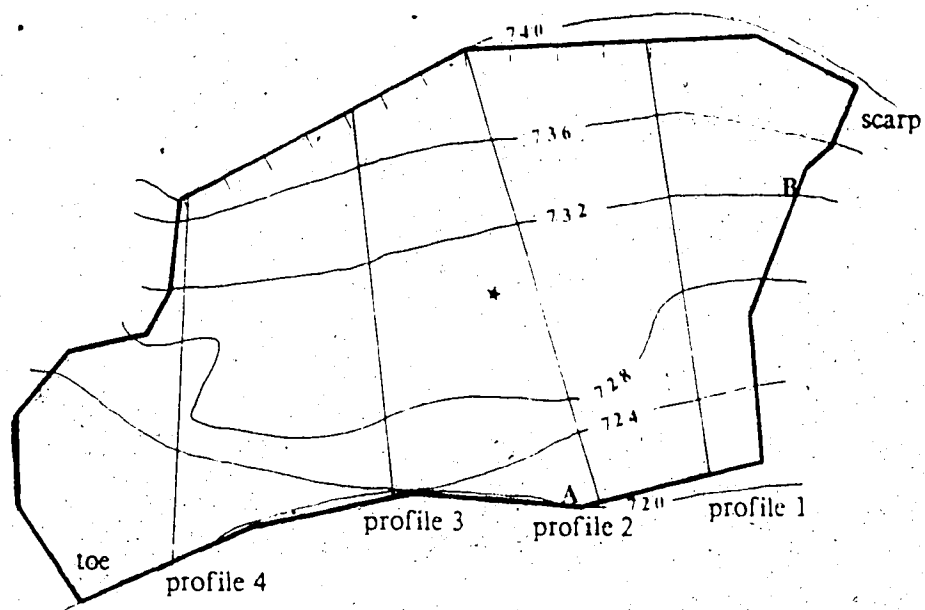


Figure 4.21 Slope profiles and contour map of S&2



0 10 20m

Scale

contour interval - 4m

A pit locations

* approximate centre of failure

VE - 1.2

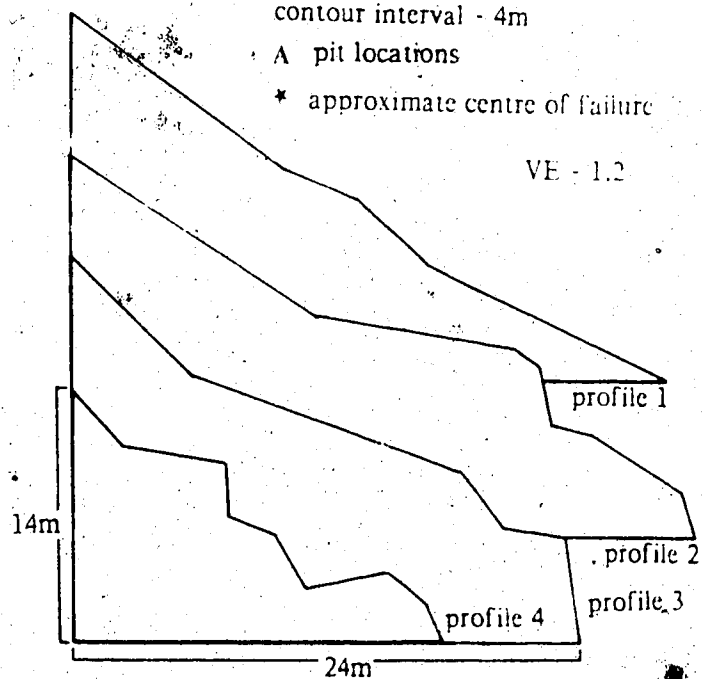


Figure 4.22 Slope profiles and contour map of Sc3

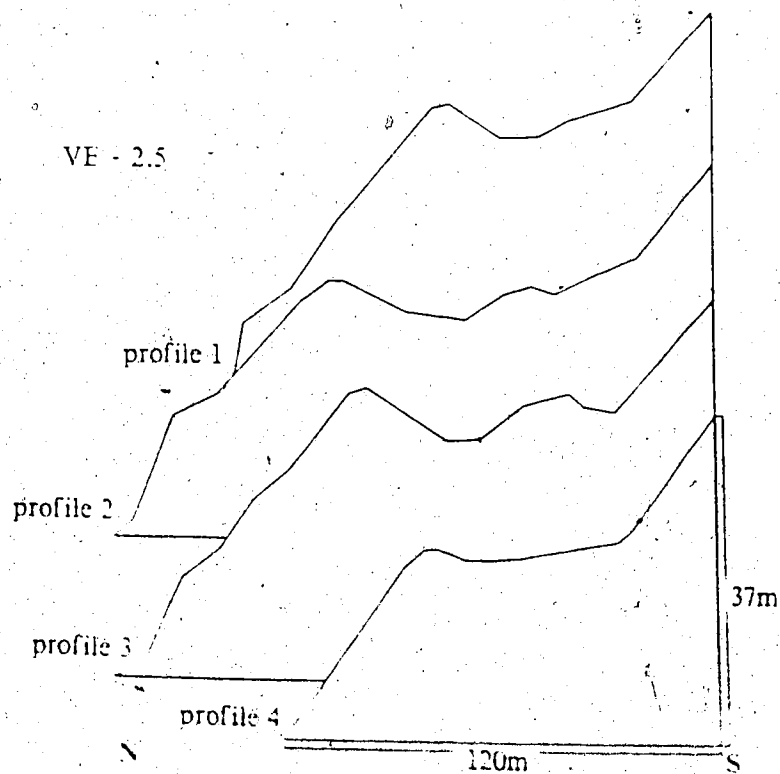
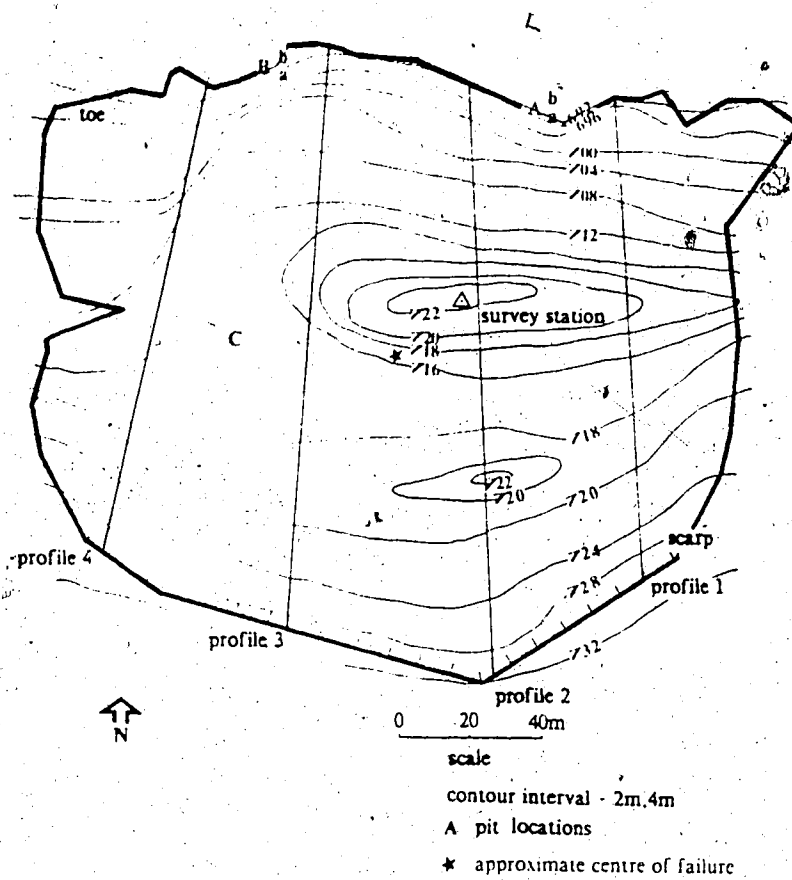


Figure 4.23 Slope profiles and contour map of Sc4

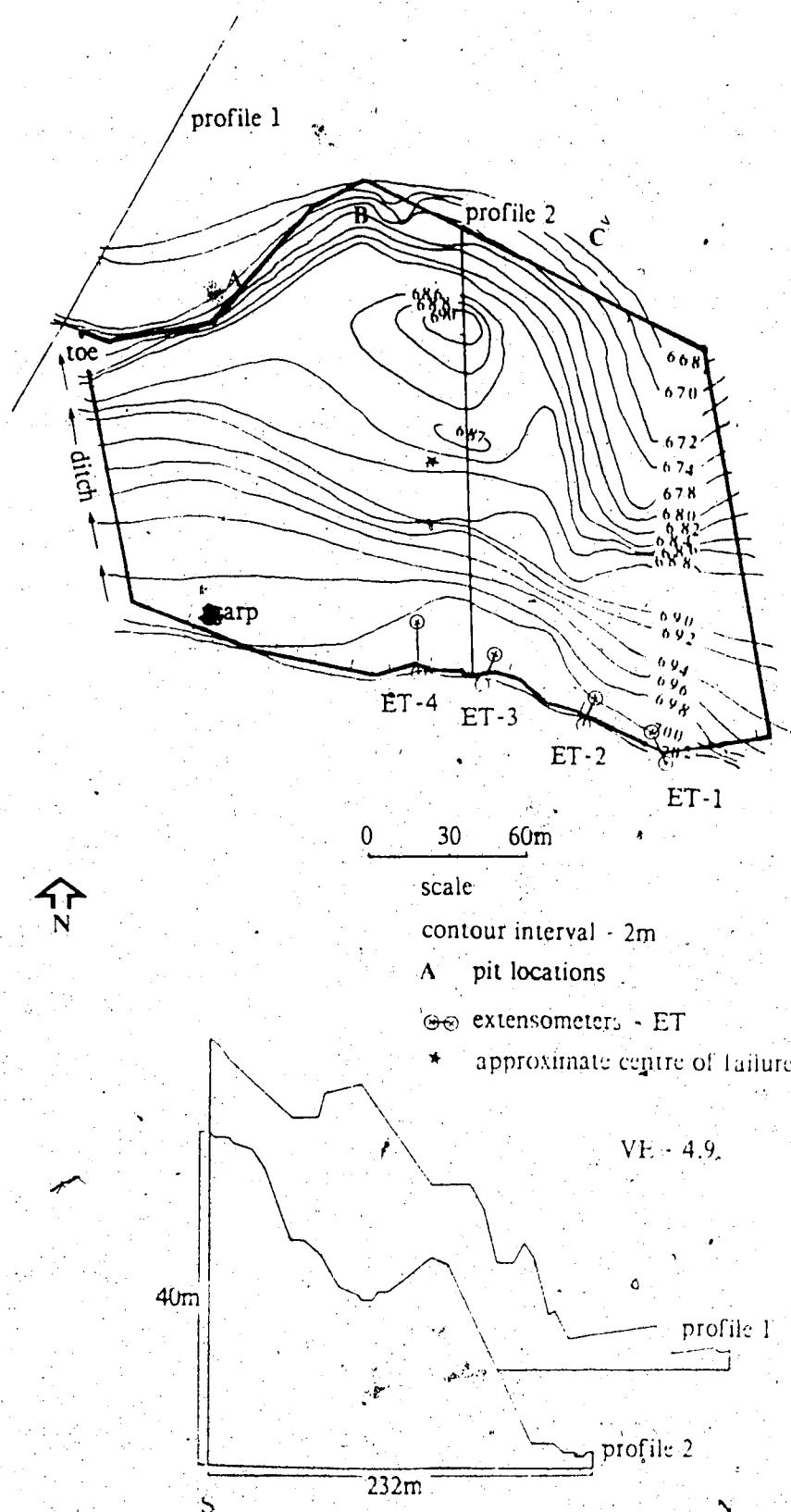


Figure 4.24 Slope profiles and contour map of Sr¹